

# The Nalunaq gold mine: a reference sample collection and compilation and interpretation of geochemical data

Denis Martin Schlatter & Simun D. Olsen

(1 DVD included)



GEOLOGICAL SURVEY OF DENMARK AND GREENLAND  
MINISTRY OF CLIMATE AND ENERGY



# **The Nalunaq gold mine: a reference sample collection and compilation and interpretation of geochemical data**

Denis Martin Schlatter & Simun D. Olsen

(1 DVD included)

# Contents

<b>Abstract</b>	<b>5</b>
Key words .....	5
<b>Introduction</b>	<b>6</b>
<b>Aim of this report</b>	<b>7</b>
Nalunaq rock library .....	7
Nalunaq geochemical database .....	7
<b>Regional geology of South Greenland</b>	<b>8</b>
<b>Regional distribution of geochemical anomalies</b>	<b>10</b>
<b>Geology of the Nanortalik peninsula</b>	<b>11</b>
<b>Exploration and mining history</b>	<b>13</b>
<b>Geological setting of the Nalunaq gold deposit</b>	<b>14</b>
Crosscutting features on Nalunaq mountain and the division into structural blocks.	17
Chemical rock definition and magmatic affinity assessed by lithochemical methods .....	17
Chemical rock definition of least altered amphibolites and dolerites .....	17
Geochemical rock definition of altered amphibolites and dolerites.....	19
Refined chemical rock definition for altered/unaltered amphibolites and dolerites ..	19
Magmatic Affinity of the least altered amphibolites and dolerites .....	22
Magmatic Affinity of the altered amphibolites and dolerites .....	24
Chemostratigraphy of the amphibolites and dolerites.....	25
Geochemical investigations of the felsic plutonic igneous rocks .....	29
<b>The Nalunaq gold deposit</b>	<b>33</b>
Physical hydrothermal alteration associated with gold mineralisation .....	33
<b>“Nalunaq rock library”</b>	<b>36</b>
<b>Compilation of geochemical Nalunaq data (gold, trace elements and major elements)</b>	<b>39</b>
<b>Gold distribution and identification of the pathfinder elements for gold on the deposit scale</b>	<b>44</b>
Distribution of gold in the main vein .....	44
Relationship between gold and the trace elements Ag, As, Sb, Bi, W and Mo .....	45

Gold-silver association .....	45
Gold-bismuth association .....	47
Gold-tungsten association .....	47
Gold-antimony association .....	48
Gold-arsenic association.....	49
<b>Semi-regional to deposit scale hydrothermal alteration</b>	<b>53</b>
Results of mass change calculations.....	54
Silicification and calc-silicate and/or carbonate alteration.....	54
Potassium and calc-silicate and/or carbonate alteration .....	56
Potassium and sodium alteration .....	58
Geochemical dispersion defined by Fe, As and gold enrichment .....	60
<b>Deposit-scale hydrothermal alteration</b>	<b>63</b>
Mass change of Si and gold enrichment.....	65
Mass change of K and gold enrichment .....	65
Mass change of Ca and gold enrichment.....	65
<b>Discussion and conclusions</b>	<b>67</b>
Nalunaq lithology .....	67
Lithogeochemistry and hydrothermal alteration.....	67
Gold deposit model.....	68
<b>Concluding remarks</b>	<b>70</b>
<b>Acknowledgements</b>	<b>71</b>
<b>References</b>	<b>72</b>
<b>List of Appendices on DVD</b>	<b>76</b>

## Abstract

Nalunaq is Greenland's first gold mine, was officially opened in August, 2004 and is located on the Nanortalik peninsula in South Greenland. The high grade gold mineralisation is located in an up to 2 m wide quartz vein and is hosted in altered amphibolite of Palaeoproterozoic age. The auriferous quartz vein is controlled by a higher-order thrust in the lowermost stratigraphy of the Nanortalik nappe. The stratigraphic column is metamorphosed at amphibolite facies grades and was redefined based on the location of the gold mineralisation: Structural Footwall (FW), main auriferous quartz vein (MV) and structural hanging wall (HW). The FW is made up of biotite granite and silicified granite. Intrusive contacts with the supracrustal wall rocks are seen at the surface and from a drill intersection. The volcanic and volcanoclastic rocks of the FW comprise a sequence of silicified siltstone containing abundant sulphides and intercalations of graphitic beds, fine-grained amphibolite, several metres thick coarse-grained dolerite sills or dykes. The MV comprises the 0.5 m to 2 m thick auriferous quartz vein and the proximal about 1 m to 1.5 m wide hydrothermal alteration halo, which occurs on both sides of the vein. The MV can be traced at surface for about one km on the east and north facing slopes of the Nalunaq mountain. The HW comprises a sequence of fine-grained amphibolite, medium-grained and coarse-grained dolerite. Several generations of pegmatite and aplite dykes or sills crosscut the lithology. Immobile-element ratios indicate seven different primary volcanic and volcanoclastic rock types: basalt 1, basalt 2, basalt 3, basalt 4, basalt X, basaltic andesite 1 and basaltic andesite 2. Most of these rocks have a tholeiitic affinity. This refined classification allowed identifying one single geochemical marker horizon; basalt X which is only found in the deeper parts of the stratigraphic column. The La/Yb ratio and the gold content allowed discriminating the felsic plutonic igneous rocks into pegmatite from the "Pegmatite fault", silicified granite and biotite granite; only the silicified granite contains anomalous levels of gold (up to 200 ppb). The most proximal part of the hydrothermal alteration system is the auriferous quartz vein. The medial hydrothermal alteration zone comprises biotite-altered bands of about 15 cm thickness containing arsenopyrite, löllingite, pyrrhotite, pyrite, and chalcopyrite. The distal hydrothermal alteration zone is about 1.5 m thick and is made up of calc-silicate and silicified amphibolite. The sequence of volcanic rocks located at the base of the mineralised thrust sheet of the deep footwall comprises strongly sulphide altered siltstone. Pathfinders to gold are Ag, As, Sb, Bi and W, and hydrothermal alteration assessed by mass change calculations showed that favourable alteration is characterised by mass gains of Si and K.

In this work we present on the attached DVD a comprehensive geochemical database including the gold analyses of almost 16,000 samples and geochemical whole rock analyses of >4,700 rock samples from the mine or from areas near Nalunaq. A rock library comprises 186 representative rock samples including the auriferous quartz vein the hydrothermal alteration zones and the least-altered wall rocks, which were sampled from all three structural blocks of the Nalunaq gold mine. The "Nalunaq rock library" is located at GEUS at the Geocenter and can together with the compiled geochemical data be used as a basis of future investigations and help to define further exploration targets in the area.

An exploration model for gold in South Greenland should include the search for meta-volcanic rocks that are intruded by silicified granite; or other rocks which are associated with intrusive plutonic and altered rocks. Within these rocks a shear zone associated with Si and K enriched rocks with anomalous levels of Au, As, Ag, Sb, Bi and W represent a particular good target.

### Key words

Vector to the ore · Mass change calculations · Geochemical rock classification Immobile element ratios · Hydrothermal alteration · Nalunaq rock library · Pathfinder elements to gold · Orogenic gold deposit · Psammite Ketilidian Orogen

## Introduction

Nalunaq is the first and only gold mine in Greenland, and gold was produced more or less continuously from 2004 to 2008 (Secher 2009, Secher et al. 2008). The production from 2004 to the end of February 2008 was 9,901,680 grams of gold (318,346 troy ounces of gold). The Nalunaq ore body was found during regional exploration by stream sediment sampling (Gowen et al. 1993). The source of the gold was finally located in the fall of 1992 in Kirkespirdalen (Kirkespir valley is the name of the valley at the foot of the mountain named Kirkespiret) and represents a 0.5 m to 2 m thick quartz-vein with visible gold (Gowen et al. 1993; Kaltoft et al. 2000). The Nalunaq ore body yields high gold grades with several hundred g/t of gold and underground samples with gold contents of up to 5200 g/t (Kaltoft et al. 2000). Although an excessive amount of data was reported by several exploration and mining companies in the form of printed reports to GEUS, these data have not been compiled in a comprehensive manner and were not made available digitally. These data were reported by the following companies: Cyprus Greenland Corp., NunaOil A/S, Mindex ASA, Nalunaq I/S, Crew Development Corporation and Nalunaq Gold Mine A/S. Here we present the result of the compilation of these data. Also lacking is a reference rock library with representative rock samples from Nalunaq. This lack of a comprehensive database and the lack of a reference sample collection may be part of the reason that only limited scientific work has been carried out and reported on the Nalunaq gold mineralisation. In the following we describe how we have compiled geochemical data and how we have built a reference sample collection in order to compile data and rocks from Nalunaq.

This report aims to provide some inspiration in the process of defining new gold targets in South Greenland and results of this study can be used for further exploration in the Nalunaq area and regionally in the Nanortalik area. It is expected that gold exploration efforts in South Greenland will be increased in the near future, because of the recent commissioning of an underground processing crushing, screening and Carbon in Pulp (CIP) plant inside the Nalunaq mine (Chadwick 2010) which will enable in the future to treat gold ore at a low cost level.

## **Aim of this report**

This report aims at providing **(a)** a comprehensive rock library including all rock types, hydrothermal alteration types and ore types of the Nalunaq deposit and **(b)** an updated database which includes all the geochemical data from the ore body, from the vicinity of the mine and from regional sampling programmes.

It has been shown from other closed mines, e.g. from the historical Boliden Cu-Au-As deposit, that a data compilation and a desk-top approach provides a rich source of information and allows new and innovative interpretations (Hallberg 2001). Sundblad (2003) compiled all past information from gold occurrences from Northern Europe, and his work allowed very useful new interpretation of the regional metallogeny of gold deposits. But now here, in the following we present a data compilation and a desk-top approach from the Nalunaq gold deposit.

## **Nalunaq rock library**

The “Nalunaq rock library” contains 186 representative rock samples from the Nalunaq auriferous quartz-vein, the hydrothermally altered contact rocks adjacent to the ore and the unaltered wall rocks. The “Nalunaq rock library” is located at GEUS at the Geocentre in Copenhagen and is easily accessible by simply making an appointment with GEUS staff.

## **Nalunaq geochemical database**

This report provides the compiled geochemical Nalunaq database, new interpretations regarding the host rocks and hydrothermally altered rocks from Nalunaq.

New interpretation of the compiled geochemical data from Nalunaq can help to better understand the high grade Nalunaq gold deposit. The Nalunaq rock library allows to select specific samples for analysis or examination.

This will help to define additional exploration targets and lead to follow-up field work which potentially could lead to new gold discoveries on the Nanortalik peninsula or elsewhere in South Greenland.

# Regional geology of South Greenland

The Ketilidian orogen evolved between 1850 Ma to 1725 Ma during supposedly northward subduction of an oceanic plate under the southern margin of the Archaean North Atlantic craton. The Ketilidian orogen is divided into four geological domains: the Ketilidian border zone, the Julianehåb batholith zone, the Psammite zone and the Pelite zone (Fig. 1).

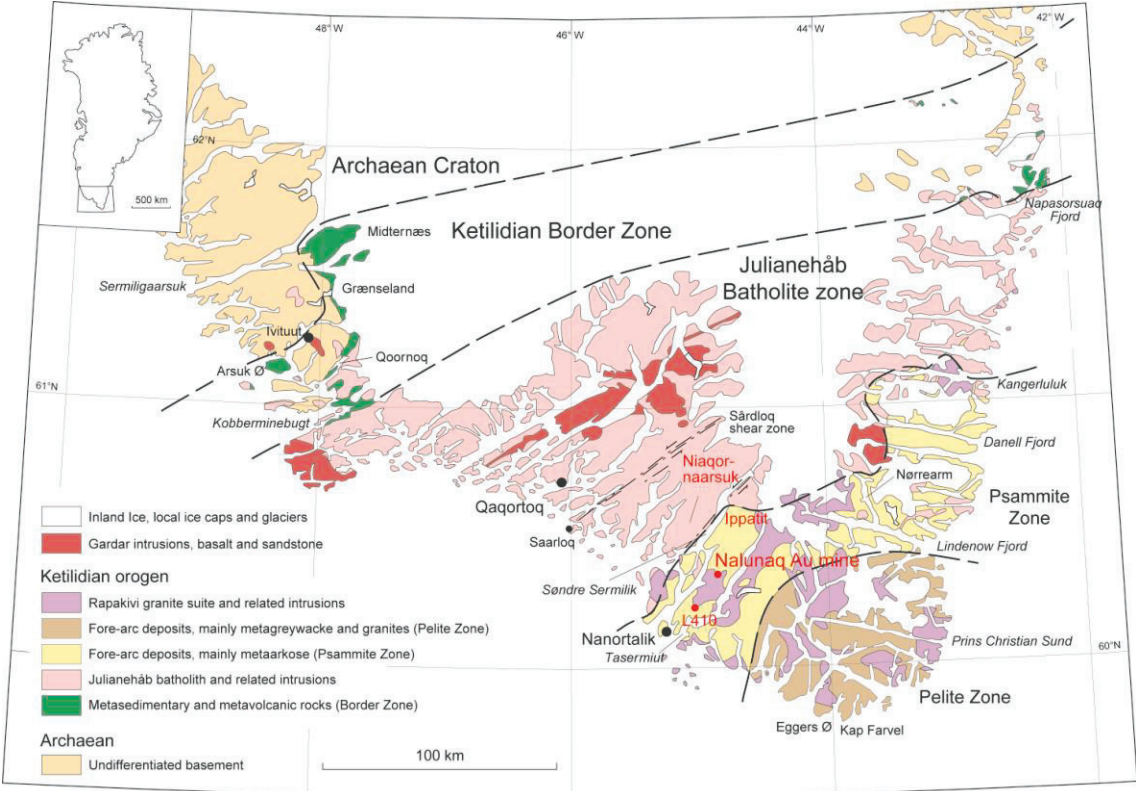


**Figure 1.** Summary map of the Ketilidian Orogen, South Greenland modified from Chadwick and Garde (1996) showing the main divisions: Foreland, Border Zone, Julianehåb Batholith, Psammite Zone and Pelite Zone. The Nalunaq gold mine is located in the Psammite zone and is about 35 km NE of Nanortalik. A second prospect with gold potential is “Lake 410” which is located about 20 km SW of Nalunaq. Other areas near Nalunaq where gold has been reported are, Ippatit and Niaqornaarsuk.

Below, the four domains are described by using information from Secher et al, 2008, however the description is only brief and the interested reader is referred to Windley (1991) and Chadwick and Garde (1996).

The *Ketilidian border zone* comprises the Palaeoproterozoic metavolcanic rocks of Midternæs and Grænseland and reworked Archaean basement rocks, forming the foreland of the orogen (Fig. 1).

The *Julianehåb batholith zone* represents the central part of the Ketilidian orogen and is dominated by one large, multi-phase, continental calc-alkaline batholith (Fig. 1), which is emplaced between 1854 and 1795 Ma. The major stages of deformation formed several NNE- or NE-trending, sinistral shear zones crosscutting the batholith.

The *Psammite Zone* comprises mafic volcanic rocks, variably migmatized pelitic and semi-pelitic rocks, calcareous metasediments, bedded massive-pyrrhotite/graphite-cherts, dolerites, syn- to post-kinematic appinite dykes as well as post-kinematic rapakivi granites. The sediments represent erosional material from the Julianehåb batholith and were deposited in fluvial and shallow marine environments between the batholith and an oceanic environment to the south. They are interpreted to represent intra- and fore-arc sediments, in molasses-type sedimentation and pelitic metasediments are suggested to be formed in flysch-type sedimentation. The Nalunaq gold deposit and also other gold occurrences on the Nanortalik half island (Fig. 1) are located in this zone and are hosted in mafic metavolcanic rocks.

The *Pelite Zone* at the southern tip of Greenland comprises mainly flat-lying, intensely migmatized pelitic rocks. The pelitic rocks consist mainly of turbidite, deposited in a deeper offshore part of the marine sedimentary basin in a flysch-type sedimentation.

All rocks from the Nanortalik peninsula are metamorphosed and in the following the prefix "meta" is omitted for simplicity.

## Regional distribution of geochemical anomalies

South Greenland has been recognized as a gold province since the early 1990ies (Stendal and Schönwandt 2000; Stendal and Frei 2000). Elements such as As, Sb, Sc and Cs are associated with the gold occurrences in South Greenland (Steenfelt 2000). The Psammite zone was recognized by Steenfelt (2000) as a zone which is regionally elevated in As based on stream sediment data (Fig. 2).

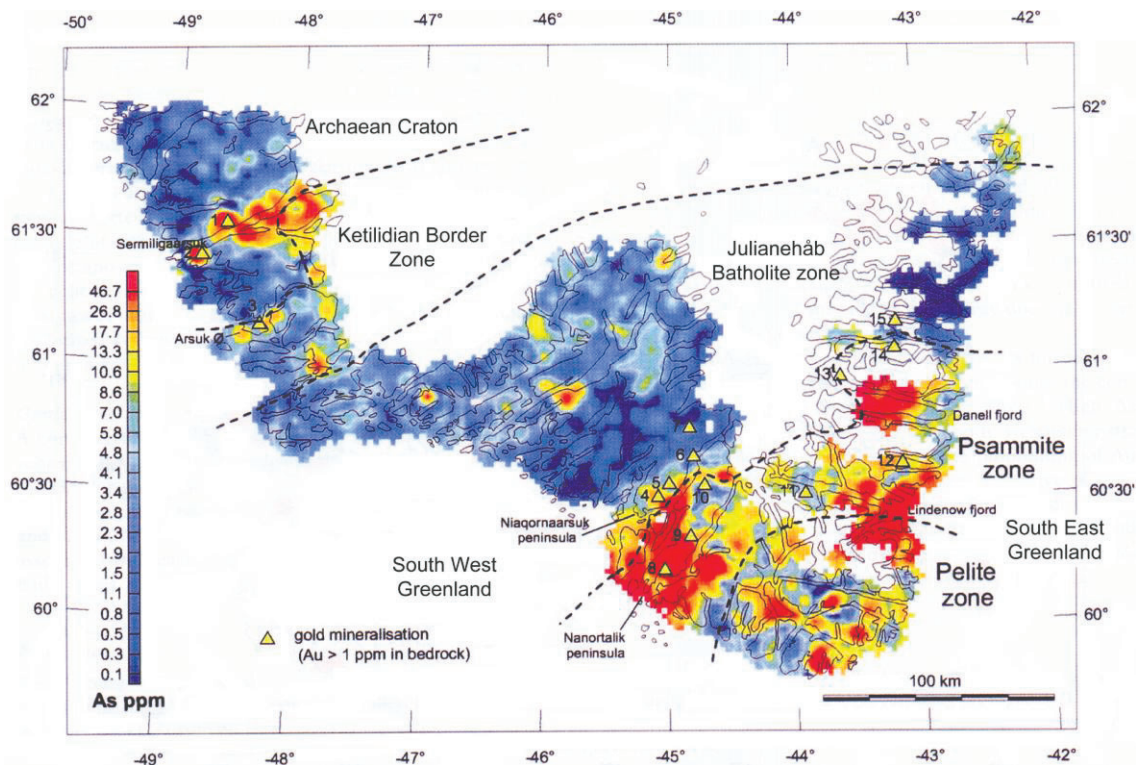


**Figure 2.** Gold occurrences in South Greenland and arsenic distribution outlined from stream sediment samples (modified from Steenfelt 2000). The Psammite Zone represents an area strongly elevated in arsenic. A second area with strongly elevated arsenic is located at Sermiligaarsuk about 250 km NW of Nalunaq and corresponds to the Achaean Tartoq greenstone belt. Gold occurrences in South Greenland are 1) Iterlak, 2) Nuuluk, 3) Arsuk Ø, 4) Niaqornaarsuk Valley, 5) Qoorormiut Valley, 6) Søndre Sermilik, 7) Isortup Qoorua, 8) Lake 410, 9) Nalunaq, 10) Ipattit. Gold occurrences in South-East Greenland are 11) West of Sønderarm, 12) Kutseq Fjord, 13) Sorte Nunatak, 14) Kangerluluk, 15) Igutsaat Fjord.

Gold occurrences are located either in the areas with the highest arsenic anomalies (as, e.g., the Nanortalik peninsula) or they are located close to the boundaries of areas with elevated arsenic contents and low arsenic contents (as, e.g., the Niaqornaarsuk peninsula; Fig. 2). Steenfelt (2000) has also shown from stream sediment data that in South Greenland a spatial correlation between Au and As-Sb-Sc occurs.

The Nalunaq gold mine is located in the Psammite zone (Kaltoft et al. 2000). From the same zone, several other gold occurrences are known, such as e.g. "Lake 410" (Stendal and Frei 2000, Petersen et al. 1997).

Other areas north-west of the Ketilidian mobile belt are also elevated in arsenic, e.g. Arsuk Ø and an area north-east of Sermiligaarsuk (Fig. 2; Evans and King 1993; Appel and Secher 1984; Petersen and Madsen 1995).

## Geology of the Nanortalik peninsula

The Nalunaq gold deposit is located in the Psammite zone (Figs. 1 and 2) on the Nanortalik peninsula (Fig. 2). The area is dominated by arkose, biotite- and rapakivi granite, volcanic rocks and gneiss (Fig. 3).

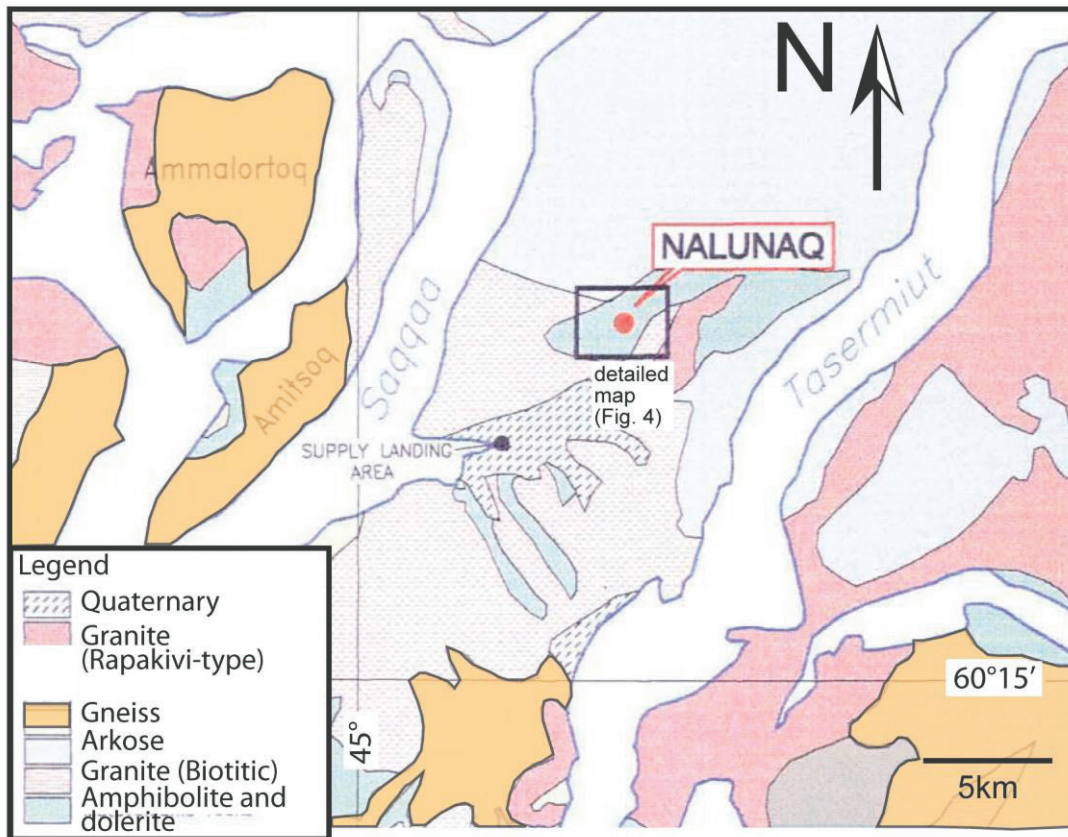


**Figure 3.** Simplified geological map of the Nalunaq area (after Allaart 1976). The Nalunaq area comprises mainly granites, gneiss and arkose; relatively small areas are amphibolite and dolerite which are the host rock of the gold mineralisation.

The volcanic rocks which host the main auriferous quartz-vein (Nalunaq MV) in the Nalunaq mine represent a nappe, which was thrust over an arkose basement (Petersen 1993). After the structural emplacement of the nappe, the volcanic rocks were intruded by granite (Petersen 1993). The contact between arkose and volcanic rocks is made up of a unit consisting of several tens of meters thick sulphide-impregnated rocks which are interpreted as volcanoclastic rocks (Fig. 4).

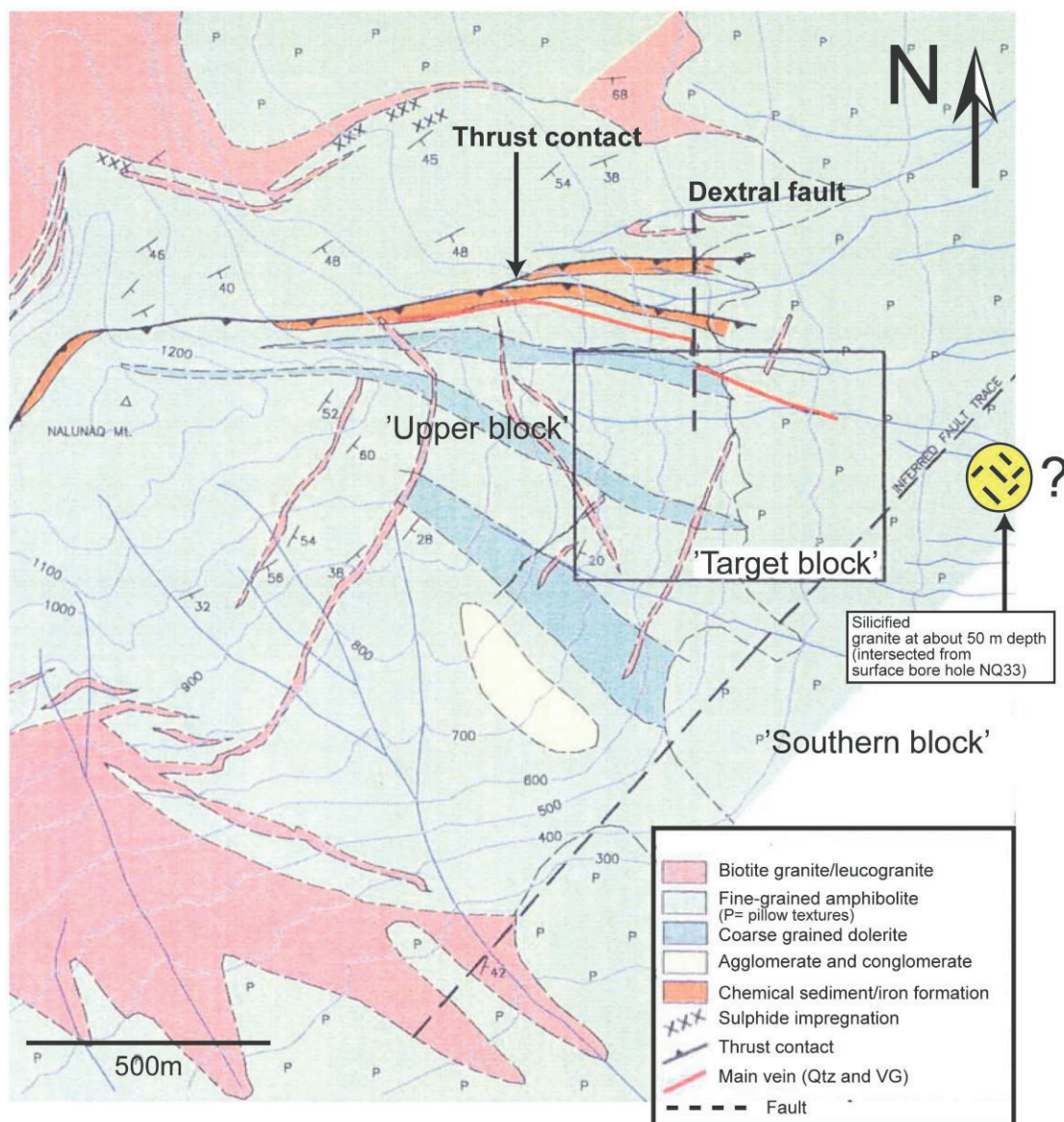


**Figure 4.** Detailed map around the outcropping Nalunaq quartz-gold vein (modified from Petersen 1993). The map shows that the Nalunaq quartz-gold vein is mainly hosted in fine-grained amphibolite but locally the main vein is also hosted in dolerite. The small “P” symbols indicate areas where relict pillow textures in fine-grained amphibolite were observed by Petersen (1993).

These sulphide-rich rocks represent the basis of the nappe and contain gold up to several hundred ppb (Kaltoft et al. 2000).

Similar nappe sheets occur elsewhere on the Nanortalik peninsula, e.g., the “Lake 410” area which is located 20 km south-west of Nalunaq and in the Ippatit area which is located 25 km north-east of Nalunaq (Fig. 1). At “Lake 410” the volcanic rocks are under-roofed by granite as seen from Nalunaq and gold occurrences are known from “Lake 410” and from Ippatit (Petersen et al. 1997). Although the Archaean volcanic rocks from the Tartoq group in South Greenland are not part of the Ketilidian orogen (Appel and Secher 1984), it is noteworthy that the gold found in volcanic rocks of the Tartoq group area are also interpreted to be related to thrusting. Similar to the setting of the gold in the Ketilidian mobile belt, the gold mineralisation at Tartoq is interpreted to be structurally controlled (Evans and King 1993; Appel and Secher 1984; Petersen and Madsen 1995; Schlatter and Kolb 2011, Schlatter et al. 2011).

## **Exploration and mining history**

A quartz-vein of 0.5 m to 2 m thickness with visible gold has been found in 1992 in Kirkespirdalen that is located on the Nanortalik peninsula about 35 km north-east of Nanortalik (Fig. 2). Previous to the discovery, geochemical exploration using gold analyses from stream and scree sediment samples (Gowen et al. 1993) identified the Kirkespirdalen area as a gold target because the sediment samples contained five to ten times higher gold than samples collected elsewhere in the area. After the discovery of the high grade gold vein at Nalunaq, exploration work and resource estimation based drilling was intensified between 1993 and 2003 including establishment of an investigation adit in 1998 and pilot production and processing in 2000 (Dumka and Thalenhorst 2001; Lind et al. 2001; Porritt 2003; Secher et al. 2008). To date, 237 drill holes totaling 5,572 m were drilled from underground drill positions and 172 drill holes totaling 30,477.85 m were drilled from surface including 14,219 m of drilling that was carried out in the period 1993 to 2003.

After a positive bankable feasibility study and necessary Government approvals Greenland's first gold mine was officially opened in August, 2004.

## Geological setting of the Nalunaq gold deposit

The volcanic rocks and the Nalunaq auriferous quartz-vein of 0.5 m to 2 m thickness are outcropping at about 500 m elevation and can be followed on surface more or less continuously to the 850 m elevation on the east-facing slope of the 1340 m high Nalunaq mountain (Fig. 5).

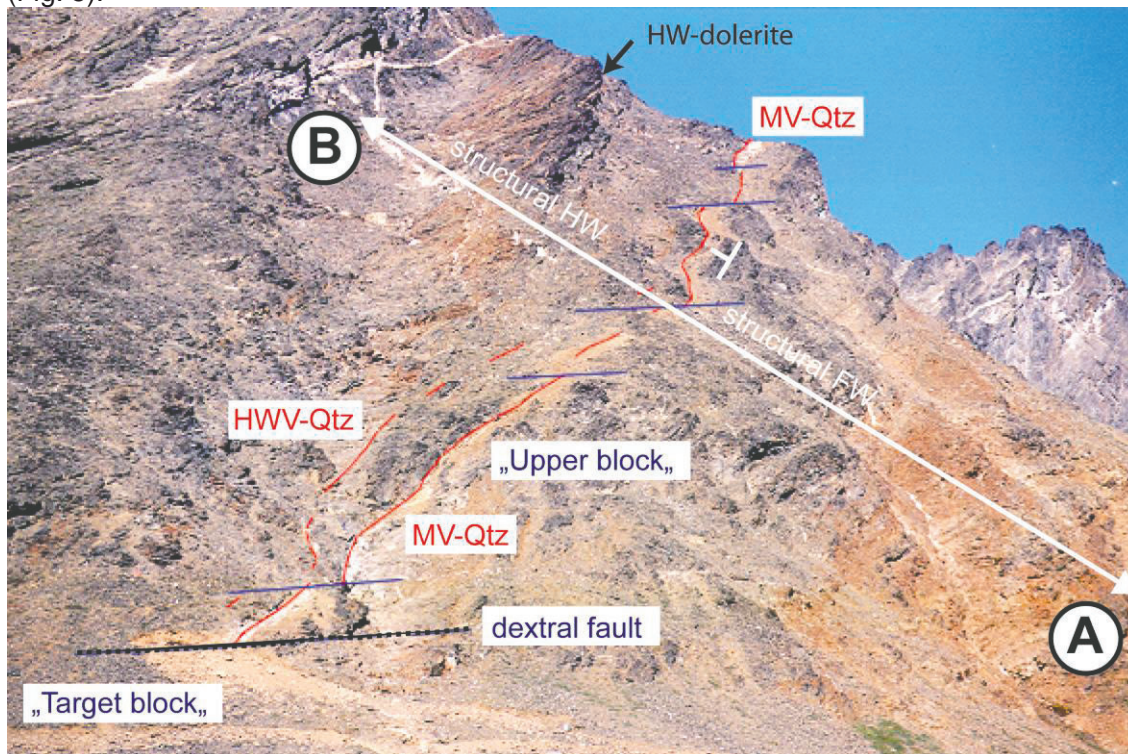


**Figure 5.** Nalunaq mountain, south-east face (looking in the NW direction). Main gold-quartz vein (MV-Qtz) in the centre of the photograph. Above the MV-Qtz, the hanging-wall complex (structural HW) and below the MV-Qtz the footwall complex (Structural FW). In the structural HW outcrops of the hanging-wall dolerite (HW dolerite) can be seen. The fault which separates the “Upper block” from the “Target block” is marked in black and stippled patterns. It is seen that the Nalunaq MV is slightly oblique to the main foliation. The dextral fault separates the “Target block” from the “Upper block”. Details of the Nalunaq-setting seen in the photograph are provided in Figure 6 (section A-B).

From the 850 m elevation the outcropping auriferous quartz-vein can be further followed on the north-facing slope but access to these outcrops involves climbing. The auriferous quartz vein is interpreted to be associated with a several meter thick shear zone (Secher et al. 2008). The Nalunaq auriferous quartz vein is hosted in a sequence of volcanic host rocks, which have been metamorphosed to upper greenschist to amphibolite facies grades. Prehnite-bearing rocks were metamorphosed retrograde at the prehnite-pumpellyite facies grade (Porritt 2000). Gold mineralisation was formed under retrograde metamorphic conditions, and fluids related to the gold mineralisation have caused retrograde metamorphism of rocks that were originally at amphibolite facies grades (Porritt 2000).

Data from detailed geological mapping (Petersen 1993; Kaltoft et al. 2000) and detailed information from drilling programmes (Schlatter 1997; Schlatter 1998; Kludt and Schlatter 2000; Schlatter and Aasly 2001) were reviewed. The review of these data was synthesized into a simplified stratigraphic lithological column (Fig. 6).

## Simplified stratigraphic column through the Nalunaq ore horizon (MV-Qtz)

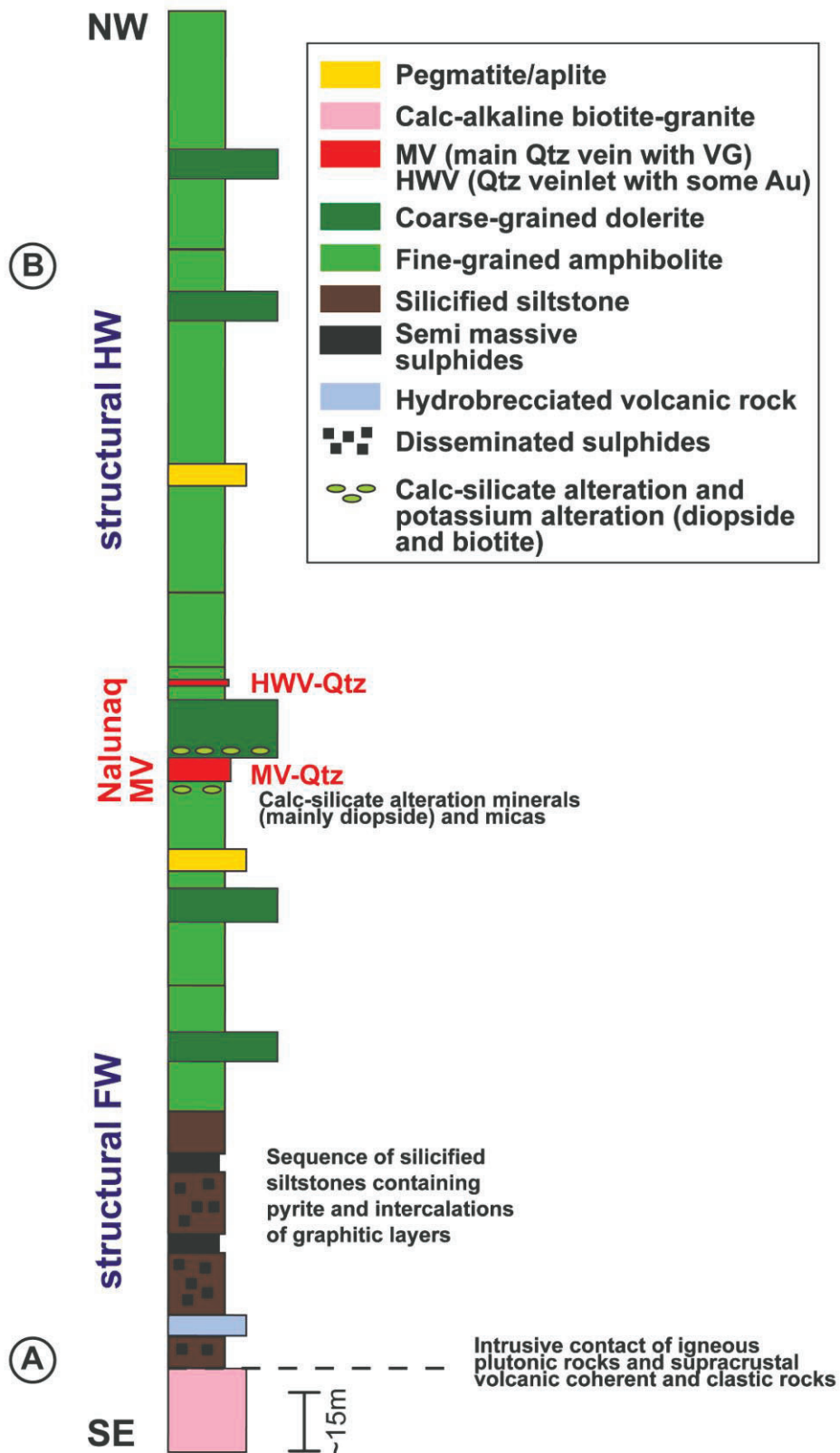


**Figure 6.** Simplified stratigraphic column of Nalunaq. The Nalunaq setting is relatively simple and consists mainly of fine-grained amphibolites and coarse-grained dolerite. Between the granite of the deep

*footwall and the amphibolite and dolerite of the shallow footwall, silicified and pyrite-impregnated siltstones with intercalation of graphitic beds and a package of altered fine-grained siltstones occur. The gold mineralised quartz vein is located at or close to the contact of fine-grained amphibolite and coarse-grained dolerite. The Nalunaq rock sequence comprises numerous pegmatite and aplite dykes at various stratigraphic levels.*

The true stratigraphic way up is unknown because of the lack of primary volcanic textures. Because the age relation of the rock sequence is unknown, it is labelled into structural footwall (FW) and structural hanging wall (HW) with respect to the main gold-quartz vein (Nalunaq MV). A second, less continuous and thinner auriferous quartz vein occurs about 15 to 20 m above the Nalunaq MV and is known as the Nalunaq hanging-wall vein (HWV); (Fig. 6).

#### *Structural Footwall (FW)*

The structural footwall is made up of biotite granite underlying the volcanic rocks (Figs. 3, 4 and 6). Intrusive contacts between granite and volcanic rocks are seen at the surface and from a drill intersection of borehole NQ-93-2 (Guy 1993). The volcanic and volcanoclastic rocks of the FW comprise a sequence of silicified siltstone containing abundant sulphides and intercalations of graphitic beds, fine-grained amphibolite and several metres thick coarse-grained dolerite sills or dykes and some thin aplite dykes or sills (Fig. 6). The sequence of sulphide-rich volcanic rocks represents the base of the mineralised thrust sheet located in the lowermost stratigraphy of the Nanortalik nappe (Fig. 4).

#### *Nalunaq MV: the ore*

The ore horizon comprises the 0.5 m to 2 m thick auriferous Nalunaq MV and the proximal about 1 m to 1.5 m wide hydrothermal alteration halo, which occurs on both sides of the vein. The characteristics of the hydrothermal alteration are discussed later. The Nalunaq MV can be traced at surface for about one km on the east and north facing slopes of the Nalunaq mountain and is slightly cross cutting the foliation (Fig. 5).

#### *Nalunaq HWV:*

The Nalunaq HWV comprises a few tens of centimetre thick quartz vein sometimes with visible gold. Along strike the Nalunaq HWV thins out and in places is only recognizable in the form of few centimetre thick seams of calc-silicate altered and silicified volcanic rocks or is not present at all. In summary the Nalunaq HWV is less continuous, thinner and contains less gold than the Nalunaq MV and might represent a splay structure off the Nalunaq MV (Fig. 5).

#### *Structural Hanging wall (HW)*

The Structural hanging wall comprises a sequence of fine-grained amphibolite; medium-grained and coarse-grained dolerite. Several generations of pegmatite and aplite are crosscutting the lithology.

## **Crosscutting features on Nalunaq mountain and the division into structural blocks**

The Nalunaq area was affected by late-stage (post mineralisation) faulting, which resulted in the breakup of the rock sequence into several blocks. The Nalunaq ore deposit comprises from SE to NW the “Southern block”, the “Target block” and the “Upper block”, sometimes also referred to as the “Mountain block” (Fig. 4; Kaltoft et al. 2000, Lind et al. 2001). The most important fault is a NE-SW trending reverse fault with a dextral component. The structural movement resulted in the uplift of the “Southern block” relative to the “Target block” (Fig. 4 in Kaltoft et al. 2000). This fault is well exposed on the south-facing slope of the Nalunaq mountain and is intruded by granitic pegmatite. The Target block is separated from the Upper block by a dextral fault (Fig. 4) but only with minor displacement movement in the order of a few meters. The movement on the late-stage faults created offsets on the mine scale which considerably complicated the planning and mining of the ore (Lind et al. 2001).

## **Chemical rock definition and magmatic affinity assessed by litho-geochemical methods**

### **Chemical rock definition of least altered amphibolites and dolerites**

Least altered samples from the “Target block” were selected on the basis of low gold and silver contents, low contents of As, Bi, Sb, Ba Mo, W and low loss on ignition. Least altered samples, 12 in number, from different lithologies or rocks of the Nalunaq stratigraphy were identified (Fig. 7a; appendix b).

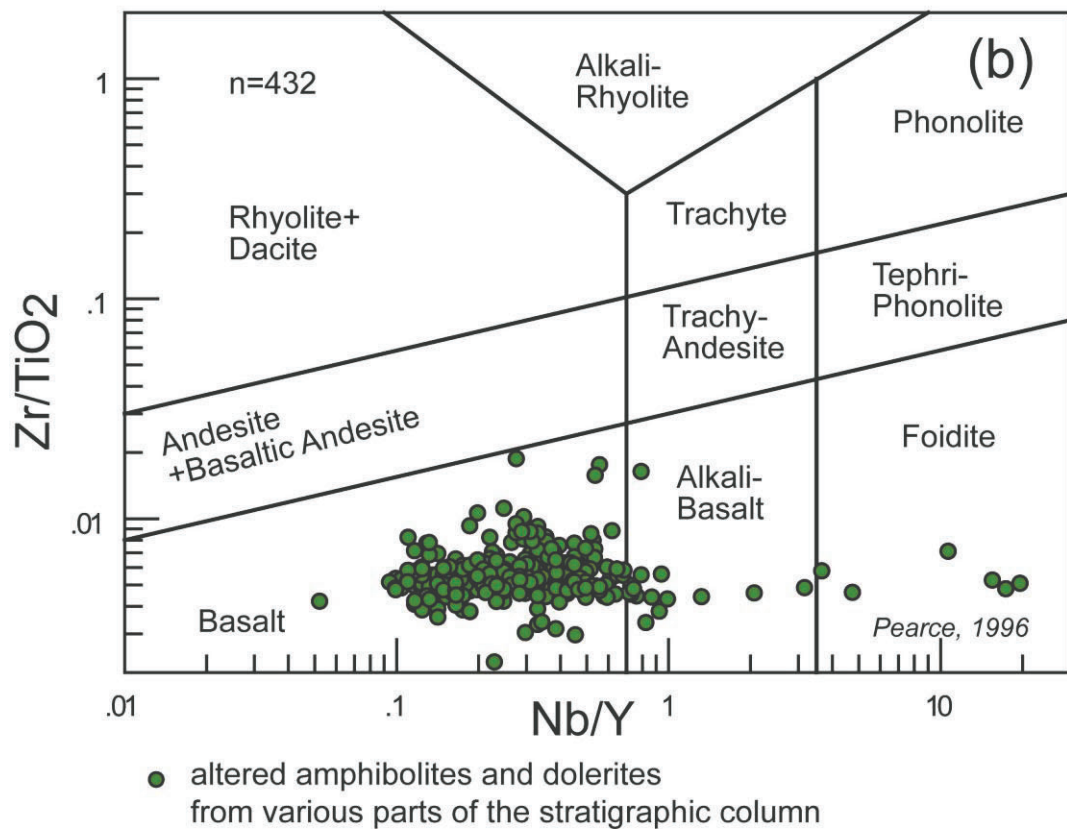
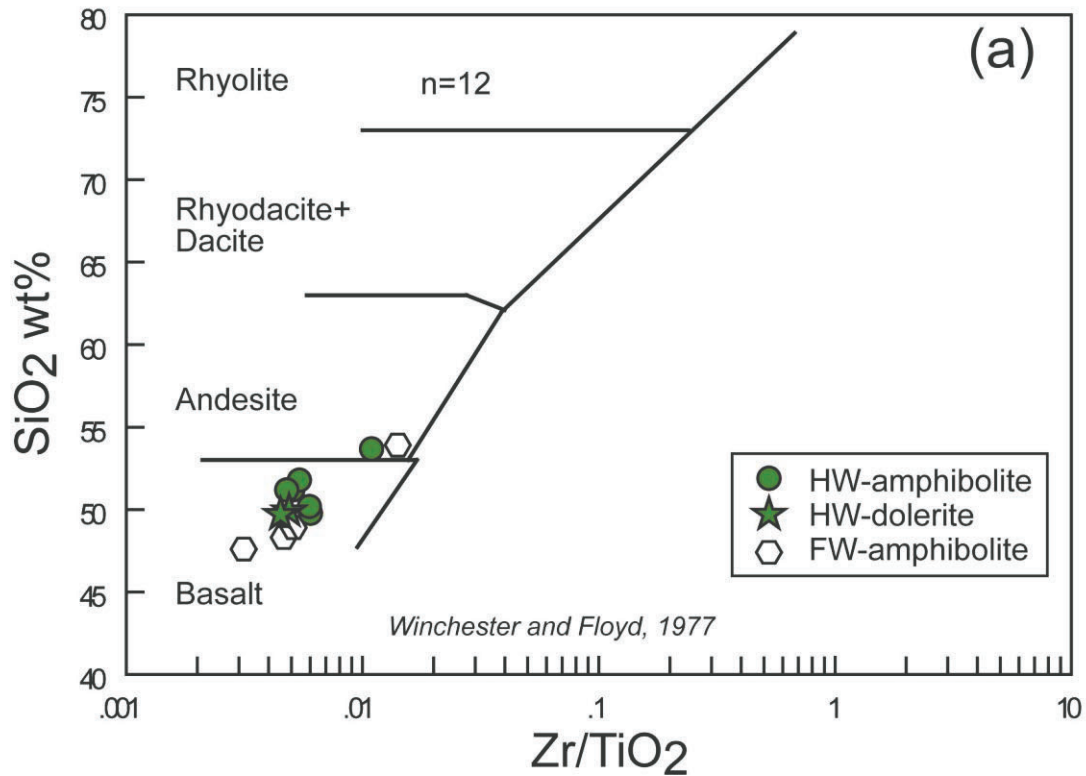


**Figure 7.** Chemical classification of volcanic rocks from the Nalunaq stratigraphy. (a) Least altered rocks, 12 in number from the “Target block” and the “Upper block” are plotted into the diagram by Winchester and Floyd (1977). The sample identifications (ID) of the 12 least altered samples used in the diagram are NAL RCO 74411, NAL RCO 74410, NAL RCO 74368, NAL RCO 194737, NAL RCO

194733, NAL RCO 194729, NAL RDC 330592, NAL RDC 330589, NAL RDC 197542, NAL RDC 74959, NAL RDC 75058, NAL RDC 75053. The interested reader can find the data in appendix b. The rocks are mostly basalt and two samples (194729 and 74959) are basaltic andesites. (b) The primary rock type of altered rocks from the "Target block" and the "Upper block is determined by the use of a diagram based on two immobile element ratios (Pearce 1996). The geochemical data used in (a) and (b) can be found in appendix b.

The geochemical data was plotted in a standard rock classification diagram (Winchester and Floyd 1977; Fig. 7a). Most of the least altered amphibolites and dolerites from Nalunaq yield a basaltic composition with only two samples having a basaltic-andesitic composition (Fig. 7a).

## **Geochemical rock definition of altered amphibolites and dolerites**

In order to assess the primary rocks types of the altered samples a rock classification diagram involving two immobile element ratios was used. Plots of one immobile-element ratio versus another removes mass change effects caused by hydrothermal alteration because the immobile element ratio of an altered rock is identical with the immobile element ratio of the precursor rock (Finlow-Bates and Stumpfl 1981; MacLean and Barrett 1993). Therefore it is possible to use rock classification diagrams which are based on immobile element ratios also for altered rocks.

All altered samples yield basaltic composition in the rock classification diagram by Pearce (1996); (Figure 7b). Only one sample straddles the boundary of the basalt and basaltic andesite fields (Fig. 7b). Only a few samples fall in the fields of alkali basalt or foidite (Fig. 7b). In summary, the majority of altered volcanic rocks fall in the basalt field and most of the samples from the "Target block" have similar primary geochemistry (Fig. 7b).

## **Refined chemical rock definition for altered/unaltered amphibolites and dolerites**

In order to refine the geochemical classification, we used immobile element ratios involving  $Zr/TiO_2$ ,  $Zr/Al_2O_3$  and  $Al_2O_3/TiO_2$  (MacLean and Barrett 1993). Such a refined classification allows to further group the samples with the aim to establish the chemostratigraphy. Table 1 reveals that seven chemical groups can be distinguished based on their distinct  $Zr/TiO_2$ ,  $Zr/Al_2O_3$  and  $Al_2O_3/TiO_2$  ratios.

**Table 1.** Characteristic immobile-element ratios are used to define the Nalunaq samples into seven chemical groups: basalt 1, basalt 2, basalt 3, basalt 4, basalt X, basaltic andesite 1 and basaltic andesite 2. The chemical rock types basalt 2, basalt 3 and basalt 4 have very similar ranges in their Zr/TiO<sub>2</sub>, Zr/Al<sub>2</sub>O<sub>3</sub> and Al<sub>2</sub>O<sub>3</sub>/TiO<sub>2</sub> ratios. Basalt X has distinctly different Zr/TiO<sub>2</sub> and Zr/Al<sub>2</sub>O<sub>3</sub> ratios. The Zr/Y ratio was used together with the REE pattern to assess the magmatic affinity, ratios <4 define a tholeiitic magmatic affinity, whereas ratios between 4 and 7 indicate a transitional (between tholeiitic and calc-alkaline) affinity; divisions from Barrett and MacLean (1994).

Chemical groups (only mafic rocks)		Zr/TiO <sub>2</sub>	Zr/ Al <sub>2</sub> O <sub>3</sub>	Al <sub>2</sub> O <sub>3</sub> /TiO <sub>2</sub>	Zr/Y	
<b>Basalt 1</b> n=116	<b>mean</b>	<b>65.7</b>	<b>4.3</b>	<b>15.4</b>	<b>3.2</b>	
	st. deviation	7.6	0.6	1.2	0.7	
<b>Basalt 2</b> n=87	<b>mean</b>	53.0	3.5	15.2	2.7	<b>very similar rocks</b>
	st. deviation	1.3	0.3	1.2	0.4	
<b>Basalt 3</b> n=208	<b>mean</b>	<b>45.5</b>	<b>3.0</b>	<b>15.1</b>	<b>2.8</b>	
	st. deviation	2.6	0.3	1.0	0.5	
<b>Basalt 4</b> n=20	<b>mean</b>	45.8	4.8	9.6	2.6	
	st. deviation	3.8	0.4	0.3	0.3	
<b>Basalt X</b> n=6	<b>mean</b>	27.4	1.7	16.4	1.4	
	st. deviation	4.1	0.3	1.1	0.2	
<b>Basaltic andesite 1</b> n=4	<b>mean</b>	106.8	6.7	16.1	4.1	
	st. deviation	3.7	0.7	1.8	0.2	
<b>Basaltic andesite 2</b> n=6	<b>mean</b>	161.8	9.9	16.3	5.5	
	st. deviation	12.1	0.5	1.1	1.9	

The samples are classified into basalt 1, basalt 2, basalt 3, basalt 4, basalt X, basaltic andesite 1 and basaltic andesite 2 (Table 1). It can be seen from table 1 that the basalt 2, the basalt 3 and the basalt 4 have similar geochemical characteristics. The criteria which were used to classify each sample into one of these chemical groups allow classifying any given sample from the Nalunaq area into one of the seven chemical rock groups (Table 1). Generally, chemical groups with low values in their immobile element ratios are basalts, whereas the basaltic andesites show slightly higher values in their immobile element ratios (Table 1).

The chemical basalt 1, basalt 2, basalt 3 and basalt 4 fields are located in the same part of the scatter plot (Figure 8a).

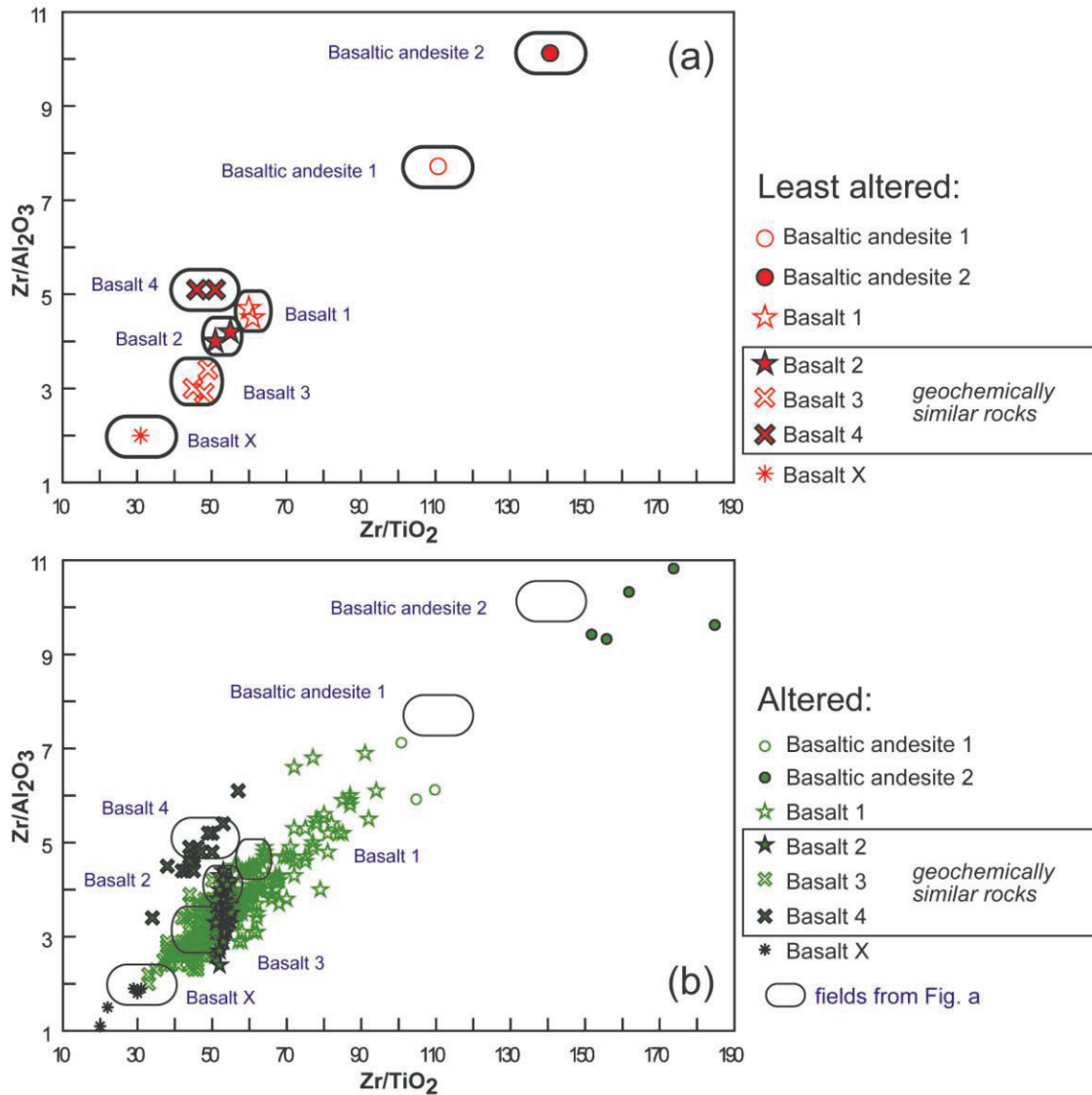


**Figure 8.** Immobible element ratio-ratio plots for Nalunaq samples. (a) Least altered rocks from Nalunaq. The  $Zr/TiO_2$  versus  $Zr/Al_2O_3/TiO_2$  diagram shows that rock types can be classified into seven groups based on immobile element ratios. The chemical rock types are basalt 1, basalt 2, basalt 3, basalt 4, basalt X, basaltic andesite 1 and basaltic andesite 2 (divisions from Barrett and MacLean 1994). (b) The  $Zr/TiO_2$  versus  $Zr/Al_2O_3$  diagram for altered rocks from Nalunaq. Fields from the least altered rocks (see diagram a) are superimposed (divisions from Barrett and MacLean 1994). Appendix a and appendix b provide the geochemical data of the rocks shown in (a, b and c) and lists the chemical rock type for each rock.

Hence these chemical rock groups have a similar immobile element geochemistry. However basalt 1, basalt 2, basalt 3 and basalt 4 can be distinguished from their different Zr/Al<sub>2</sub>O<sub>3</sub> ratios (Table 1, Fig. 8a). In figure 8b, the altered samples from Nalunaq are plotted and most of the chemical groups form fairly tight clusters. However some chemical groups fall into well defined fields in the immobile element ratio-ratio plot (Fig. 8b), whereas other chemical groups show less clustering. For example, basalt 1 rocks define a rather large field in the diagram, which is also seen from high standard deviation values for basalt 1 rocks (Table 1). In summary, the chemical grouping reveals that basalt X, and two varieties of basaltic andesite can be distinguished, whereas basalt 2, basalt 3 and basalt 4 show very similar characteristics in terms of their immobile elements. Samples from basalt 1 have the largest spread in their immobile element ratios. It will be shown in a later section that basalt X mainly occurs in the footwall of the Nalunaq stratigraphy and therefore can be used as a good geochemical marker.

### **Magmatic Affinity of the least altered amphibolites and dolerites**

The magmatic affinity was assessed by plotting the least altered samples in an AFM diagram, which involves the mobile oxides Na, K, Mg and Fe (Fig. 9a).

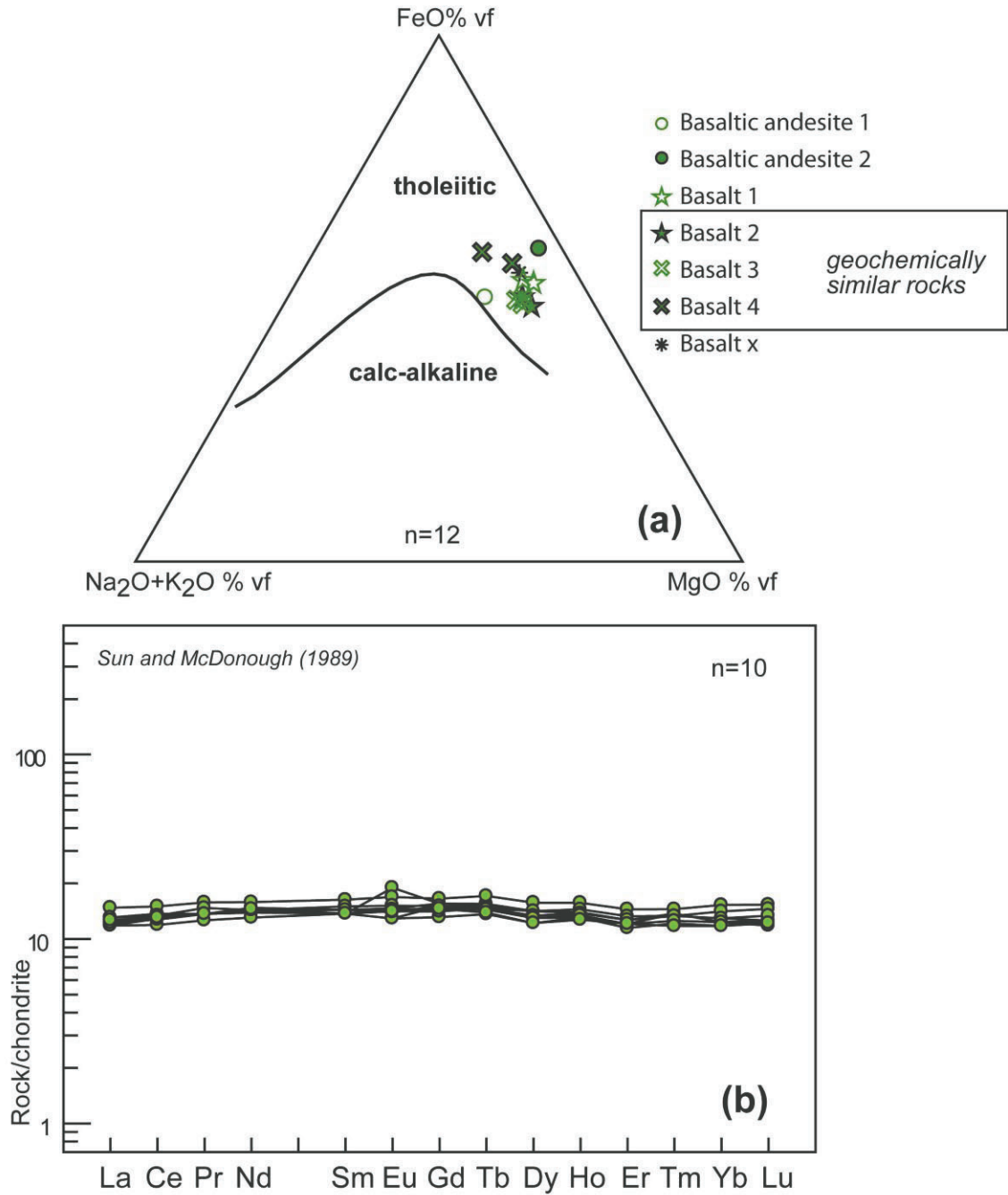


**Figure 9.** (a) Least altered Nalunaq rocks are plotted into the AFM diagram. All samples fall into the tholeiitic field. The data were normalized after loss on ignition (LOI); vf = volatile free basis. For details of calculation see Schlatter (2007). (b) Least altered and moderately altered samples: A chondrite-normalized plot shows that the pattern for basalt 1, basalt 2 and basalt 3 is flat from La to Lu, which is typical for rocks of tholeiitic magmatic affinity. Basalt 1, basalt 2 and basalt 3 show only minor differences with respect to their REE content. Samples in (b) are NAL RDC 330506, 330507, 330511, 330517, 330518, 330527, 330528, 330535, 330539 and 330540.

All samples have tholeiitic affinity except of one basaltic-andesite 1 sample, which straddles the boundary between the tholeiitic and the calc-alkaline field. Chondrite-normalized REE patterns are shown for least altered rocks of basalt 1, basalt 2 and basalt 3 compositions in figure 9b. All the samples have flat REE patterns, which is typical for a tholeiitic magmatic affinity (Fig. 9b). This is in agreement with earlier work, where it was shown that samples from the Nalunaq area have tholeiitic magmatic affinity (Petersen et al. 1997).

## Magmatic Affinity of the altered amphibolites and dolerites

In order to assess the magmatic affinity of the altered rocks, a discrimination diagram based on two immobile elements was applied. A plot involving Zr and Y reveals that most of the altered rocks are tholeiitic and only a few have a transitional magmatic affinity (Fig. 10). Rocks with transitional magmatic affinity are basaltic andesite 1, basalt 1 and a few basalt 3, whereas the basalt X has a distinct low Zr/Y ratio and is tholeiitic (Fig. 10; Table 1).

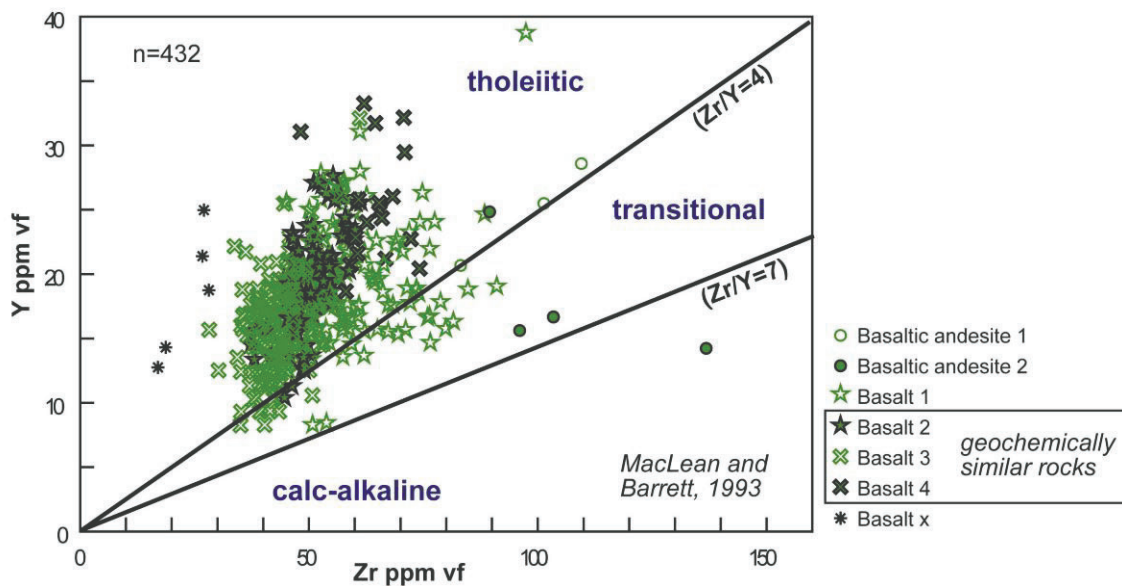


**Figure 10.** (a) The Zr-Y diagram reveals that most of the samples are tholeiitic and transitional. Only a few samples plot in the transitional field. The data set includes three scree sediment samples. These are the samples 74510 (Zr=50 ppm, Y=12.5 ppm); 74511 (Zr 72.1 ppm, Y=17.8 ppm) and 74509 (Zr=137 ppm, Y=14.1 ppm). Sample 74509 is an outlier, plots in the calc-alkaline field and this scree sediment certainly represents a mixture of mafic and felsic material. (Divisions from Barrett and MacLean 1994; vf = the data were normalized after loss on ignition on a volatile free basis).

## **Chemostratigraphy of the amphibolites and dolerites**

The stratigraphic column was described in an earlier section of this report (Fig. 6), where the lithological variation from the deep structural footwall to the hanging wall were discussed. Here we aim to establish the chemostratigraphy of a selected part of the stratigraphy comprising the amphibolite and dolerite units located above and below the Nalunaq ore horizon (Fig. 11).

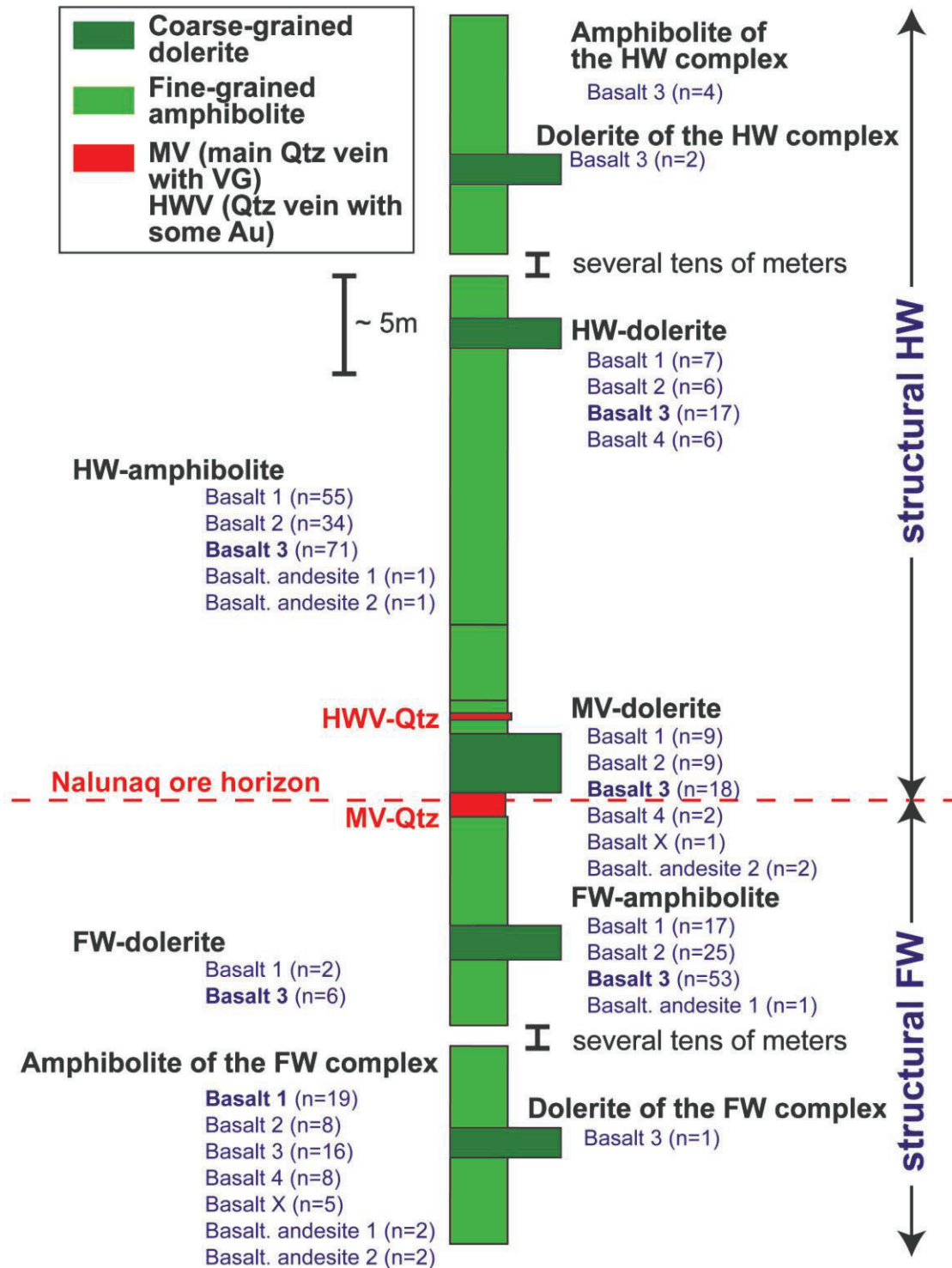


**Figure 11.** Chemostratigraphic relation seen from the stratigraphic column. The rock sequence comprises from the structural footwall (FW) to the structural hanging wall (HW): Amphibolite in FW complex, Dolerite in FW complex, FW amphibolite, FW-dolerite, MV-Qtz, MV-dolerite, HWV-Qtz, HW-amphibolite, HW-dolerite, dolerite in HW complex and amphibolite in HW complex. Pegmatites and effects of hydrothermal alteration as well as the sequence of silicified siltstone occurring in the structural footwall are removed from the stratigraphic column. The column consequently only shows the amphibolite-

lite and dolerite units, the MV and the HWV quartz. Rocks from each of the above units were classified according to their geochemical characteristics. It was not possible to identify an unique geochemical marker horizon however the distinct basalt X occurs only in the structural FW and the distinct basaltic andesite 1 and basaltic andesite 2 never occur in the upper part of the structural HW. Raw data can be found in appendix b.

The selected part of the stratigraphy comprises from footwall to hanging wall (Fig. 11): amphibolite of the FW complex, dolerite of the FW complex, FW-amphibolite, FW-dolerite, MV-Qtz, MV-dolerite, HWV-Qtz, HW-amphibolite, HW-dolerite, dolerite of the HW complex and amphibolite of the HW complex. We examine the geochemical characteristics of the stratigraphy (Fig. 11) by using the refined geochemical classification (Table 1) and define the chemostratigraphy:

*The amphibolite in the FW complex:* comprises basalt 1, basalt 3, basalt 2, basalt 4, basalt X, basaltic andesite 1 and basaltic andesite 2.

*The dolerite in the FW complex* consists of basalt 3.

*The FW-amphibolite* comprises basalt 1, basalt 2, basalt 3 and basaltic andesite 1.

*The FW-dolerite* comprises basalt 3 and basalt 1.

*The MV-dolerite* comprises basalt 1, basalt 2, basalt 3, basalt 4, basaltic andesite 2 and basalt X.

*The HW-amphibolite* comprises basalt 1, basalt 2, basalt 3, basaltic andesite 1 and basaltic andesite 2.

*The HW-dolerite* comprises basalt 1, basalt 2, basalt 3 and basalt 4.

*The dolerite in the HW complex* consists of basalt 3.

*The amphibolite in the HW complex* consists of basalt 3.

One unit – the dolerite of the FW complex - consists of one single geochemical rock type – basalt 3. The geochemical investigation also shows that basalt X only occurs in the FW complex and that all the dolerites comprise basalt 3. Although the amphibolites and the dolerites can be easily distinguished from drill cores and from surface mapping by their different grain size, they interestingly have very similar immobile element ratios. In summary, geochemical differences are not seen on the metre-scale, but differences can be seen from lower and upper part of the stratigraphy. For example the basalt 3 rocks are more abundant in the hanging wall than in the footwall. Amphibolite units of the footwall and of the hanging wall cannot be distinguished based on their immobile element ratios and possibly represent very similar basaltic flows. After the emplacement of this package, the rocks were intruded by mafic sills (MV-dolerite; FW-dolerite) and it is suggested that both rocks were derived from the same magma, since the geochemistry of the fine-grained amphibolite and the coarse-grained dolerite is very similar (Fig. 12).

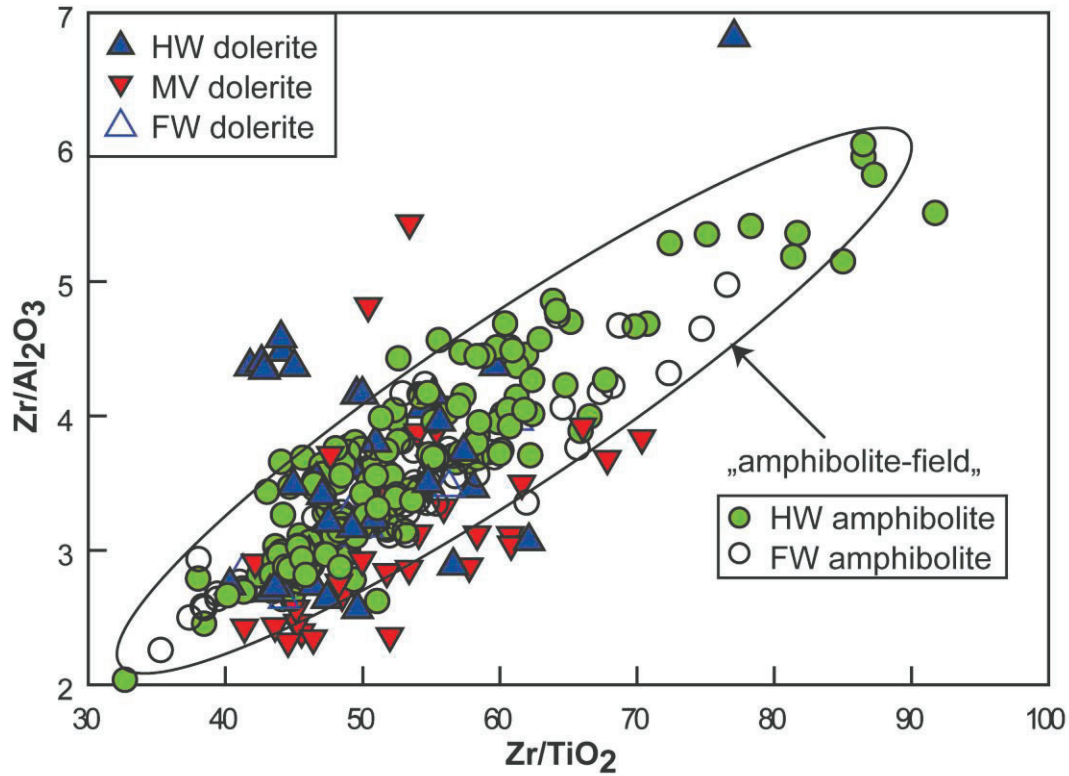


**Figure 12.** An immobile element ratio-ratio plot is used to characterize primary lithology. The amphibolite samples fall into an elongated field. While all samples from the FW-dolerite fall into this elongated field the HW-dolerite and the MV-dolerite fall inside and outside this field.

The HW-amphibolites and the FW amphibolites fall in the same field of the diagram (“amphibolite field”; Fig. 12), which means that they cannot be distinguished based on immobile element geochemistry. A few of the dolerite samples show different primary geochemical signatures and fall outside the “amphibolite field” (Fig. 12). These minor geochemical variations possibly indicate minor fractionation of the dolerites.

## Geochemical investigations of the felsic plutonic igneous rocks

The basement of the Nalunaq mountain consists of biotite granite of whitish colour, which can easily be distinguished from the dark mafic volcanic rocks which make up the upper parts of the Nalunaq mountain (Fig. 13).

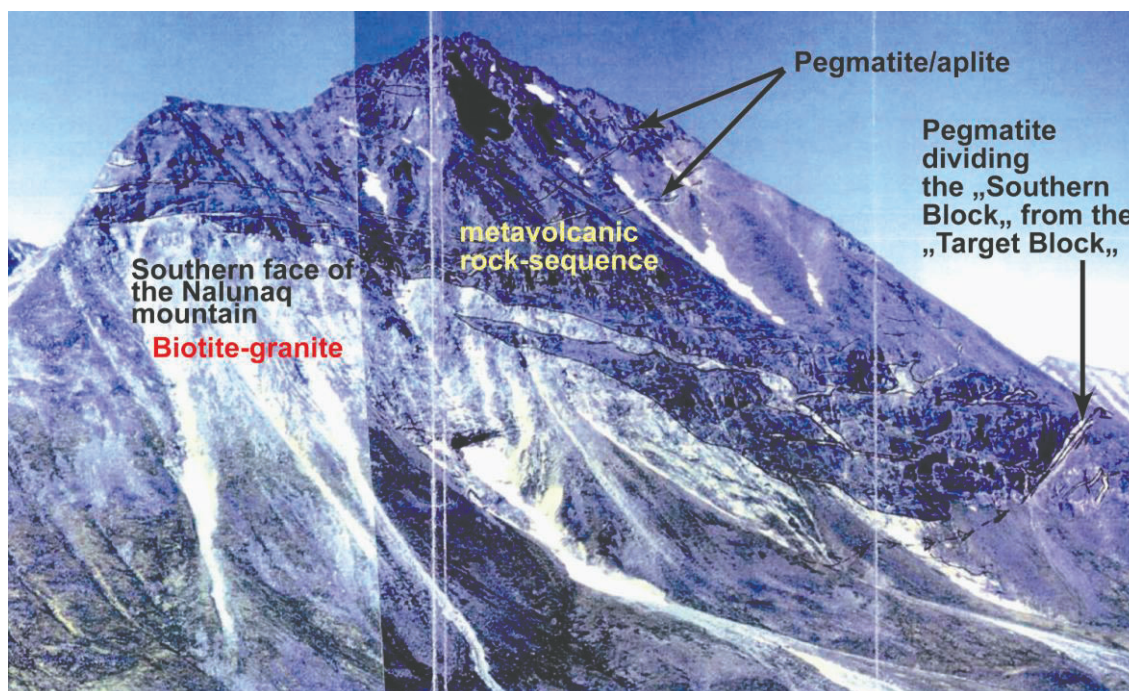


**Figure 13.** *Nalunaq southern face: a large body of granite under-roofs the volcanic rocks which are also intruded by several generations of aplite and pegmatite dykes. The picture also shows the location of the “Pegmatite fault”, which divides the “Target block” from the “Southern block”. (Picture and super-imposed sketches by Petersen, 1993).*

The intrusive contact of the biotite granite with the dark volcanic rocks and the inter-fingering of the biotite granite as narrow sheets into the volcanic rocks can be clearly seen from figures 4 and 13. The thrust fault which moved the “Southern block” relative to the “Target block” (Fig. 4) is intruded by pegmatite (Fig. 13). Yet a different felsic unit, best described as the silicified granite was encountered from surface drill hole NQ 33 (Fig. 4), and it is unclear from the drill core logging if they represent aplite, pegmatite or granite.

Here we show how we have used litho-geochemical methods to geochemically characterise the biotite granite, the pegmatite, the aplite and the silicified granite. The granite from the southern face and from the northern face plot into the same field and, therefore, probably represents a single intrusive body (Fig. 14).

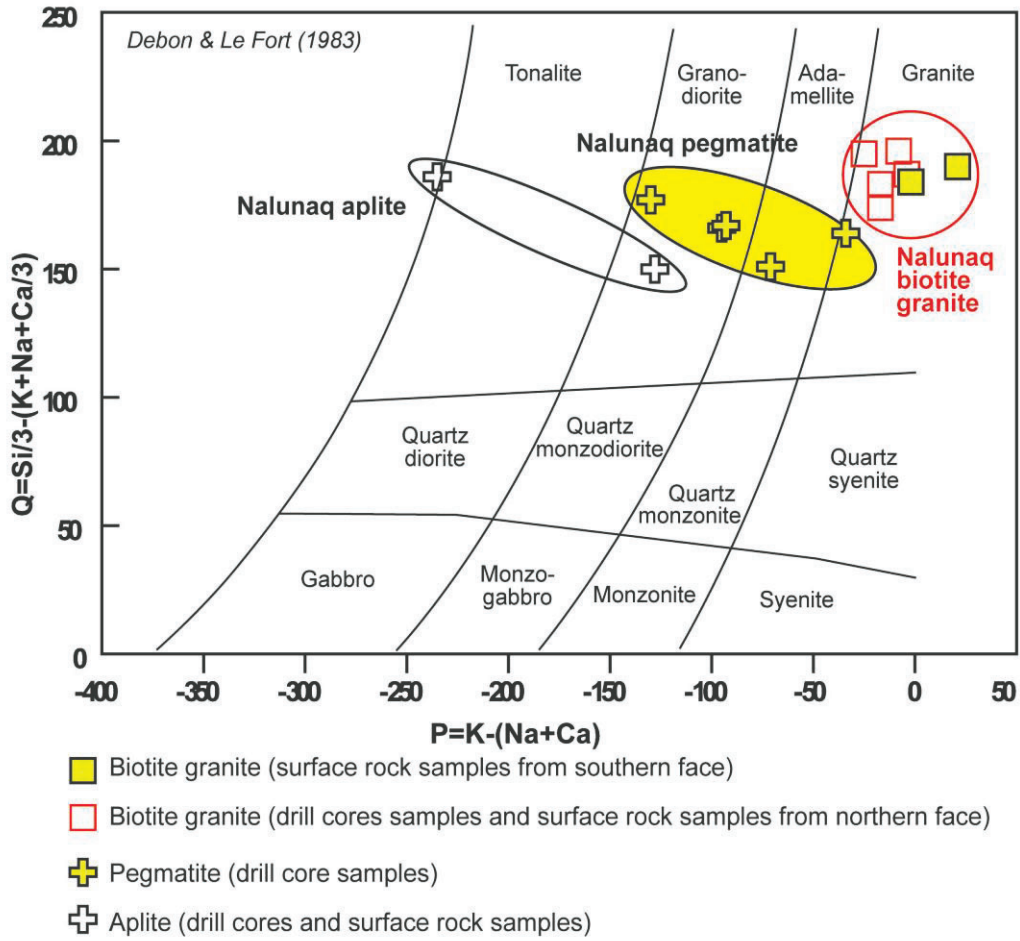
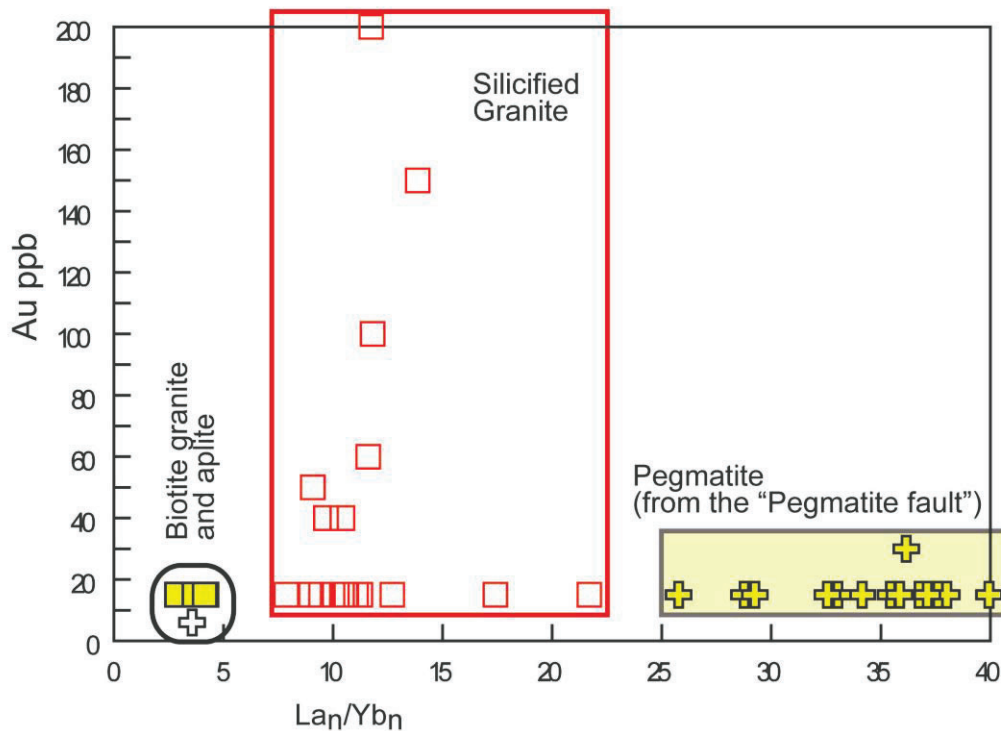


**Figure 14.** The igneous rocks are classified in the Debon & Le Fort (1983) diagram, where rocks are discriminated based on ratios involving major oxides. From the diagram it can be seen that rocks identified from grab samples as granite cluster tightly in the “granite field”. Samples identified as pegmatite and aplite show larger variation and plot into the fields of granite, adamellite, granodiorite, and one outlier is of tonalitic composition. The data can be found in appendix b.

The pegmatites plot in the granodiorite, the adamellite and the granite fields and the aplites plot either in the tonalite or the granodiorite fields (Fig. 14).

The biotite granite, aplite, silicified granite and pegmatite can also be distinguished by their different  $La_n/Yb_n$  ratios and gold contents (Fig. 15).



- Least altered biotite granite (drill core samples from the end of bore hole NQ 33)
- Silicified granite about 60 m thick, some samples with xenoliths of volcanic rocks (drill core samples from bore hole NQ 33)
- + Pegmatite, a few ten meters thick (drill core samples from bore hole NQ 31)
- ⊕ Aplite (surface rock sample from the structural footwall)

**Figure 15.** The igneous rocks are plotted in a diagram involving the  $La/Yb$  ratio and the gold content. The only samples containing elevated gold are from the silicified granite.  $La/Yb$  ratios indicate the slope of the REE pattern and in turn provides an idea about the affinity of the rocks. The granite samples have  $La/Yb$  ratios between 3 and 5, the silicified granite samples have  $La/Yb$  ratios between 7 and 22 and the pegmatite samples have  $La/Yb$  ratios between 25 and 40. The suggested extent of the silicified granite is shown in figure 4. REE data were normalized to the chondrite values of Sun and McDonald (1989). (Details of the samples used can be found in appendix e).

All the samples from the pegmatites of the “pegmatite fault” fall into a distinct field whereas the samples from the silicified granite fall into another field (Fig. 15). The biotite granite and the aplite samples have low  $La_n/Yb_n$  ratios and fall into a third distinct field (Fig. 15). The only samples containing elevated gold are the silicified granite (Fig. 15). Five samples yielded gold  $\geq 50$  ppb and one of these samples contained 200 ppb gold. The gold enrichment is likely the result of hydrothermal alteration involving fluids anomalous in gold. The silicified granite can also be distinguished from the biotite granite by their different REE patterns (Fig. 16).

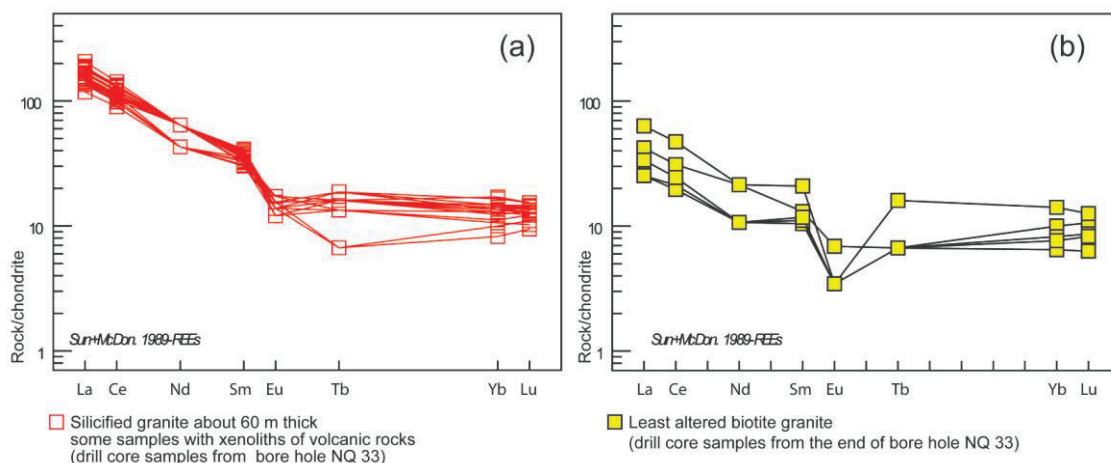


**Figure 16.** Magmatic affinity for selected igneous rocks. (a) Silicified granites are plotted on a chondrite-normalised plot, showing a relatively steep pattern from La to Lu which is typical for rocks of calc-alkaline magmatic affinity. (b) The least altered biotite granites show a flatter REE pattern than seen from the silicified granite; and also display a pronounced Eu-anomaly. (a and b) REE data were normalized to the chondrite values of Sun and McDonald (1989). Please note that several REE data were originally not included in the analytical package. (Details of the samples used can be found in appendix e).

The silicified granite may represent a small igneous body, such as for example a stock. However it is not possible to attribute a size to this suggested stock or tackle the time relation between the biotite granited and the silicified granite because the silicified granite was only encountered in one drill hole (Fig. 4).

## **The Nalunaq gold deposit**

Kaltoft et al. 2000 suggested that the Nalunaq gold deposit is a shear zone hosted orogenic gold deposit. The authors have classified Nalunaq in this deposit class because the Nalunaq deposit shows several characteristics which are typical for orogenic gold deposits such as, e.g., hydrothermal alteration minerals that are associated with the gold mineralisation. The hydrothermal alteration minerals diopside, Ca-rich amphibole and Ca-rich plagioclase are typically associated with hypozonal orogenic gold deposits elsewhere (Eilu and Groves 2001; Groves et al. 2003).

Furthermore fluid inclusion studies and arsenopyrite thermometry by Kaltoft et al. 2000 reveal that the conditions of formation were about 580°C and 3 kbar. This is in agreement with the regional metamorphic grade and the hydrothermal alteration assemblage. In summary, the mineral assemblage, fluid inclusion studies and results of arsenopyrite thermometry suggest that the deposit was formed at high temperature and about 10 km crustal depth by using a geothermal gradient (Best 1982).

### **Physical hydrothermal alteration associated with gold mineralisation**

The most abundant hydrothermal alteration minerals are quartz, biotite, diopside, Ca-rich amphibole, Ca-rich plagioclase, carbonates, muscovite, epidote, scheelite, chlorite, tourmaline and sphene (Kaltoft et al. 2000; Grammatikopoulos and Kristic 1999). The ore minerals are gold, maldonite, löllingite, arsenopyrite, pyrrhotite, pyrite, chalcopyrite and Bisulphosalts (Kaltoft et al. 2000).

The most *proximal* part of the hydrothermal alteration system is the auriferous quartz vein (MV); 17a).

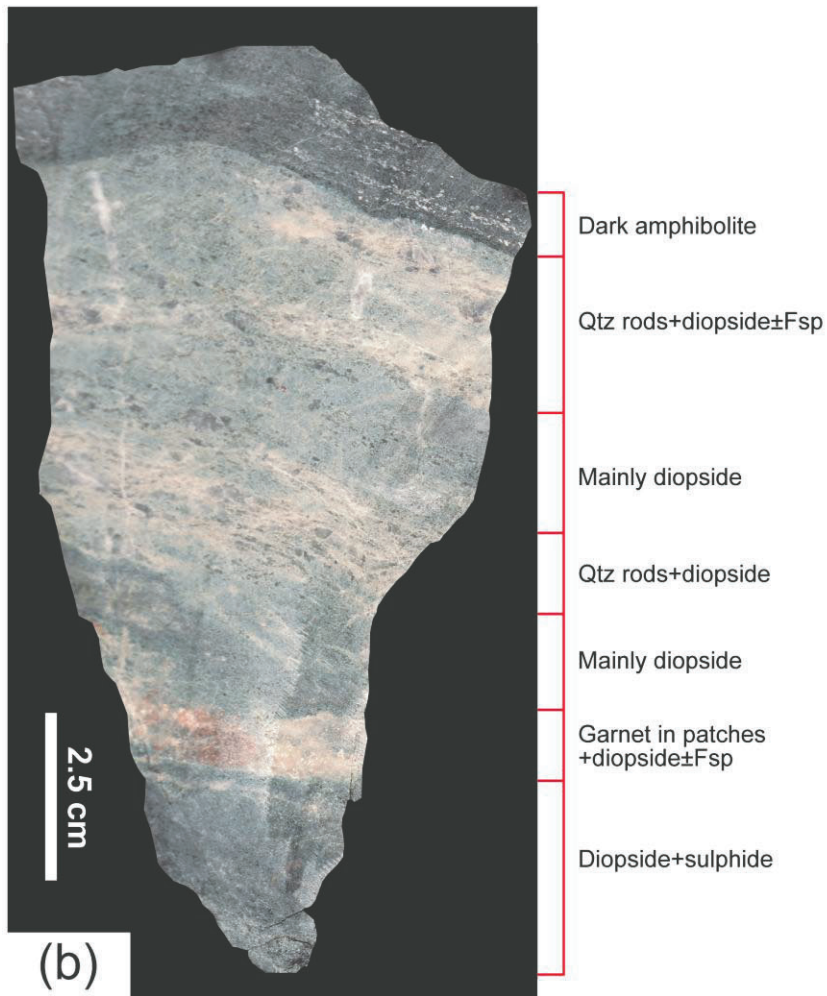
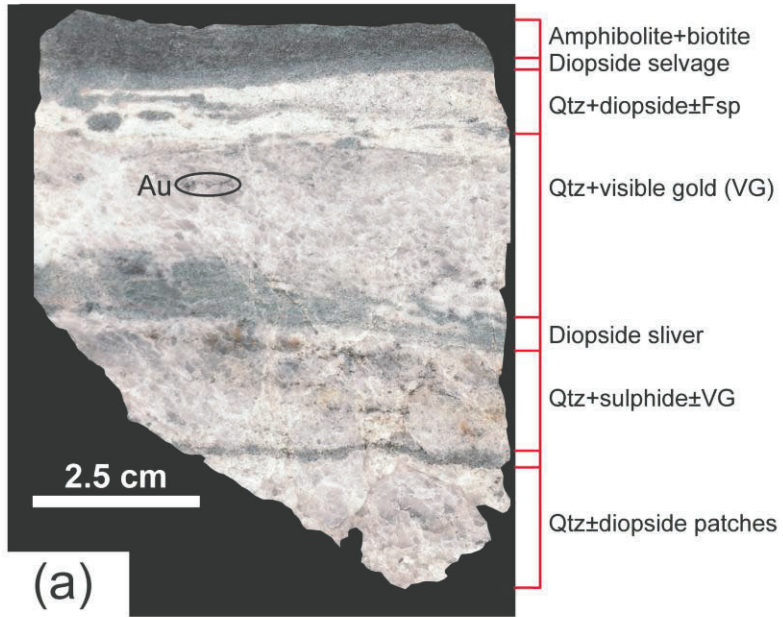


**Figure 17.** Photographs of two rock samples from the Nalunaq rock library. (a) Sample 477097 from the 450 m level of the target block at 458.75 m altitude, showing a quartz vein with calc-silicate altered

*selvages (mostly diopside). Zones of lighter parts are quartz veinlets and the darker and green parts represent diopside slivers. An area with abundant gold grains is indicated. (b) Sample 477117 is a calc-silicate altered volcanic rock from a sub-level at 360.67 m altitude of the target block. The main hydrothermal alteration minerals are pale green diopside and red-brownish garnet. A few patches of sulphide are also present in the rock and Qtz rods are abundant in the entire rock sample. The calc silicate altered volcanic rock in (b) does not contain visible gold. Detailed rock description and the location of the samples 477097 and 477117 are provided in appendix I: (List of all the samples contained in the “Nalunaq rock library”).*

The *medial* hydrothermal alteration zone comprises biotite-altered bands of about 15 cm thickness containing sulphides. The *distal* hydrothermal alteration zone is about 1.5 m thick and is made up of calc-silicate and silica-altered amphibolite and dolerite rocks (Schlatter 1997). Host rocks of the MV and hydrothermally altered zones can be amphibolite or dolerite because of the cross cutting nature of the MV (Fig. 4).

These hydrothermal alteration zones occur symmetrically on both sides of the MV. The thickness of the hydrothermal alteration zones varies between several tens of centimetres and up to a few meters (Schlatter 1998).

Although the gold mineralisation is always associated with distal calc-silicate alteration (Fig. 17a) strongly calc-silicate altered amphibolites (Fig. 17b) also occur in non gold mineralized rocks. The rock shown in figure 17b e.g. is not associated with economic gold mineralisation. Similar alteration as shown in figure 17b also occurs in the footwall and in the hanging wall of the MV-Qtz and therefore is far away from the Nalunaq ore horizon. However, these hydrothermal alteration zones are not associated with economic gold mineralisation and likely were caused by fluids, which were not carrying gold. It will be shown in a later section of this report how lithogeochemical techniques have helped to separate the hydrothermal alteration systems carrying gold from the ones that are barren.

## “Nalunaq rock library”

The “Nalunaq rock library” comprises 186 rock samples and the library is representative since all parts of the Nalunaq mine were sampled and all major rock types occurring at Nalunaq are contained in the library (Fig. 18, table 2).

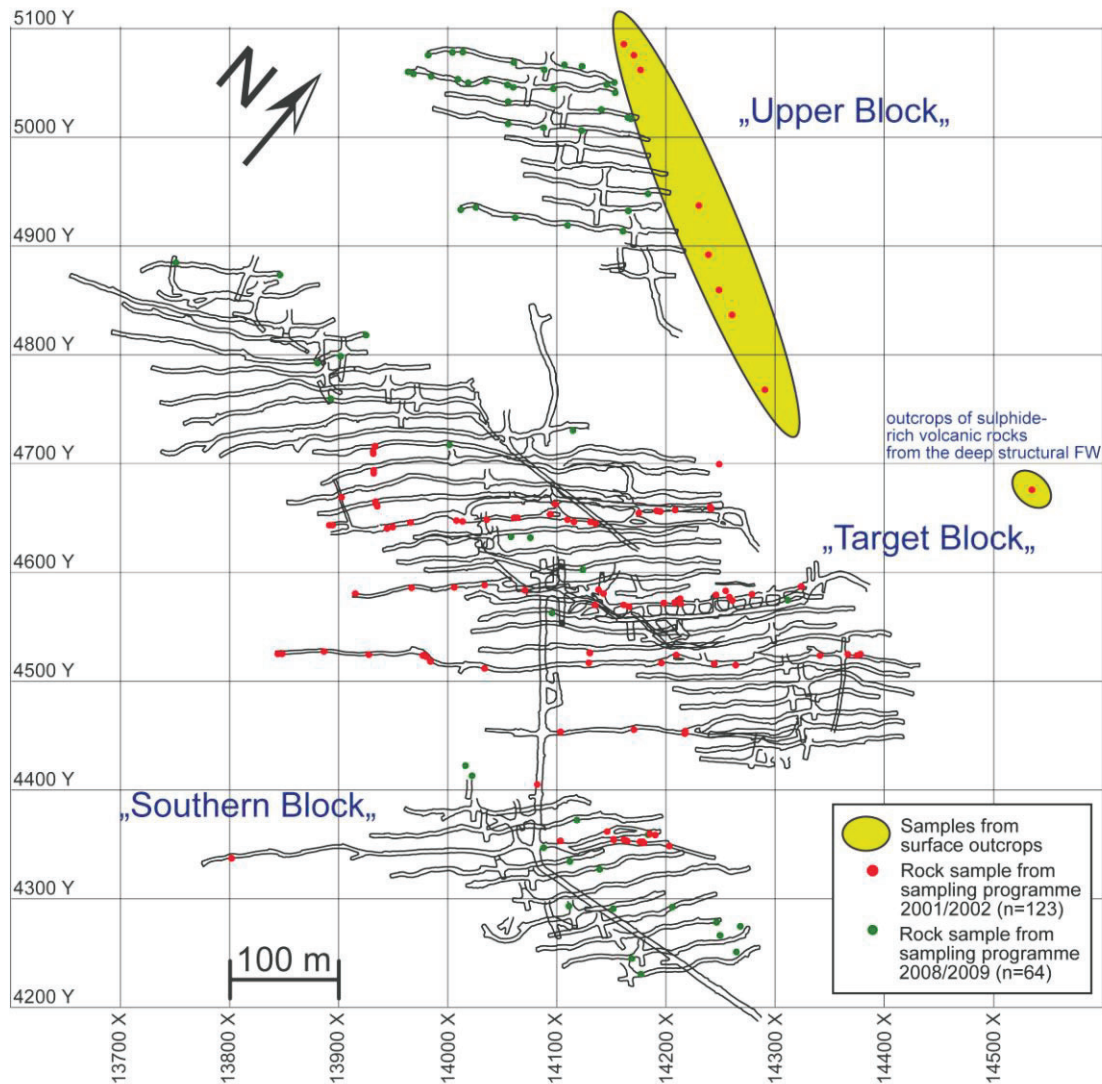


**Figure 18.** Underground development of the Nalunaq mine and locations of the 186 samples of the “Nalunaq rock library”. The map shows a longitudinal section where underground workings and sample locations and results of gold analyses are projected onto the main vein plan of the “Upper block”, the “Target block” and the “Southern block”. Strike direction of the main vein is NE-SW and the dip of the main vein is in average 35° SW degrees. It can be seen that the strike direction of the main vein is equal to the direction of the drives. However, small kinks of the drives were made in order to follow the main vein, which, in places, is offset by small late-stage dextral faults. Most of the samples of the “Nalunaq rock library” were collected from underground exposures, whereas a few samples were collected at an elevation between 526.5 m and 759.5 m from the outcropping main vein where surface exposures occur. The FW was sampled from outcrops at 398.5 m elevation. Details of the rock samples are provided in appendix I.

**Table 2.** Summary information of 186 samples contained in the “Nalunaq rock library”. More details of these samples (e.g. in which drawer that a given rock is stored, rock description or the coordinates of a given rock sample) are given in Appendix I (on the DVD).

**Nalunaq rock library (n=186)**

<b>Provenance of sample</b>	<b>Number of rock samples</b>
Rock sample from the "Upper block"	42
Rock sample from the "Target block"	113
Rock sample from the "Southern block"	31
<b>Sampling programme</b>	
Programme 2001/2002	122
Programme 2008/2009	64
<b>Rock type</b>	
Amphibolite	31
Aplite and pegmatite	17
Qtz vein and amphibolite wall rock; Qtz $\geq$ 90% of sample	56
Qtz vein and amphibolite wall rock; Qtz <90% of sample	82
<b>Rock sample type</b>	
Surface samples	14
Samples from underground exposures	172
<b>Samples with visible gold (VG)</b>	<b>54</b>
<b>Samples without visible gold (VG)</b>	<b>132</b>

Representative rocks, were sampled in 2001/2002 by Mogens Lind, Sven Monrad Jensen and Lars Lund Sørensen from underground exposures and at the surface on the eastern slope of the Nalunaq mountain. From this sampling programme 122 representative samples were sent to GEUS where the rocks were described and organized with the purpose to establish a reference sample collection (Table 2). Because after the original sampling in 2001/2002 a lot of progress was done on the mining, it has been suggested to carry out additional sampling and this was done during 2008/2009 by Mogens Lind. This sampling programme comprised samples from underground exposures of the MV structure and samples from granitic pegmatites. Overall 64 samples were collected in the 2008/2009 sampling programme (Table 2) and this programme covered those parts, which were not included in the earlier sampling programmes (see figure 18) and included also pegmatites associated with faults. Particularly samples from underground exposures of the “Upper block”, the NW extension of the “Target block” and from the “Southern block” were collected. The samples of the 2008/2009 sampling programme were received at GEUS at the end of 2010 and these additional samples are organized and amalgamated into the “Nalunaq rock library”.

Figure 18 shows the sample locations of all the 186 rock samples included in the “Nalunaq rock library”. Most of the rocks were sampled from underground exposures (n=172) and a few (n=14) were sampled at surface. The rocks of the sampling programmes 2001/2002 and 2008/2009 were shipped to GEUS located in the Geocenter in central Copenhagen. At GEUS, these rocks and additional six rocks from underground exposures collected by Lucy Porritt and Denis Schlatter in the summer of 2001 were incorporated into the “Nalunaq rock library”. Table 2 provides a summary of the samples that make up the “Nalunaq rock library” whereas appendix I provides relevant sample information such as e.g. geological rock description, sample location, information about previous analyses and how to find a given sample in the “Nalunaq rock library”. The “Nalunaq rock library” contains 31 samples from the “Southern block”, 113 samples from the “Target block” and 42 samples from the “Upper block” (Table 2). Finally, four samples were sampled from the strongly pyrite-enriched volcanic rocks occurring in the structural footwall (Figs. 5 and 6). In the “Nalunaq rock library”, 56 samples are from rocks with more than 90 % quartz material from the Nalunaq main vein, 82 samples comprise less than 90 % quartz material and 31 rocks are from calc-silicate and silica altered volcanic rocks which show variable hydrothermal alteration (Table 2, appendix I). 17 samples are from granitic pegmatite or aplite (Table 2). In summary, the “Nalunaq rock library” contains rocks from all the mining blocks and the rock-sampling was carried out in most areas of the mined deposit. Furthermore, all important rock types (amphibolite, dolerite, quartz veins) and the most typical hydrothermal alteration types (calc-silicate alteration, biotite alteration, sulphide impregnation) are represented. Moreover, samples with a wide variation of gold contents are represented, including 54 samples with visible gold. Twenty-one samples were analysed for major elements and selected trace elements and these samples are marked in bold green colour in appendix I. Detailed geochemical information is available from three samples from the “Southern block”, 17 samples from the “Target block” and one sample from the “Upper block”. Finally, it can be added that each rock sample weighs between a few hundred grams to up to a few kilograms (averaging about half a kilogram for each sample, for details see Appendix I). Consequently, a large enough portion of each sample is available to allow further geochemical analyses or other type of analyses. Such potential additional work certainly will help to better understand the formation of the high grade Nalunaq gold deposit and to better define future exploration efforts in the surroundings of Nalunaq or elsewhere in South Greenland.

## Compilation of geochemical Nalunaq data (gold, trace elements and major elements)

Extensive surface and underground exploration was carried out between 1993 and 2004 (Kaltoft et al. 2000; Porritt 2003; Lind et al. 2001). In the years 1993 to 2004, exploration efforts were focussed in achieving geological base line data for the scoping study, the pre-feasibility and bankable feasibility studies, and after the positive review of the bankable feasibility study and granting of the necessary government approvals, the Nalunaq gold mine was built and inaugurated on August 26, 2004 (Secher et al. 2008).

Typically, drilling from the surface was carried out ahead of the drifting of the adits and raises; in order to guide and facilitate the underground work. Drill cores and underground exposures were mainly sampled with the purpose to obtain information about the gold content of the rocks, i.e. grade control. Other elements than gold were only analysed for a relatively small portion of the samples.

The results from the gold analysis and geochemical analysis were provided by the exploration companies. All the gold analyses from surface samples, drill cores and underground work were initially well organised and stored in a 3D database. GEUS uses the geology and mine planning software "Gemcom Gems" which incorporates the data in a 3D working environment. Furthermore images and fully interactive 3D visuals can be exported for use in presentation software and on the Web. While all the gold analyses from surface samples, drill cores and underground work were initially well organised and stored in the Gemcom Gems database, the existing major element and trace element data from the surface samples, drill cores and underground works were only available in company reports. These reports were once a year sent by the exploration companies to the Greenlandic authority; the Bureau of Minerals and Petroleum (BMP) and The Geological Survey of Denmark and Greenland (GEUS). Many of these company reports contain interesting geochemical data, however in the Gemcom Gems database, initially, only the gold values were captured.

This report, documents how all available geochemical data have been gathered and how a comprehensive and complete geochemical database has been compiled by simply adding the geochemical data to the existing Gemcom Gems gold database. For example > 4500 samples were analysed for the trace elements As, Mo, Sb, Bi, W, Ag and the major oxide K<sub>2</sub>O and we have now added these data to the database.

### Samples with gold analysis - the "Nalunaq gold database"

Nalunaq samples were analysed from the early nineties to the end of 2003 by commercial laboratories, such as the XRAL laboratories in Toronto (now a division of SGS Canada). Since 2004, when the Nalunaq gold mine started commercial production, gold was analysed by the operating company Nalunaq Gold Mine A/S in their own on-site laboratory (Secher et al. 2008). Between 2004 and 2009 Nalunaq Gold Mine A/S reported the results to GEUS where the data were continuously compiled in the "Nalunaq gold database". The data of the "Nalunaq gold database" were then plotted in 3D by using the Gemcom Gems software. The "Nalunaq gold database" is maintained and updated by GEUS. In detail, the database contains all the past gold analyses from **surface drill cores** (Tables 3 and 4; Appendix 1), from **outcropping surface rocks** (Tables 3 and 4; Appendix 2), from **underground drill cores** (Tables 3 and 4; Appendix 3); from **underground grade-control samples from exploration adits and raises** (Table 3; Appendix 4), from **underground samples from development workings** (Tables 3 and 4; Appendix 5) and a few **underground samples** which are not from the MV structure (Tables 3 and 4; Appendix 6). The underground samples listed in the appendices 5 and 6 were collected in connection with development workings in the mine for grade verification purposes and were analysed only for gold.

The "Nalunaq gold database" contains in total about 16,000 samples (Table 3); about half of the samples are from surface or from surface boreholes and the other half are from underground exposures.

**Table 3.** *Summary of the samples analysed for gold. Almost 16000 samples were analysed for gold and >7000 of these samples are from drill cores.*

**Gold database**

<b>Type of sample</b>	<b>Number of rocks with gold assays</b>
Drill core samples from surface drillholes	7164
Surface rock samples	458
Drill core samples from underground drillholes	723
Underground exploration rock samples	2041
Underground development rock samples	5478
Miscellaneous samples (not MV samples)	104
<b>SUM</b>	<b>15968</b>

**Table 4.** Details of the gold database structure. The data can be found in the appendices 1 to 6 on the DVD.

Appendix No (and file ID)	Worksheet name	Description	n=	Comments
<b>Appendix 1</b> (App_1_surface_drillholes.xlsx)  <i>(highest Au value=3777 ppm)</i>	ASSAYS	<b>Samples from surface drill holes</b>		
	HEADER	<b>Au assay results of drill cores</b>	<b>7164</b>	Gold assay of drill cores
	LITHOLOGY	Coordinates	<b>173</b>	Coordinates of NQ 1 to NQ 172
	MAIN_VEIN	Lithology	<b>8000</b>	Logs of cores including rock type and alteration description of each section
	SURVEYS	MV interval	<b>139</b>	Au content of MV intersection
	THICKNESS	Surveys	<b>791</b>	Survey of of drill holes including Azimuth and dip measurements
			<b>352</b>	True thickness of intersected lithologies
<b>Appendix 2</b> (App_2_surface_samples.xlsx)  <i>(highest Au value=2935.8 ppm)</i>	ASSAYS	<b>Samples from outcropping surface</b>		
	HEADER	<b>Au assays</b>	<b>458</b>	Samples from outcropping MV
	SURVEYS	Coordinates	<b>458</b>	Coordinates of samples, sampling method and sampling date
			<b>458</b>	Azimuth, dip and sample length
<b>Appendix 3</b> (App_3_underground_drillholes.xlsx)  <i>(highest Au value=476.9 ppm)</i>	ASSAYS	<b>Underground drill holes</b>		
	GEOLOGY	<b>Au assay</b>	<b>723</b>	Samples and Au assay
	HEADER	Geology	<b>9</b>	From and To, rocktype and rockcode
	MAIN_VEIN	Coordinates	<b>237</b>	Coordinates, length, ore block, azimuth, dip and drill year
	SURVEYS	MainVein	<b>64</b>	From and To, gold grade, length and elevation of samples from MV intersection
			<b>237</b>	Azimuth, dip and sample length
<b>Appendix 4</b> (App_4_underground_samples.xlsx)  <i>(highest Au value=2831 ppm)</i>	ASSAYS	<b>Underground samples (from adit and raises)</b>		
	HEADER	<b>Au assay</b>	<b>2041</b>	Hole-ID (smpl treatet as a drill hole), from-to, smpl ID lab report, rock type, code
	SURVEYS	Coordinates	<b>2041</b>	Coordinates, sample length, solid (code), method and sampling year
			<b>2041</b>	Sampling length, azimuth and dip
<b>Appendix 5</b> (App_5_Underground_development_samples.xlsx)  <i>(highest Au value=2233.8 ppm)</i>	ASSAYS	<b>Underground samples from development</b>		
	HEADER	<b>Au assay</b>	<b>5478</b>	Hole-ID (sample treated as a drill hole), from-to
	SURVEYS	Coordinates	<b>5480</b>	Coordinates, sample length, sub-level, sample wall, solid nr. sampling date
			<b>5476</b>	Sample length, azimuth and dip
<b>Appendix 6</b> (App_6_underground_miscellaneous_samples.xlsx)  <i>(highest Au value=1673.3 ppm)</i>	ASSAYS	<b>Underground samples not belonging to MV</b>		
	HEADER	<b>Au assay</b>	<b>104</b>	Hole-ID (sample treated as a drill hole), from-to
	SURVEYS	Coordinates	<b>106</b>	Coordinates, sample length, sub-level, sample wall, solid (code), sampling date
			<b>101</b>	Sample length, azimuth and dip

### Samples with geochemical analyses - the “Nalunaq geochemical database”

We present in the form of EXCEL spreadsheets a compiled database containing the geochemical data, XYZ locations and geological information of more than 4700 samples (Table 5). About 4500 of these samples were collected from or near the Nalunaq ore body and about 200 samples were collected regionally on the Nanortalik peninsula. 2902 samples are drill core samples and 1832 samples were collected from surface outcrops, from underground exposures, or from scree sediments. Table 6 finally gives a summary of the data that are included in the “Nalunaq geochemical database” and provides a key where to find the relevant data in the appendices. From table 6 it can also be seen that different sample types were analysed by different geochemical methods of analysis. For example drill core samples were analysed for a variety of elements, but large bulk samples were only analysed for trace elements and gold (Dumka and Thalenhorst 2001, Lind et al. 2001).

In summary, the “Nalunaq geochemical database” provides newly compiled data in an organised manner. Furthermore it is the plan to add these analyses into the central GEUS database (Tukiainen and Christensen 2001).

**Table 5.** *Summary of the samples analysed for major oxides and trace elements. More than 4700 samples were analysed with various analytical methods and for a number of different elements. Most of the samples that were analysed are drill core samples.*

#### Geochemical database

Type of sample	number of Nalunaq rocks
Drill core samples from surface drillholes	2902
Surface rock samples	531
Samples from underground	994
Sediment samples from around the Nalunaq mountain	114

Type of sample	number of regional rocks <sup>*1</sup>
Surface rock samples	193
<b>SUM</b>	<b>4734</b>

\*1= from regional sampling from the Nanortalik peninsula

**Table 6.** Details of the structure of the database containing the geochemical data. The data can be found in the appendices a to k on the DVD. The samples are mainly from the Nalunag area (appendices a to i). Fewer samples were analysed from the northern and southern part of the Nanortalik peninsula and from an area west of Nalunag (appendix j and k). Abbreviations used are MV=main vein; INAA= instrumental neutron activation analysis; GSC=Geological Survey of Canada; REE=rare earth elements; WR=whole rock lithochemical analysis.

Appendix No (and file ID)	Description	number of data	Comments
<b>Appendix a</b> (App_a_samples_with_trace_elements_and_K2O.xlsx)	<b>Samples with trace elements<sup>*1</sup> and K<sub>2</sub>O<sup>*2</sup>; (and gold)</b>	n= 4520	about 1/3 of samples include K <sub>2</sub> O
	drill cores		<b>2902</b> NQ 2 to NQ 89 (from 88 BBH)
	surface rocks		<b>435</b> some with additional trace elements
	surface rocks from MV		<b>96</b> trace elements but no K <sub>2</sub> O, 18 rocks from NE face
	scree sediments		<b>114</b>
	rocks from mine		<b>582</b> from 400m adit (1998)
	50 to 60 t bulk samples from mine		<b>391</b> from grade verification program, Strathcona 2001
<b>Appendix b</b> (App_b_samples_with_extended_geochemical_data.xlsx)	<b>Samples with extended geochemical data<sup>*3</sup> (and gold)</b>	n=510	<b>For source of data see appendices and text</b>
	drill cores		<b>374</b> NQ 2 to NQ 72 (from 18 BBH)
	surface rocks		<b>110</b> rocks from profiles and spot samples
	scree sediments		<b>3</b>
	rocks from mine		<b>23</b> rocks are in rock library stored at GEUS
<b>Appendix c</b> (App_c_samples_with_sulphur.xlsx)	<b>Samples with sulphur analyzes (and gold)</b>	n=75	
	drill cores		<b>43</b>
	surface rocks		<b>6</b>
	100 kg bulk samples from surface		<b>5</b>
	rocks from mine		<b>21</b>
<b>Appendix d</b> (App_d_samples_with_CO2.xlsx)	<b>Samples with CO<sub>2</sub> analyzes (and gold)</b>	n=36	drill core samples
	drill cores		<b>36</b>
<b>Appendix e</b> (App_e_samples_with_neutron_activation.xlsx)	<b>Samples with NA analyzes (and gold)</b>	n=196	
	drill cores		<b>101</b> from drill holes NQ 31 and NQ 33
	surface rocks		<b>19</b> from profiles 6 and 7
	scree sediment samples		<b>76</b> from Nalunag Mt; at hardrock-scree interface
			from key drill holes NQ 17, 18, 19; analyzed by GSC
<b>Appendix f</b> (App_f_samples_with_high_quality_GSC_GEUS_analyses.xlsx)	<b>Samples with high quality GSC analyzes REE analyzes</b>	n=13	
	drill cores		<b>13</b>
<b>Appendix g</b> (App_g_samples_with_Pt_and_Pd.xlsx)	<b>Samples with PGE (Pt and Pd) analyzes</b>	n=151	from surface
	surface rocks		<b>109</b>
	drill cores		<b>42</b>
<b>Appendix h</b> (App_h_samples_from_rock_library.xlsx)	<b>Rock library contains 186 rocks and 21 are analyzed</b>	n=21	21 with WR analyzes
	rocks from mine		<b>21</b>
<b>Appendix i</b> (App_i_samples_Kirkespiret_GEUS_Green.xlsx)	<b>Kirkespiret area (GEUS Green); (and gold)</b>	n=95	WR and/or traces
<b>Appendix j</b> (App_j_regional_samples.xlsx)	<b>Regional WR major elements from Nanortalik peninsula<sup>*4</sup></b>	n=98	
	surface rocks from Kirkespiret area		<b>67</b> coordinates and sample description missing
	surface rocks from L410 area		<b>14</b> coordinates and sample description missing
	surface rocks from Ippalit area		<b>10</b> coordinates and sample description missing
	surface rocks from Ufo Mt. area		<b>4</b> coordinates and sample description missing
	surface rocks from Amphibolite ridge		<b>3</b> coordinates and sample description missing
<b>Appendix k</b> (App_k_regional_samples.xlsx)	<b>Regional WR major and trace element Data from Lake 410</b>	n=79	
	surface rocks from L410 area		<b>79</b> ICP trace elements
			<b>18</b> including WR major elements

\*1= Six trace elements are analyzed by ICP (a few samples were also analyzed for additional trace elements)

\*2= A few samples with additional trace elements are listed in a separate spreadsheet

\*3= 11 major elements and three trace elements were analyzed by XRF (a few samples were also analyzed for additional trace elements); 32 trace elements were analyzed by ICP

\*4= Data from Jon S. Petersen, (1993), reported in GEUS file no 21357

\*5= Data from NunaOil report, (1996), reported in GEUS file no 21517

# Gold distribution and identification of the pathfinder elements for gold on the deposit scale

## Distribution of gold in the main vein

The Nalunaq gold deposit is divided into three domains (Fig. 4): these are from north-west to south-east “Upper block”, the “Target block” and the “Southern block”. With respect to the geochemical interpretation it is important to treat the data separately for each of these three domains because the post-ore movements of each of the blocks relative to the other ones are not known and therefore each domain represents a separated entity. Figure 19 shows the distribution of gold from samples of the “Target block”.

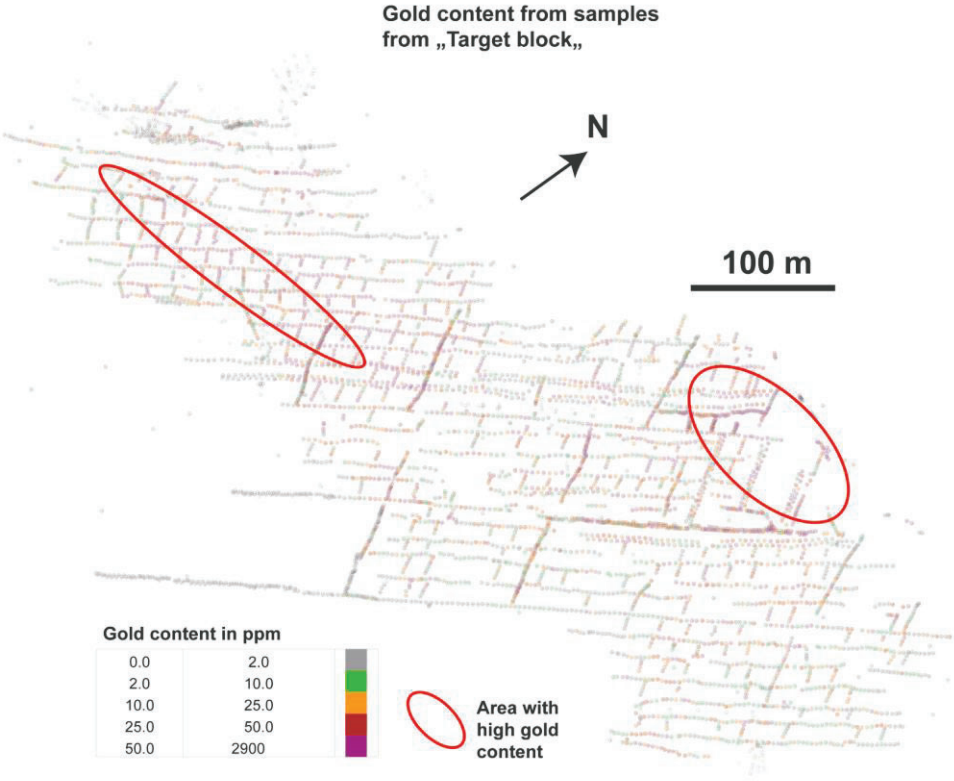


**Figure 19.** Gold distribution on the main vein plan shown on a longitudinal section. The gold contents were plotted in this longitudinal section by using the Gemcom Gems software. Samples with high gold content are displayed in purple and pink colours; samples with gold contents below 2 ppm are in grey colour. Only samples from the “Target block” are shown and the areas with highest gold contents are hand contoured. Data used to construct the diagram can be found in the appendices 1 to 5.

The distribution of gold on the main vein surface is best shown from samples from the “Target block” (Fig. 19) because it represents the area that is most extensively sampled from exploration adits (sampled along strike), mine drives (sampled along strike) and raises (sampled in up dip direction). From the gold-distribution map it can be seen that the areas with the highest gold contents are roughly E-W oriented panels (Fig. 19). The areas with the highest gold contents are located in the upper parts of the “Target block”.

## Relationship between gold and the trace elements Ag, As, Sb, Bi, W and Mo

Background values from unmineralised rocks from the Earth’s crust are a few ppm for the elements As, Sb, Bi, W and Mo and less than one ppm for Ag (Rose et al. 1979). Consequently, rocks which yield higher contents than the background values of As, Sb, Bi, W and Mo and Ag were likely exposed to metasomatic hydrothermal processes, which added these elements. A relationship between gold and trace elements such as Ag, As, Bi, Sb, Te and W has been shown from other studies (Eilu and Mikucki 1998; Eilu et al. 2001). Other investigations have shown that pathfinder elements can define a vector to the gold (Eilu and Groves 2001).

From the Nalunaq gold deposit, it was shown that samples proximal to the main vein are enriched in As, Sb, Bi, W and Ag (Schlatter 1997; Kludt and Schlatter 2000; Porritt 2000). Dumka and Thalenhorst (2001) observed, based on analysed bulk samples from adits, some correlation between Au and As and Au and Zn.

We investigate here, based on >4000 samples, if the elements Ag, As, Sb, Bi, W and Mo show correlation with gold and, in a next step, we try to define a vector to the ore.

In order to identify elements which are associated with gold, we have calculated correlation coefficients between gold and a number of potential pathfinder elements (Table 7).

**Table 7.** Correlation coefficients between gold and pathfinder elements Ag, As, Sb, Bi, W and Mo. The  $r^2$  and Spearman rank correlation coefficients were calculated by using the chemical data from 391 bulk samples, 582 samples from underground exposure, 182 surface rock samples and 2902 drill core samples.

Correlation of Au and trace element	Ag	As	Sb	Bi	W	Mo
$r^2$ (square of the correlation coefficient)	0.820	0.010	0.005	0.060	0.004	0.000
Spearman rank corr. coef.	0.680	0.641	0.449	0.525	0.582	0.097

The best correlations between gold and pathfinders are seen for Ag, As, Sb, Bi and W (Table 7). Ag and gold show high correlation coefficients and the elements As, Sb, Bi and W yield moderate correlation coefficients for the Spearman rank correlation coefficient (Table 7). Mo is not associated with gold (Table 7).

## Gold-silver association

The gold-silver association is shown in figure 20 and reveals moderate correlation between Au and Ag. The gold content of Nalunaq samples is about ten times higher than the silver content (Fig. 20).

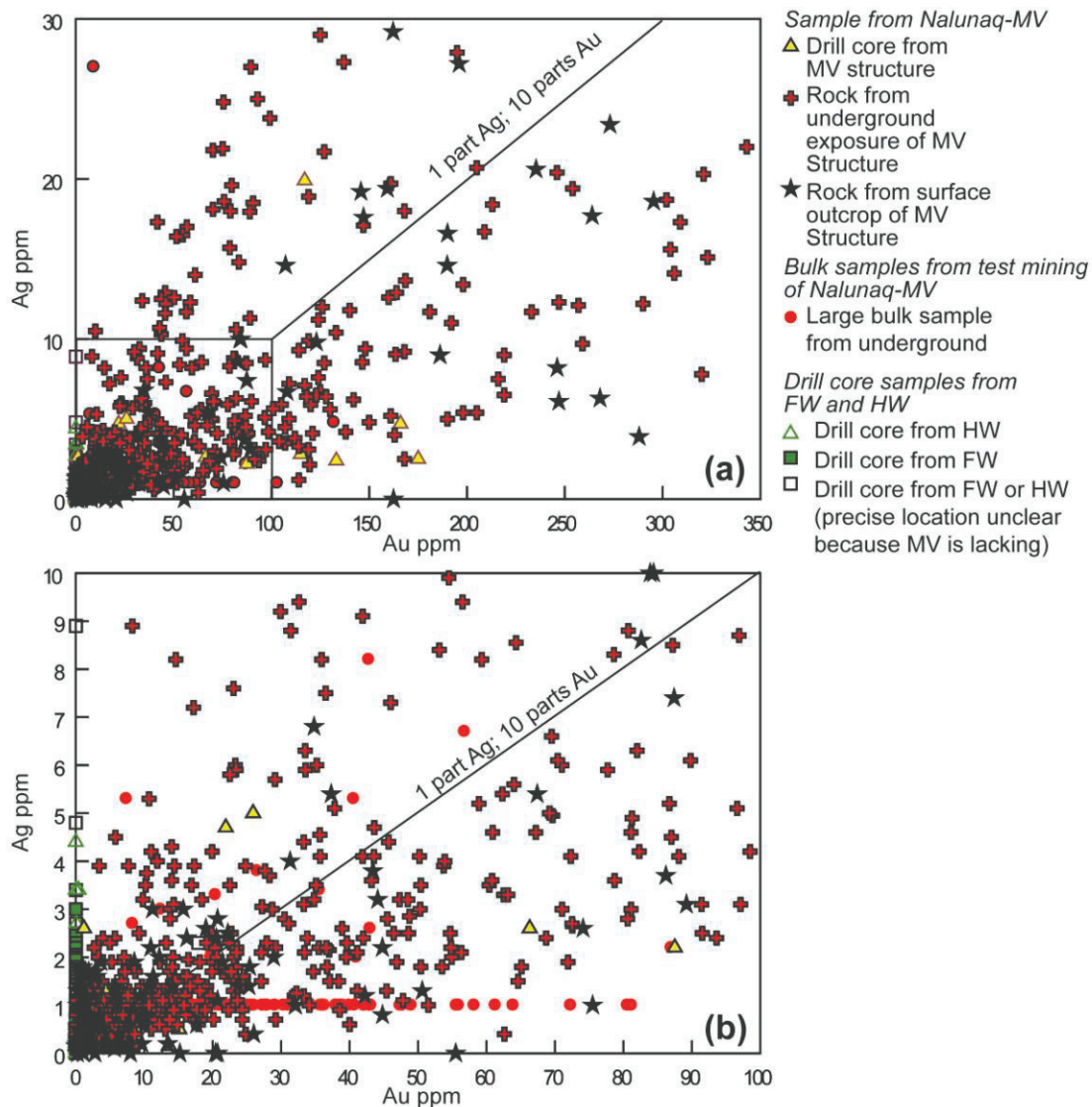


**Figure 20.** Gold and silver distribution. (a) Scatter plot of Au versus Ag for samples with Au content between 0 and 350 ppm and Ag content of 0 to 30 ppm. (b) Scatter plot of Au versus Ag for samples with Au content between 0 and 100 ppm and Ag content of 0 to 10 ppm. Only a few bulk samples yielded Ag above the detection limit. Correlations between Au and Ag are independent of sample type, e.g. rocks from underground showings and rocks from outcrops have similar correlations. The data set for the diagrams shown in (a) and (b) can be found in appendix a.

This is in agreement with results from microprobe investigations which showed that 25 analysed gold grains contain between about 5 and 15 at% silver (Kaltoft et al. 2000).

A good gold-silver correlation is seen for most of the samples (Fig. 20). However, Ag analysis of the bulk samples generally yielded only 1 ppm Ag and only few of the bulk samples show a good Au-Ag correlation. This is possibly caused by difficulties while analysing the bulk samples for Ag.

## Gold-bismuth association

Gold shows a weak correlation with bismuth (Table 7). The occurrence of the alloy maldonite ( $\text{AuBi}_2$ ) in the ore proves a correlation between both elements (Petersen et al. 1997). All bulk samples except of one yield bismuth below the detection limit (Fig. 21a) which makes a statistical assessment impossible.

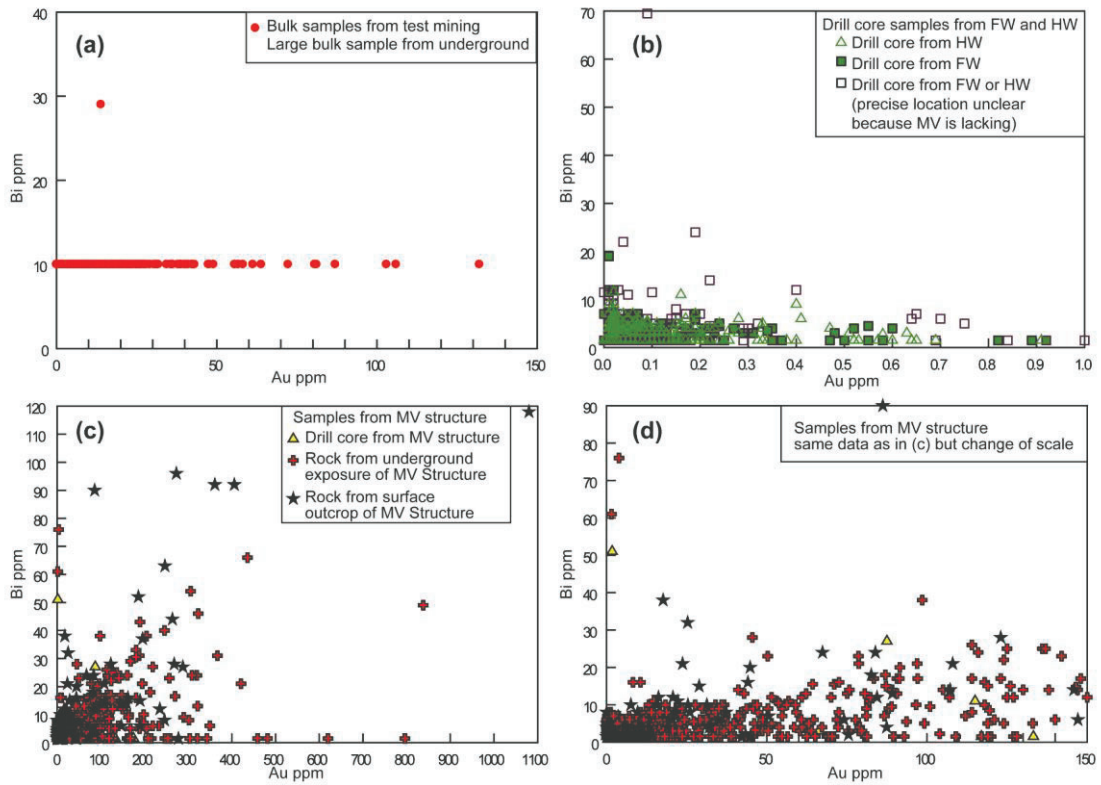


**Figure 21.** Gold and bismuth distribution. (a) Scatter plot of Au versus Bi for bulk samples. (b) Scatter plot of Au versus Bi for drill core samples with Au content between 0 and 1 ppm and Bi content of 0 to 70 ppm. (c) Scatter plot of Au versus Bi for drill core samples, underground rock samples and surface samples from the main vein or main vein structure. Au contents of these samples are between 0 and 1100 ppm and Bi contents are between 0 and 120 ppm. (d) The same data set as used in (c) but only samples with Au < 150 ppm are shown. The data set for the diagrams shown in (a) to (d) can be found in appendix a.

Although most of the drill core samples have low contents of bismuth, 148 samples have Bi contents above 10 ppm and most of these samples are also elevated in gold (Fig. 21b). Samples from the footwall and from the hanging wall have distinctively lower contents of bismuth than samples from the MV structure (Figs. 21b and 21c).

## Gold-tungsten association

Tungsten only weakly correlates with gold (Fig. 22) and the Spearman rank correlation coefficient between Au and W is >0.5 (Table 7).

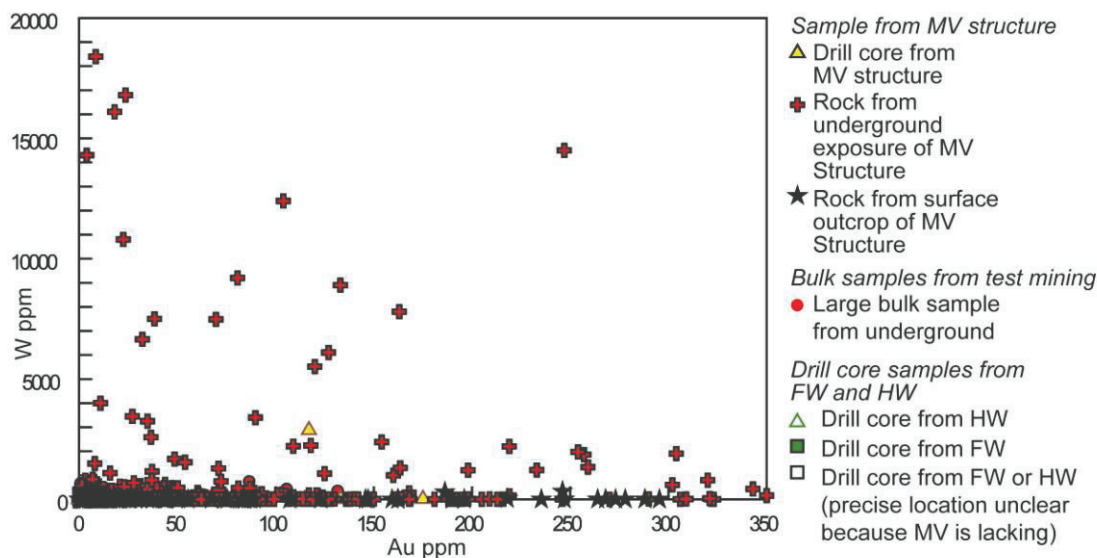


**Figure 22.** Gold and tungsten association. Rock samples from underground exposures show better correlation than rock samples from surface. Several rock samples from underground exposures are highly elevated in tungsten. The data set for the diagrams shown in the figure can be found in appendix a.

Several samples from underground exposures have strongly anomalous W contents and the highest values are above 1 wt. % W and about hundred samples from underground have W content between 1000 ppm and 1 wt. %, which is clearly elevated and must have been introduced to the rock together with the fluids. These very high W contents is also explained by the observation of scheelite from underground exposures, e.g. from several parts of the 400 m adit where scheelite was associated with the proximal hydrothermal alteration zone (Kjølsen, 1999). The modest gold and tungsten correlation is explained by either unequal distribution of tungsten and/or gold or by the nugget effect of tungsten and/or gold. For example all the samples from outcrops show consistently W contents below about 400 ppm (Fig. 22) and this could be caused by the sampling done parallel to an E-W oriented ore shoot (Fig. 19) which occurs to be low in W. These tungsten anomalies are easily detected by using an ultraviolet (UV) lamp at rock exposures in the adits of the Nalunaq gold mine or by scanning drill core samples with an UV lamp.

The W content of bulk samples is low compared to the other sample types (Fig. 22) and only a few samples yielded tungsten contents above 100 ppm. This is probably caused by the dilution of rocks from the MV structure with the wall rocks in the bulk samples. Nevertheless it is unclear why several of the bulk samples show elevated gold contents but none of the bulk samples show elevated W contents.

## Gold-antimony association

Gold shows a weak correlation with antimony (Table 7) and it has earlier been shown that gold grains from Nalunaq contain traces of bismuth and antimony (Kaltoft et al. 2000). Bulk samples were analysed for antimony, however antimony was only detected in one bulk sample whereas the other samples have antimony contents below the detection limit (Fig. 23a).

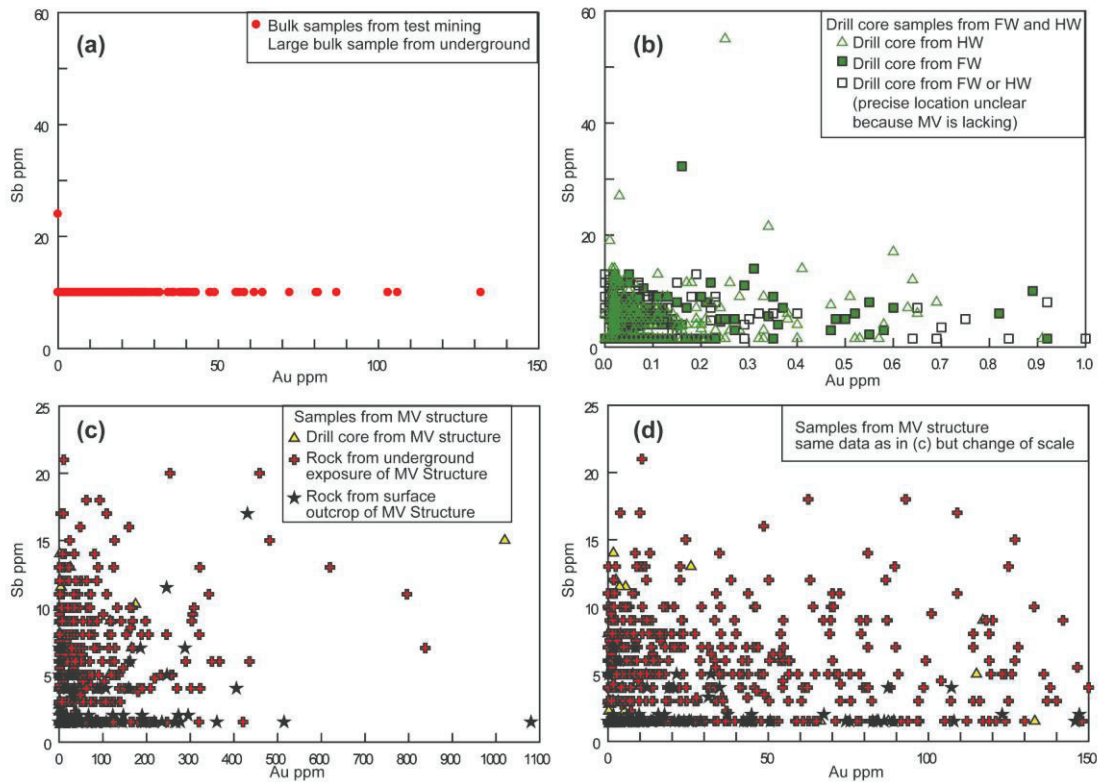


**Figure 23.** Gold and antimony distribution. (a) Scatter plot of Au versus Sb for bulk samples. Only one bulk sample yielded antimony above the detection limit. (b) Scatter plot of Au versus Sb for drill core samples with Au content between 0 and 1 ppm and Sb content of 0 to 60 ppm. Several of these drill core samples yield highly anomalous Sb contents. (c) Scatter plot of Au versus Sb for drill core samples, underground rock samples and surface samples from the main vein or main vein structure. Au contents of these samples are between 0 and 1100 ppm and Sb contents are between 0 and 25 ppm. (d) The same data set as used in (c) but only samples with Au < 150 ppm are shown. No correlation is seen between Au and Sb in the diagram (c). The data set for the diagrams shown in (a) to (d) can be found in appendix a.

Figure 23b shows that several samples from the footwall and the hanging wall contain Sb > 20 ppm. Scatter plots of Au and Sb from samples from the main vein structures show a weak correlation but the Sb content of these samples is always low. Interestingly, strongly gold mineralised samples (>200 ppm) from the main vein structure are either slightly elevated in Sb or they only contain Sb below the detection limit (Fig. 23c).

## Gold-arsenic association

Arsenic is known to occur in elevated concentrations in the vicinity of vein type gold deposits and it has been shown from many gold deposits that As is a good pathfinder to gold (Rose et al. 1979; Eilu and Groves 2001; Goldfarb et al. 2005). Although most of the bulk samples yield Bi and Sb contents below detection limit (Figs 21 and 23) most of the bulk samples yield As contents above the detection limit (Fig. 24a; Fig 7 in Dumka and Thalenhorst 2001).

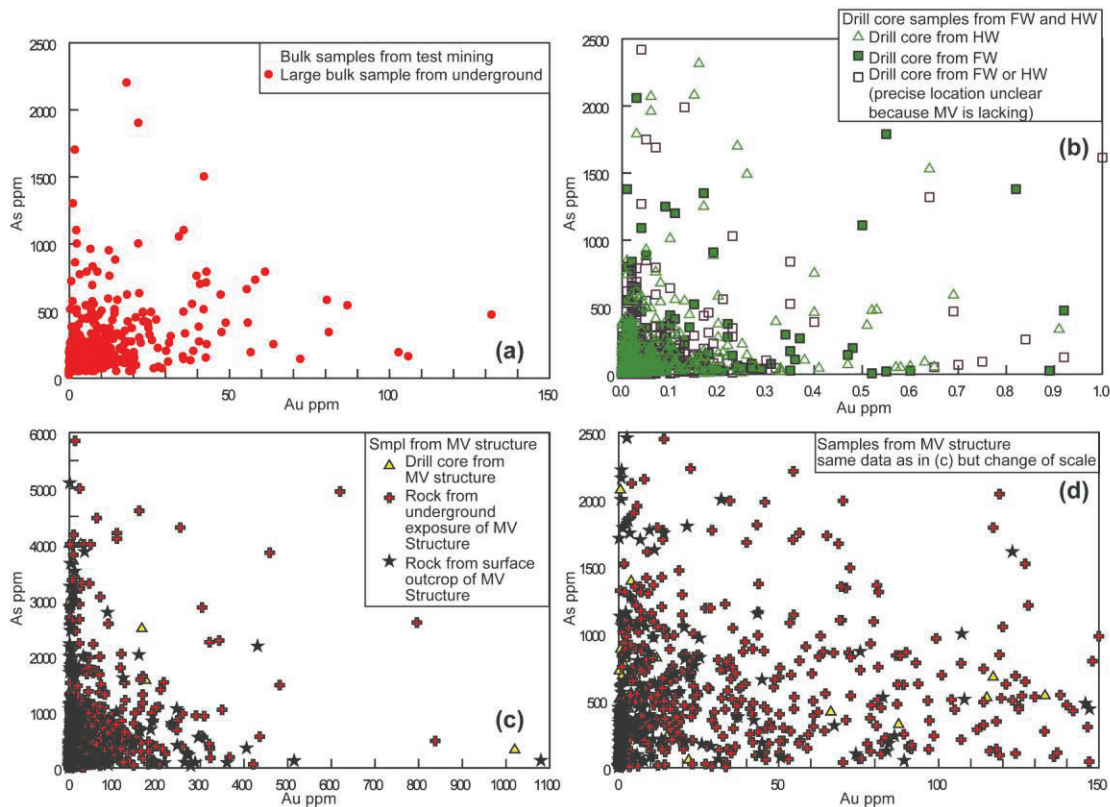


**Figure 24.** Gold and arsenic distribution. (a) Scatter plot of Au versus As for bulk samples. The correlation between gold and arsenic is moderate with a Spearman rank correlation coefficient of 0.482. (b) Scatter plot of Au versus As for drill core samples with Au content between 0 and 1 ppm and As content of 0 to 2500 ppm. Several of these drill core samples yield highly anomalous As contents. (c) Scatter plot of Au versus As for drill core samples, underground rock samples and surface samples from the main vein or main vein structure (main vein structure = ore horizon where hydrothermal alteration is present instead of the MV-Qtz). Au contents of these samples are between 0 and 1100 ppm and As contents are between 0 and 6000 ppm. (d) The same data set as used in (c) but only samples with Au < 150 ppm are shown. (c). The data set for the diagrams shown in (a) to (d) can be found in appendix a.

Figure 24a shows a weak correlation between gold and arsenic for the bulk samples, although there is not a straight forward correlation (Fig. 24a). The arsenic contents of most of the bulk samples are high, averaging about 250 ppm which is about 100 times higher than the As content from a unaltered Nalunaq rock. Several bulk samples yielded arsenic higher than 1500 ppm (Appendix a) and similar high arsenic values are also seen from numerous drill core samples (Fig. 24b). Some of the drill core samples are elevated in gold but have rather low arsenic contents (Fig. 24b). Interestingly, the samples from the footwall and the samples from the hanging wall are equally arsenic-enriched, which suggests that the hydrothermal alteration systems responsible for addition of arsenic occurred on both sides of the Nalunaq main vein. This is in agreement with the observation from other orogenic gold deposits where arsenic enrichment occurred on either sides of the ore zone (e.g. Bulletin lode-gold deposit in Western Australia, see Eilu and Mikucki 1998). Although no clear correlation occurs, most of the samples have elevated arsenic contents. Some samples contain several thousand ppm of arsenic and no gold (Figs. 24c and 24d). It is noteworthy that gold doré produced from Nalunaq yield high arsenic content (Chadwick 2010) which is in agreement with analyses from bulk samples which also yield high arsenic (Dumka and Thalenhorst 2001).

Drill cores and samples from underground exposures show slightly higher Au-As correlation (Spearman rank correlations =0.387 for drill cores and 0.293 for underground samples) than samples from surface (Spearman rank correlations =0.038). The large amount of Nalunaq samples with arsenic contents above the detection limit allowed displaying the data in a 3D space. An area in the mine covering the north-eastern extension of the Nalunaq main vein at the 400 m level was particularly well covered by samples which were analysed for arsenic (Fig. 25).

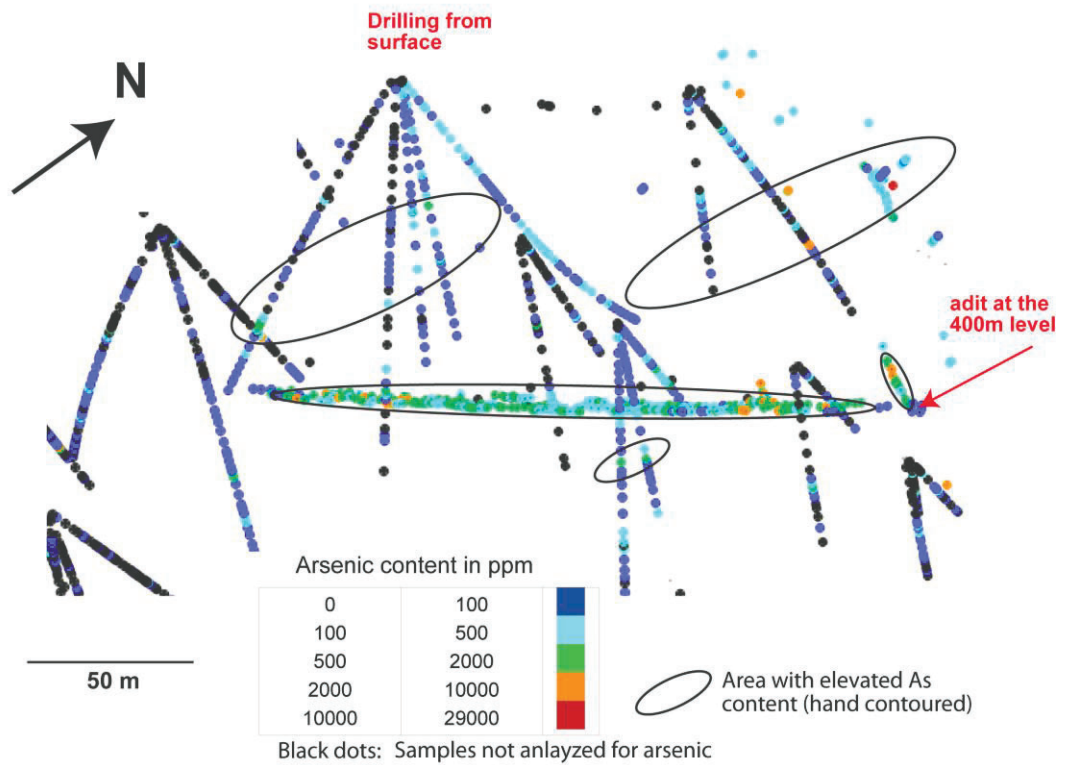


**Figure 25.** Arsenic contents of drill core samples, underground samples and a few surface samples are plotted on a longitudinal section using the Gemcom Gems software. The area around and at the adit 400 m level is shown. Arsenic contents from drill core samples and samples from underground exposures show that most samples with high arsenic contents come from the 400 m adit, but several samples with strongly elevated arsenic contents are also from the footwall or the hanging wall. The data set for the diagram can be found in appendix a.

It becomes evident that the arsenic contents from samples of the gold mineralized main vein generally are high (Fig. 25). This is in agreement with the earlier observation that gold is associated with arsenic (Fig. 24). Several areas with rocks that are strongly elevated in arsenic (>2000 ppm) occur along strike of the main vein at the 400 m level (Fig. 25).

However, other areas with rocks that are strongly elevated in arsenic also occur in the footwall and in the hanging wall of the Nalunaq main vein and define haloes of elevated arsenic (Fig. 25). It is suggested that these haloes were formed by fluids. These fluids however did not enrich the rocks with gold. This is in agreement with trends seen from scatter diagrams involving Au and As (Fig. 24). From figure 24 it becomes apparent that a population of samples is defined by high arsenic and low gold and corresponds to rocks from areas located distal to the ore body in the hanging wall and in the footwall of the Nalunaq main vein. Enrichment of arsenic away from the gold horizon is seen from other gold deposits and is a distinct characteristic of orogenic gold deposits (Eilu and Groves 2001). It remains unclear if the arsenic dispersion away from the Nalunaq main vein is related to Au mineralisation or if it was related to hydrothermal alteration stages previous or later to Au mineralisation.

## Semi-regional to deposit scale hydrothermal alteration

Lithogeochemical methods allow to reveal the style of hydrothermal alteration and to quantify the alteration. In this report, we have chosen to calculate the mass changes that are caused by hydrothermal alteration by the method developed by Barrett and MacLean (1994) using the single precursor approach.

As the effects of hydrothermal alteration were calculated for each sample, hydrothermal alteration trends can be identified and described. The results of mass change calculations also allow comparing the results presented in this report to the results from gold deposits elsewhere, where similar calculations were performed. For example it is possible to compare the hydrothermal alteration seen from Nalunaq to the one seen from the Qussuk mineralisation or elsewhere in the Godhåbsfjord (Schlatter and Christensen 2010, Eilu et al. 2006).

### Basalts and basaltic andesites NW of the the „pegmatite fault,,

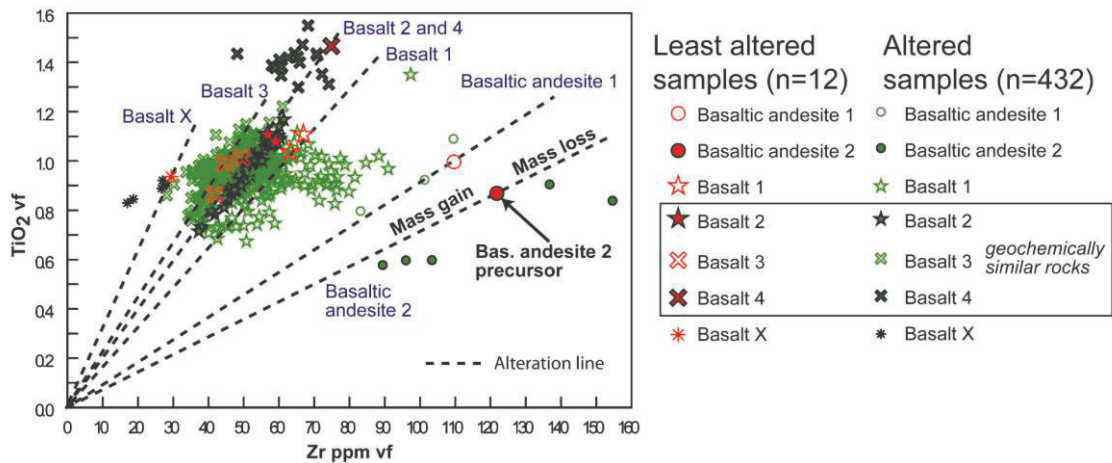


**Figure 26.** 12 least altered and 432 altered rocks are shown in a Zr versus TiO<sub>2</sub> diagram. The least altered samples are plotted in red colour. Rocks of a given primary chemical composition plot on a line. The plot shows alteration lines for basaltic andesite 1, basaltic andesite 2, basalt 1, basalt 3 and basalt X. The alteration lines for basalt 2 and basalt 4 are superimposed, because basalt 2 and basalt 4 are chemically very similar and have very similar Zr/TiO<sub>2</sub> ratios although the Zr and TiO<sub>2</sub> contents are different for altered and for unaltered samples. The Zr/TiO<sub>2</sub> ratios remain constant during hydrothermal alteration, which causes mass loss or mass gain. These changes in turn are caused by dilution and residual enrichment of mobile elements, such as during silicification or leaching of silica (divisions from Barrett and MacLean 1994; vf = the data were normalised after loss on ignition on a volatile free basis).

Effects of hydrothermal alteration are best shown on a TiO<sub>2</sub> versus Zr plot (Fig. 26). Samples belonging to the same chemical group (Table 1) form distinct alteration lines because the original immobile element ratio of a given chemical rock type remains unchanged during hydrothermal alteration (MacLean and Barrett 1993). However, hydrothermal alteration has caused mass gain or loss of the mobile elements in the rocks, which in turn results in dilution or residual concentration of the immobile elements (Fig. 26; “mass gain” and “mass loss”). Basaltic andesite 2 rocks e.g. form a distinct alteration line defined by the least altered and altered basaltic andesite 2 rocks. Altered samples located on the right hand of the least altered basaltic andesite 2 were exposed to mass loss, whereas samples located

on the left hand of the least altered basaltic andesite 2 were exposed to mass loss (Fig. 26).

Similar to the basaltic andesite 2, basalt X, basalt 3, basalt 2 and 4, basalt 1 and basaltic andesite 1 form distinct alteration lines (Fig. 26). In the next session we examine which mobile elements caused dilution of the immobile elements and which have been removed from the rocks during hydrothermal alteration.

## **Results of mass change calculations**

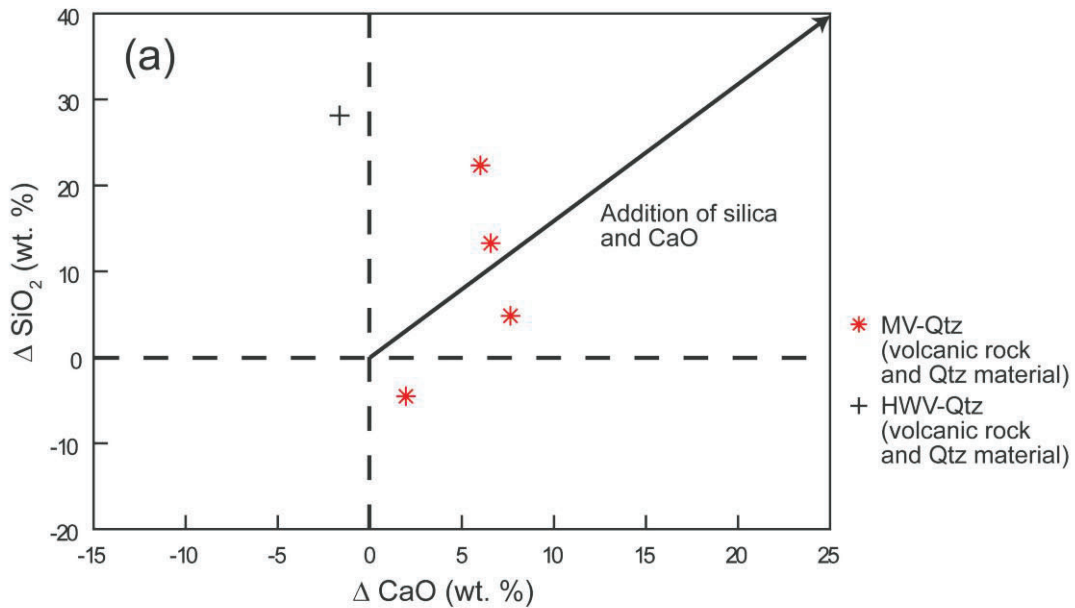
For each of the chemical rock types; (basalt 1, basalt 2, basalt 3, basalt 4, basalt X, basaltic andesite 1 and basaltic andesite 2), one or several least altered samples were identified, and the Zr-content for the precursor rock was determined. Least altered samples were selected based on the geological rock description, which indicates that the rock is a typical unaltered rock. The samples were also chosen in a way that they came from parts of the stratigraphy, which are distant to hydrothermal alteration systems. Finally, the samples were further screened by applying the following criteria: Au < 20 ppb, As < 200 ppm, Ba < 70 ppm, LOI (loss on ignition) < 2%, and Bi, W and Sb below detection limit, because the elements Au, As, Ba, Bi, W and Sb form haloes and alter the host rocks around gold deposits elsewhere (Eilu and Groves 2001).

In a next step the reconstituted value for each sample was determined (MacLean and Barrett 1993): The reconstituted value is calculated by multiplying each geochemical data by a correction factor. The correction factor is calculated by dividing the Zr-content of the precursor with the Zr-content of the altered sample. The reconstituted value represents the geochemical values of the sample previous to the hydrothermal alteration. Finally, the mass changes are calculated by subtracting the geochemical data of the reconstituted rock from the geochemical data of the precursor rock. In appendix B an example is provided how the mass change calculations were determined for the basalt 1 and appendix C provides the results of the mass change calculations for all the samples. In order to quantify quartz, biotite, diopside and plagioclase alteration, we calculated the mass gain and loss of the mobile elements Si, K, Ca and Na<sub>2</sub>O and show the hydrothermal alteration trends.

## **Silicification and calc-silicate and/or carbonate alteration**

In figure 27a hydrothermal alteration trends for the proximal alteration zone with respect to mass changes of Si and Ca are shown. Most of the rocks of the proximal hydrothermal alteration zone were affected by silicification and addition of Ca and hydrothermal alteration has caused mass gain of silica and Ca for most of the samples. This is in agreement with the observation of strong silicification in the proximal hydrothermal alteration zone.

### Hydrothermal alteration trends (proximal alteration zone)



### Hydrothermal alteration trends (medial and distal alteration zones)

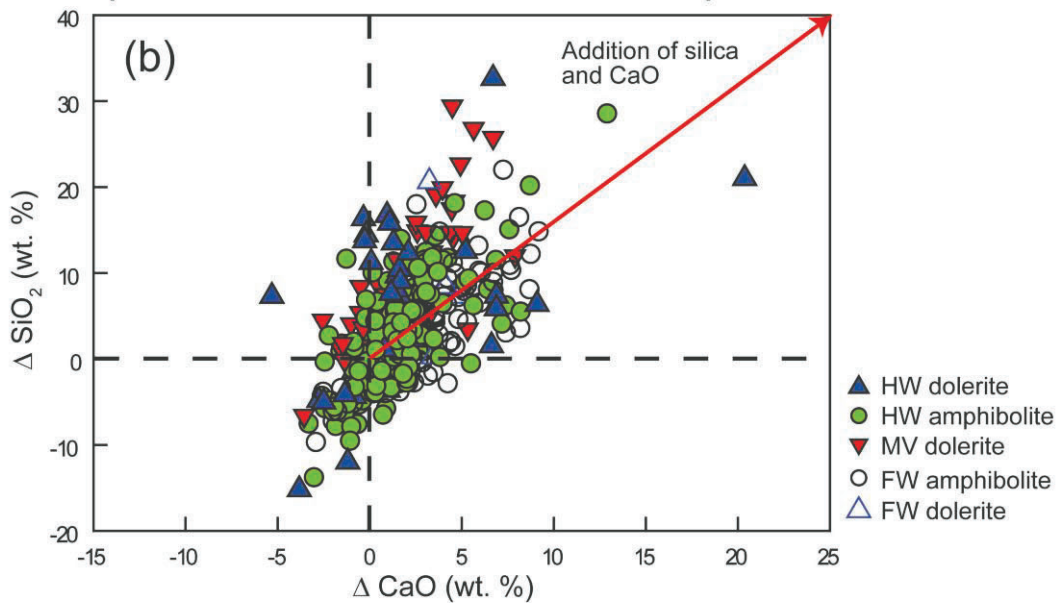


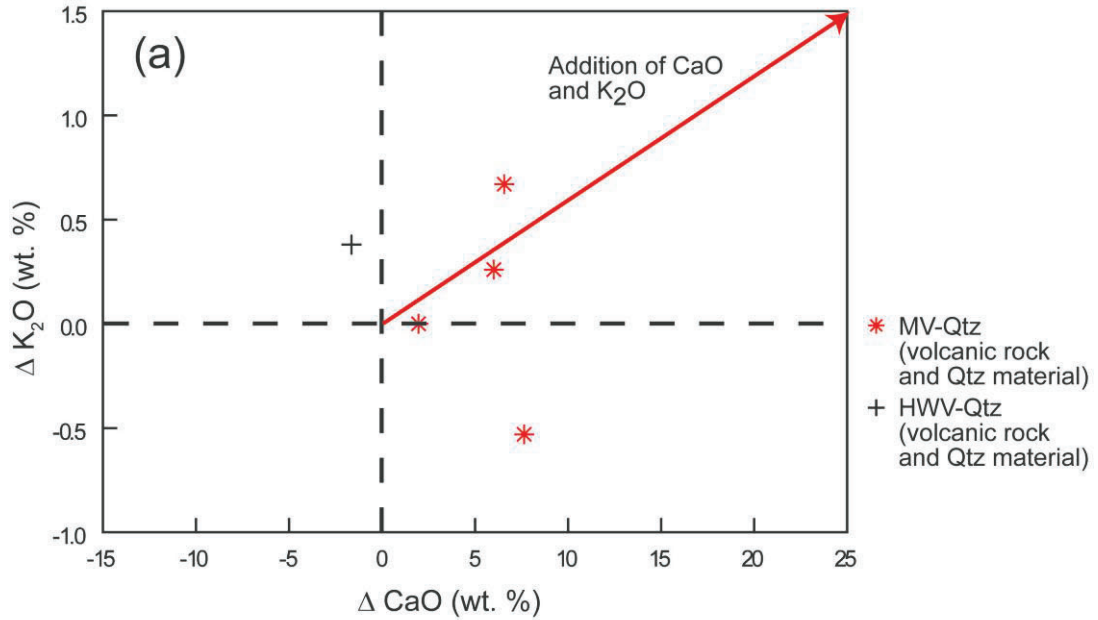
**Figure 27.** Results of mass change calculations. (a)  $\Delta \text{SiO}_2$  versus  $\Delta \text{CaO}$  for altered samples from the proximal alteration zone. Most of these samples show silicification and enrichment of CaO. (b)  $\Delta \text{SiO}_2$  versus  $\Delta \text{CaO}$  from samples of the medial and distal hydrothermal alteration zone. The amphibolites and dolerites were silicified and enriched in CaO during hydrothermal alteration and there is no relation between intensity of hydrothermal alteration and primary rock type.  $\Delta$  is the calculated mass change in wt. %.

In the medial and distal hydrothermal alteration zones (Fig 27b), the host rocks were affected by silicification with mass gains of silica up to 30 wt. % which means that for each hundred grams of rock up to 30 g silica has been added during hydrothermal alteration. Rocks also experienced addition of Ca during hydrothermal alteration with mass gains of up to 20 wt. %.

### **Potassium and calc-silicate and/or carbonate alteration**

Samples from the proximal hydrothermal alteration zone (Fig. 28a) show addition of K and Ca, which is in agreement with the field observations showing biotite alteration in this hydrothermal alteration zone

### Hydrothermal alteration trends (proximal alteration zone)



### Hydrothermal alteration trends (medial and distal alteration zones)

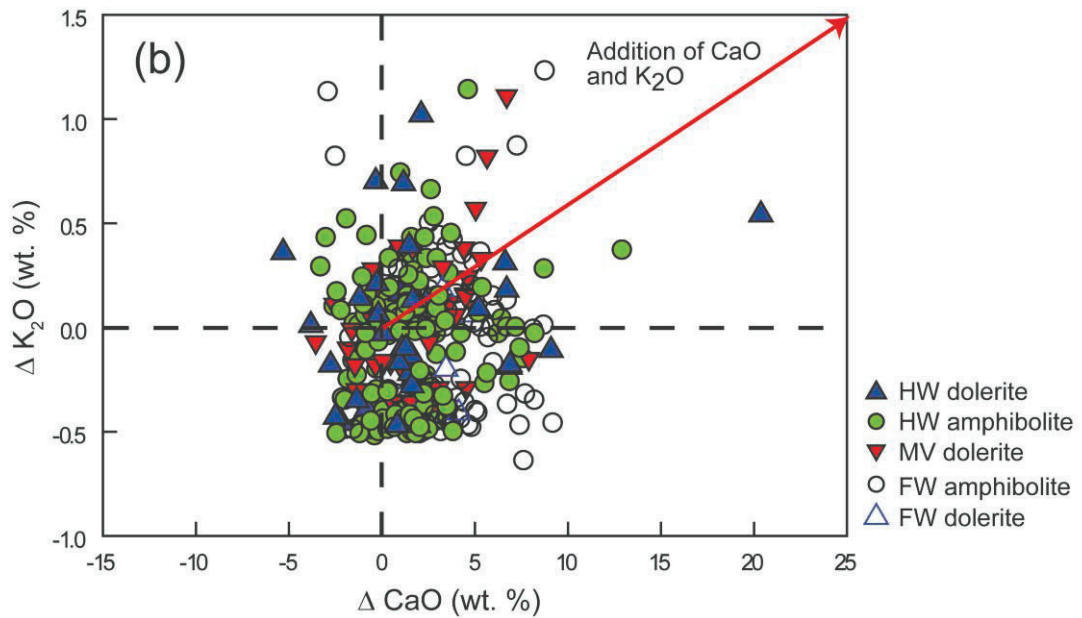


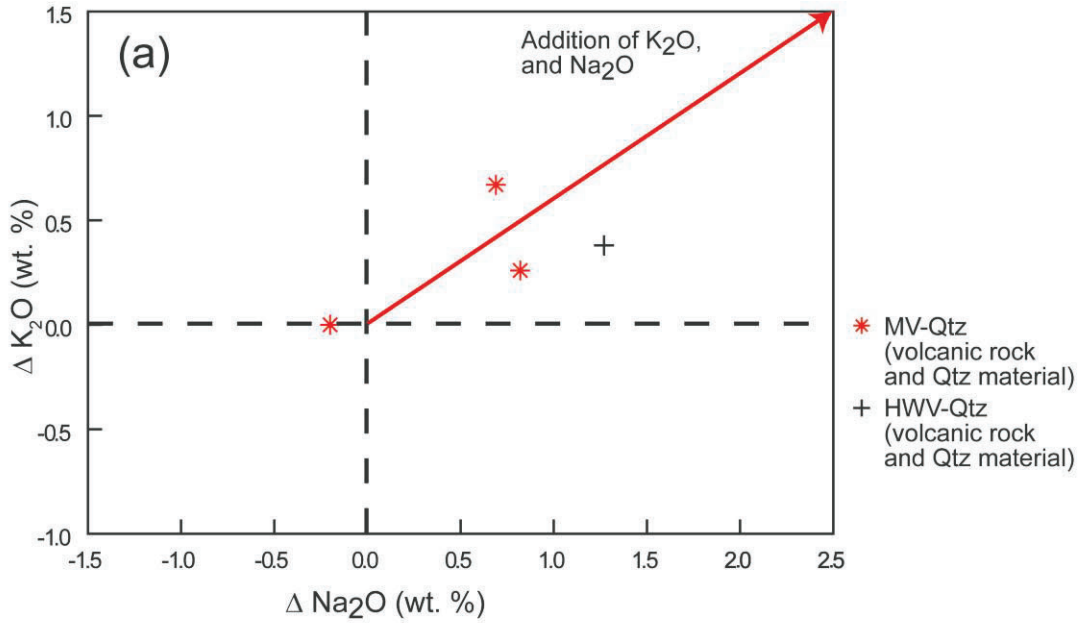
**Figure 28.** Results of mass change calculations (a)  $\Delta K_2O$  versus  $\Delta CaO$  from samples of the proximal hydrothermal alteration zone shows that most samples were affected by addition of CaO and  $K_2O$  during hydrothermal alteration. (b)  $\Delta K_2O$  versus  $\Delta CaO$  from samples of the medial and distal hydrothermal alteration zone shows that during hydrothermal alteration CaO and  $K_2O$  has been added.  $\Delta$  is the calculated mass change in wt. %.

In the medial and distal hydrothermal alteration zones (Fig 28b), the host rocks were affected by addition of  $K_2O$  of 0.5 to 1.5 wt. % and addition of  $CaO$  of 5 to 20 wt. % which is in agreement with field observations of strongly biotite altered wall rocks in the medial hydrothermal alteration zone, and calc-silicate altered rocks in the distal hydrothermal alteration zone which occur on both sides of the main vein.

### **Potassium and sodium alteration**

Samples from the proximal hydrothermal alteration zone (Fig. 29a) show addition of potassium and sodium.

### Hydrothermal alteration trends (proximal alteration zone)



### Hydrothermal alteration trends (medial and distal alteration zones)

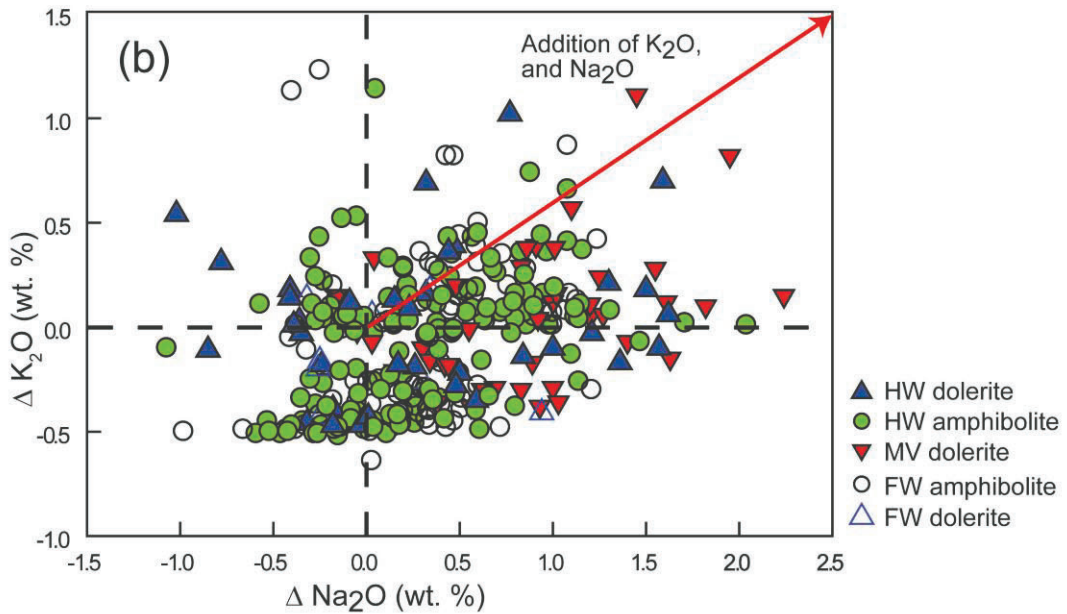


**Figure 29.** Results of mass change calculations (a)  $\Delta K_2O$  versus  $\Delta Na_2O$  plots from samples of the proximal hydrothermal zone. Three samples show mass gains of  $Na_2O$  and one sample did neither gain nor lose  $Na_2O$ . (b)  $\Delta K_2O$  versus  $\Delta Na_2O$  plot for the samples of the medial and distal alteration zone show that most of the samples show mass gains of  $Na_2O$  and only a few samples have minor losses of  $Na_2O$ .  $\Delta$  is the calculated mass change in wt. %.

Addition of Na during hydrothermal alteration commonly occurs in the hydrothermal alteration zones of gold deposits, whereas leaching of Na and Ca is typically seen in districts hosting VMS deposits. The low gold “Plateau gold mineralisation” occurring in the Qussuk area of the Gothåbsfjord in southern West Greenland for example, shows a distinct addition of Na (Schlatter and Christensen, 2010).

In the medial and distal hydrothermal alteration zones (Fig 29b), the host rocks were affected by the addition of K and Na; and most samples show gains in Na, whereas only few show losses in Na.

### **Geochemical dispersion defined by Fe, As and gold enrichment**

Other important hydrothermal alteration minerals are pyrrhotite and pyrite (Kaltoft et al. 2000), and figure 30a shows that addition of Si is followed by addition of Fe. This is in agreement with the field observation of silicified and sulphide-rich rocks, which occur for example in the medial hydrothermal alteration zone (Kjølsen 1999).

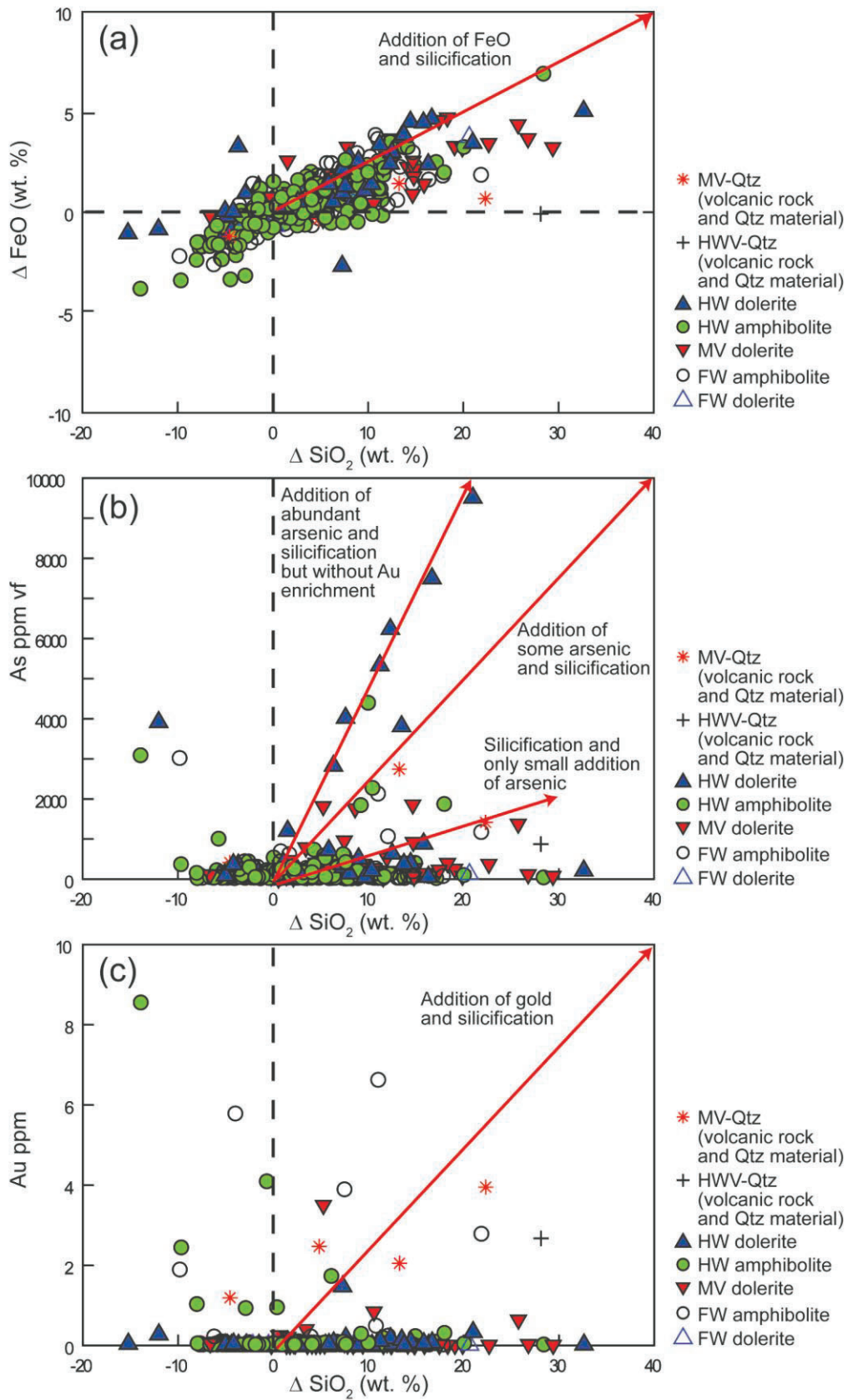


**Figure 30.** (a)  $\Delta \text{FeO}$  versus  $\Delta \text{SiO}_2$  plot for the volcanic samples of the footwall and the hanging-wall rocks and the rocks from the ore horizon. The scatter plots show that the proximal hydrothermal altera-

*tion and also the medial and distal alteration both are characterized by addition of Fe and Si. (b) As versus  $\Delta\text{SiO}_2$  plot for the volcanic samples of the footwall and the hanging-wall rocks and the rocks from the ore horizon. Some of the strongly silicified samples are strongly enriched in arsenic, whereas others are not. (c) Au versus  $\Delta\text{SiO}_2$  plot for the volcanic samples of the footwall and the hanging wall and the rocks from the ore horizon. Many samples with gold contents  $>2$  ppm are strongly silicified.*

Other main opaque minerals are arsenopyrite and löllingite (Kaltoft et al. 2000). It has been shown earlier that arsenic enrichment is seen not only from the MV level, but is also seen from the footwall and hanging wall (Fig. 25). This is in agreement with the observations from rocks, which are characterized by strong arsenic enrichment accompanied by silicification (Fig. 30b) but without gold enrichment (Fig. 30b and 30c). Anomalies of As occurring distant to the gold mineralised areas are reported from other gold deposits; e.g. from the Yilgarn craton (Eilu and Groves 2001). At Nalunaq, several silicified rocks from the HW dolerite are strongly enriched in arsenic, but they are not elevated in gold. Interestingly these rocks show larger enrichment in arsenic than the rocks from the hydrothermal alteration zones around the MV, and outcrops from the HW-dolerite (Fig. 5) are known where the dolerite yielded up to 19000 ppm As. On the other hand the rocks which are enriched in gold only show relatively small additions of arsenic.

A diagram where Au versus  $\Delta\text{SiO}_2$  is plotted (Fig. 30c) shows that samples which are elevated in gold generally also show gain of silica, which suggests that the same fluids which have added the silica also have enriched the gold.

## Deposit-scale hydrothermal alteration

The most important hydrothermal alteration minerals are quartz, biotite, muscovite, Ca-rich amphibole and Ca-rich plagioclase (Kaltoft et al. 2000). Semi-quantitative analyses (done by Scanning Electron Microscope equipped with an Energy Dispersive X-ray Spectrometer) by Grammatikopoulos and Krstic (1999) reveals that the plagioclase composition is between andesine and labradorite with An mole % between 35 and 60. As seen from the alteration minerals present, the elements Si, K and Ca are enriched as a result of hydrothermal alteration, hence the mass changes in Si, K and Ca are the most interesting parameters to characterise the hydrothermal alteration (Figs. 27, 28 and 29). However, it remains unclear, which of these alteration trends are related to economic gold mineralisation and which type of hydrothermal alteration is unrelated to gold. This is important because we aim to characterise the hydrothermal alteration, which is associated to the gold mineralisation in order to define a vector to the ore.

We group the altered samples into one group not elevated in gold ( $Au \leq 10\text{ppb}$ ) and another group elevated in gold ( $Au > 10\text{ppb}$ ), and examine the results of mass change calculations for each of the two groups.

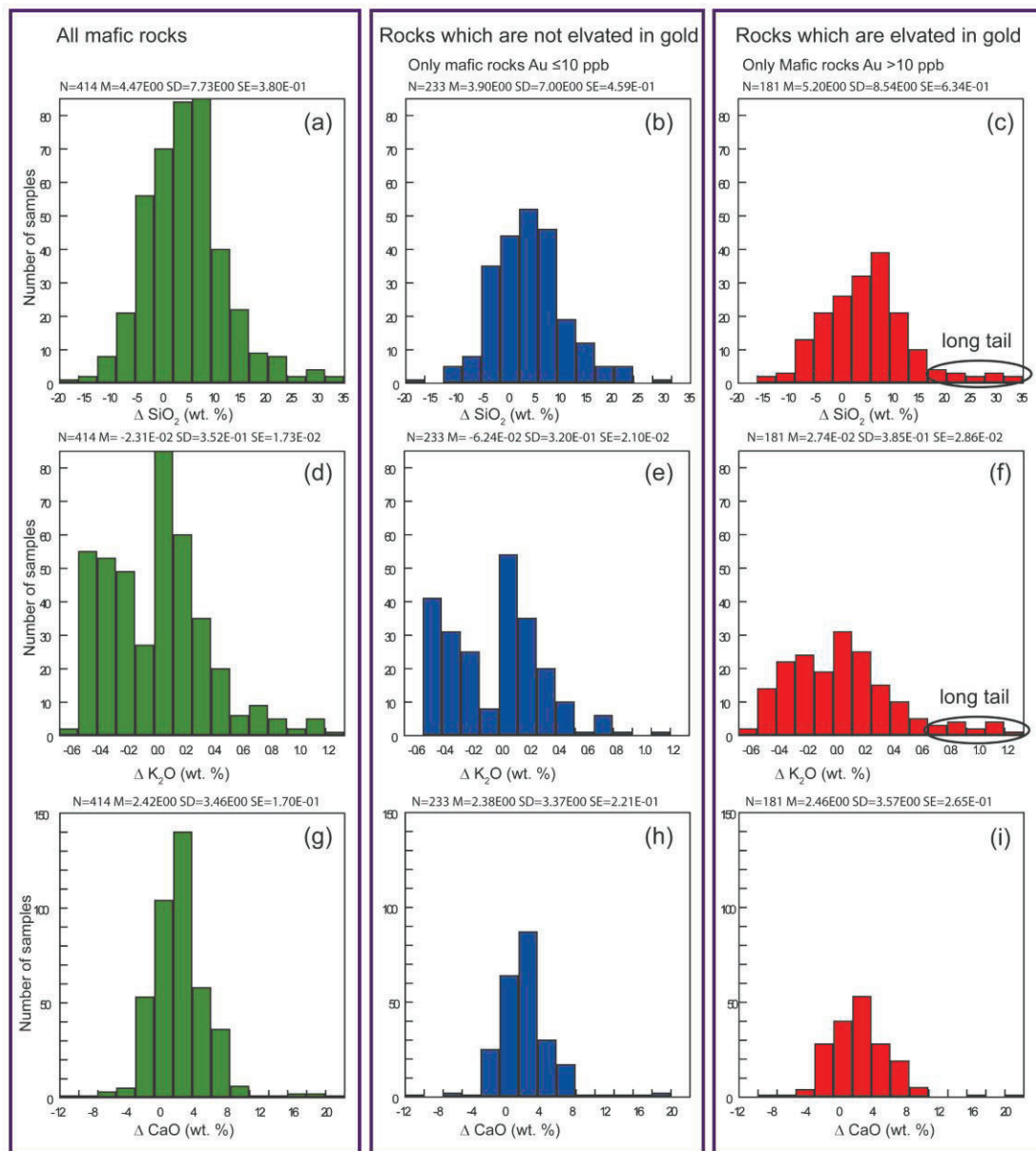


**Figure 31.** Histograms of mass changes ( $\Delta$ ) in  $\text{SiO}_2$ ,  $\text{K}_2\text{O}$  and  $\text{CaO}$ . (a), (d), (g) summarizes the results of mass change calculations for  $\text{SiO}_2$ ,  $\text{K}_2\text{O}$  and  $\text{CaO}$  of all 414 samples. (b), (e), (h) only the 233 samples with  $\leq 10$  ppb gold are plotted and in (c), (f) and (i) the 181 samples which contain gold  $> 10$  ppb are plotted. N=number of samples used; M=mean; SD=Standard deviation; SE=Standard error.

The results of mass change calculations are shown in histograms of mass changes in SiO<sub>2</sub>, K<sub>2</sub>O and CaO for all mafic rocks (Fig. 31a, d and g), for the samples with low gold-content (Fig. 31 b, e, h) and for the samples with elevated gold (Fig. 31 c, f, i).

### **Mass change of Si and gold enrichment**

Samples with Au ≤ 10 ppb display a normal distribution of mass changes in SiO<sub>2</sub> (Fig. 31b). A large number of the gold-enriched samples show SiO<sub>2</sub>-gain of >25 wt. %. It is this long tailed distribution on the histogram that is a distinct feature of the gold mineralised samples (Fig. 31c). This suggests that the hydrothermal alteration, which is associated with the introduction of gold, is characterised by addition of silica in agreement with silicification in the proximal and medial hydrothermal alteration zones (Fig. 17a).

### **Mass change of K and gold enrichment**

Samples with Au ≤ 10 ppb display a bimodal distribution of mass change in K<sub>2</sub>O (Fig. 31e) whereas relatively large number of the gold-enriched samples show K<sub>2</sub>O-gain of >0.7 wt. % (Fig. 31f). It is, as seen from mass changes in SiO<sub>2</sub> (Fig. 31c), this long tailed distribution on the histogram that is a distinct feature of the gold mineralized samples (Fig. 31f).

This suggests that the hydrothermal alteration is characterised by addition of potassium, which is in agreement with the observation of biotite in the medial hydrothermal alteration zone (Fig. 17a).

### **Mass change of Ca and gold enrichment**

Samples with Au ≤ 10 ppb display a normal distribution of mass change in Ca (Fig. 31h). The same normal distribution is seen from samples with Au > 10 ppb (Fig. 31i). Only a few samples show strong gains of Ca and they occur in the group of samples with low gold-content (Fig. 31h) as well as in the group of samples with elevated gold (Fig. 31i).

Because mineralised and unmineralised samples display very similar distribution patterns in terms of mass changes in Ca (Fig. 31h and i), it is suggested that Ca-alteration is not diagnostic for hydrothermal gold mineralisation. It is possible that Ca has been added during several pulses of hydrothermal alteration before and/or after gold mineralisation.

In summary, it appears that the hydrothermal alteration is characterised by the addition of Si, K and Au. Although Ca is enriched in haloes around the Nalunaq MV, it is not diagnostic for hydrothermal gold mineralisation. Even though that Ca-rich hydrothermal alteration minerals occur in the distal hydrothermal alteration zone (Fig. 17b), it is possible that Ca-enrichment of the wall rocks was caused by an earlier hydrothermal alteration system barren in gold (Fig. 32b). A later hydrothermal alteration stage involving Au, Si and K might then have overprinted pre-existent hydrothermal alteration (Fig. 32b).

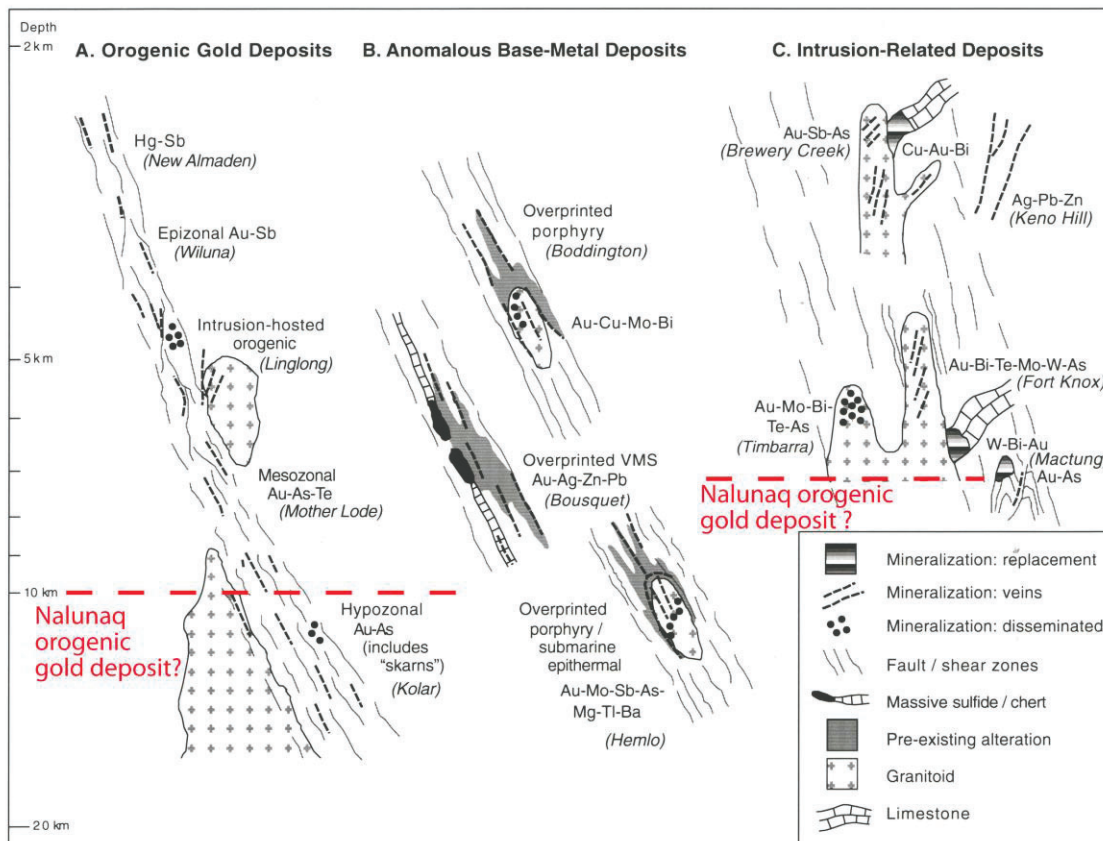


**Figure 32.** Classification of gold deposit after Goldfarb et al. 2005. The Nalunaq deposit has been formed at about 10 km depth (Kaltoft et al. 2000) and falls into the class of hypozonal orogenic gold deposits.

## Discussion and conclusions

### Nalunaq lithology

The stratigraphic column reveals that the main rock types are volcanic amphibolite, dolerite, altered volcanoclastic rocks and biotite granite, aplite and pegmatite (Fig. 6). The granite, aplite and pegmatite intruded the volcanic sequence. Minor rock types are graphite layers and sulphide-altered volcanoclastic rocks which occur in the rock sequence between the biotite-granite and the amphibole and dolerite (Fig. 6). Immediately at the contact of the biotite granite and the supracrustal rocks, skarn-like rocks occur. Although only small variations are seen from the mafic rocks, the dolerite can be distinguished from the amphibolite by its coarser grain size.

### Lithochemistry and hydrothermal alteration

Amphibolites and dolerites are classified into basaltic andesite 1 and basaltic andesite 2, basalt 1, 2, 3, 4 and X based on immobile element ratios (Table 1). A thin dolerite in the footwall complex and one thin dolerite in the hanging-wall complex is of basalt 3 composition and therefore represent good geochemical markers (Fig. 11). Basalt X only occurs in the lower part of the stratigraphic column, in the footwall of the MV-Qtz (Fig. 11) and therefore, basalt X represents a good geochemical marker.

Because the rocks are chemically very similar (Figs. 7 and 8) and have a tholeiitic affinity (Figs. 9 and 10), a comagmatic origin of the mafic Nalunaq rocks is suggested.

Rocks of low-K tholeiitic basaltic composition are known from island arc and sea floor settings. Therefore it is conceivable that the volcanic rocks at Nalunaq represent oceanic basalts formed at the sea floor. This is in agreement with relict pillow structures in fine-grained amphibolite (Petersen 1993). Tholeiitic basaltic rocks are known to be favourable host rocks to orogenic gold deposits (Dinel et al. 2008). It is, therefore recommended, to target similar stratigraphic units in South Greenland for gold exploration.

Hydrothermal alteration is characterised by the addition of Si, K, Au, As, Ag, Sb, Bi and W. These elements and the gold were transported by the hydrothermal fluids and finally trapped in the Nalunaq main vein and the hanging-wall quartz vein. Quartz veins and hydrothermal alteration zones belong to the gold mineralisation.

Calc-silicate alteration is not directly related to the gold mineralisation with quartz and biotite, as strong addition of Ca is also seen elsewhere several hundred meters away from the Nalunaq MV in barren zones without gold (Guy 1993, Petersen 1993). It is likely that several stages of hydrothermal alteration occurred. Possibly an early stage of Ca alteration was related to sea floor alteration at the time of the emplacement of the host rocks. This early Ca alteration stage (Fig. 17b) possibly was overprinted by a later Si-K-Au alteration (Fig. 17a) possibly also involving Ca alteration, which would make it difficult to distinguish both stages where they overlap. The results of mass change calculation only allow quantifying the effects of combined hydrothermal alteration stages; however it is not possible by applying lithochemical techniques to distinguish and to separate different hydrothermal alteration stages.

## Gold anomalies and pathfinders

South Greenland hosts a number of gold anomalies and numerous showings with elevated gold (Fig. 2; Stendal and Frei 2000). Most gold occurrences are known from the Psammite zone and this is also the area, which is strongly enriched in arsenic (Fig. 2).

In detail, the Nalunaq stratigraphy shows a weak correlation of Au and As however haloes of As-enrichment also occur distal to the gold mineralisation (Fig. 25). Therefore, As cannot be used solely as a vector to the gold mineralisation. It is recommended to examine areas where other pathfinder elements than As and Au, such as Bi, W and Sb are also elevated.

Interestingly, an area north of the Ketilidien in the Archaean craton also shows elevated arsenic and gold (e.g.; Sermiligaarsuk; Schlatter and Kolb 2011; Schlatter and al. 2011) and represents an interesting target for gold exploration. Association of gold with arsenic has been documented from numerous gold deposits but in detail, the correlation between both elements is not always simple (Fig. 32).

## Gold deposit model

The Nalunaq gold mineralisation age is suggested to be 1.8 to 1.77 billion years old (Stendal and Frei 2000) which is a favourable age for orogenic gold deposits elsewhere (Fig. 33); (Goldfarb et al. 2005).

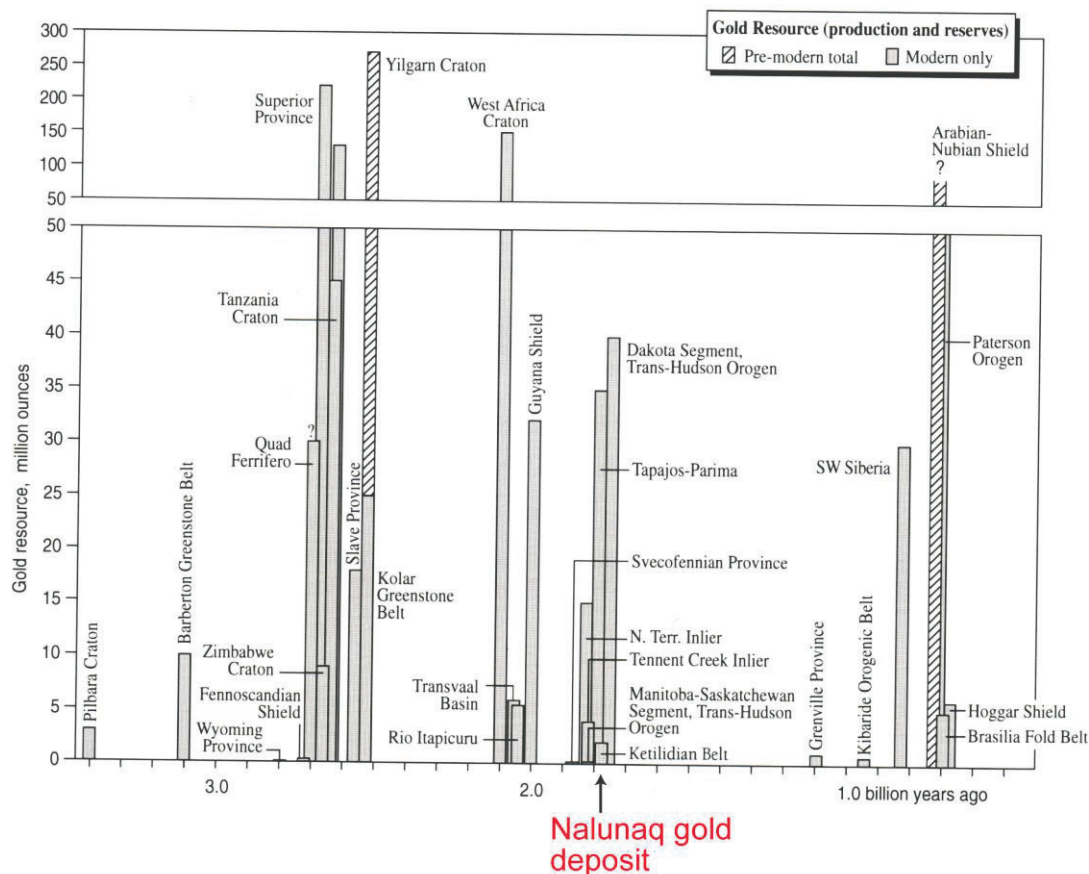


**Figure 33.** One of the favourable ages of gold mineralisation is at around 1.8 Ga. The Nalunaq gold deposit of the Ketilidian belt falls within this “golden window”. Figure from Goldfarb et al. 2005.

The Nalunaq deposit is hosted in a shear zone in an amphibolite-granite sequence. Metamorphosed host rocks in granite-greenstone belts and a spatial association with crustal-scale shear and fault zones are features characteristic of orogenic gold deposits (Goldfarb et al. 2005). The hydrothermal alteration at Nalunaq is symmetric and grades from proximal Qtz-gold to medial biotite (Fig. 17a) and distal calc-silicate+Qtz alteration. Such symmetric alteration is characteristic of orogenic gold deposits (Groves et al. 2003 and references herein). The gold-silver ratio at Nalunaq is very high (Fig. 20) which is a feature typically seen from orogenic gold deposits (Goldfarb et al. 2005).

The formation of the Nalunaq deposit took place at a crustal level of about 10 km depth (Kaltoft et al. 2000) which therefore rules out that Nalunaq was formed for example by syn-genetic processes at the sea floor.

High salinity (14-26 wt. % NaCl +CaCl<sub>2</sub> eq.) seen from fluid inclusion studies done from Nalunaq samples by Kaltoft et al. (2000) might indicate that the Nalunaq deposit is related to intrusions. It is in the intrusion related gold deposits where variable salinity has been observed whereas the "typical orogenic gold deposits" are characterized by low salinity ( $\leq$  6 wt. % NaCl eq.) fluid inclusions (Groves et al. 2003).

The gold occurrences and calc-alkaline granites in South Greenland are spatially associated. This association is well documented from Nalunaq (Figs. 4 and 13) and from "Lake 410" (Petersen 1993). The granitic rocks, which intruded the volcanic rocks at Nalunaq and "Lake 410" occupy a large volume (Fig. 4), but these granites are not elevated in gold. However at Nalunaq, silicified granitic rocks of unknown size were intersected from a single surface drill hole. They contain up to 200 ppb Au and high U (Fig. 15). Although it is unclear if the silicified granite played a role in the formation of the Nalunaq deposit, intrusion related gold deposits are recognised elsewhere and form a subgroup within the class of orogenic gold deposits (Groves et al. 2003). The Björkdal gold deposit in Northern Sweden might represent a good analogue to Nalunaq because of its similar age (1.78 to 1.79 billion years) and the spatial association of the gold mineralization with a granitic rock (Weihed et al. 2003). With respect to South Greenland, exploration was carried out in an area 25 km northwest of Nalunaq on the Niaqornaarsuk peninsula, and several gold showings were reported (Stendal and Schønswandt 2000). This area is dominated by granites and granodiorites, and represents a large target area for future exploration.

## **Concluding remarks**

The compiled geochemical data, the organized rock library and the new interpretation of the geochemical data provided some new contribution in understanding the formation of the Nalunaq gold deposit and for future gold exploration in South Greenland. South Greenland is recognised as one of the most gold-enriched areas in Greenland and numerous targets remain untested, e.g. gold targets hosted in intrusive rocks.

A good exploration model for gold in South Greenland therefore should include the search for greenstones which are intruded by silicified granite; or other rocks which are associated with intrusive plutonic and altered rocks. Within these rocks a shear zone associated with Si and K altered rocks with anomalous levels of Au, As, Ag, Sb, Bi and W represent a particular good target.

## Acknowledgements

Mogens Lind (Nalunaq Gold Mine A/S, now independent geologist), Dr. Sven Monrad Jensen (Crew Gold Corporation, now Intex resources) and Lars Lund Sørensen (Bureau of Minerals and Petroleum, now GEUS) are thanked for having sent us the samples, which are now part of the “Nalunaq rock library”. Mogens, Sven Monrad and Lars have collected the samples from Nalunaq during 2002. Mogens Lind is thanked for having collected additional samples (47 samples from underground exposures from the MV structure and 17 samples from granitic rocks associated to faults, also from underground exposures at Nalunaq in the period 2008 to 2009). We also would like to thank Kurt Christensen (Nalunaq Gold Mine A/S, now Angel Mining) for having organised shipment of the samples collected in the period 2008 to 2009 from Nalunaq to GEUS, Copenhagen and for having helped with the sampling at the Nalunaq site.

Dr. Lucy Porritt is thanked that she has sent us a copy of her Master thesis (“Alteration surrounding the main vein of the Nalunaq gold deposit, South Greenland” unpublished M.Sc. thesis, University of Exeter, 2000) and that she has given GEUS permission to add her M.Sc. thesis into the GEUS Dodex database. Please contact GEUS at [dodex@geus.dk](mailto:dodex@geus.dk) to obtain a pdf-file of the thesis.

Dr. Jason Kirk from the University of Arizona (USA) is thanked for having sent us six samples which have been sent by Crew Development Corporation to Jason in 2001 for his global research on gold deposits. These samples are now integrated.

Kristian Kaltoft is thanked for having made available to GEUS his field notes, maps and rock samples from Nalunaq. Kristian has collected rocks and information for his investigations which was leading to a M.Sc. thesis at the University of Aarhus in 2000 and to a peer reviewed article in 2000.

Dr. Henrik Stendal (BMP) is thanked for his critical comments given at the occasion of an oral presentation where the senior author has presented the preliminary results and ideas of this report.

Lars Lund Sørensen and Dr. Jochen Kolb are thanked for having critically reviewed an earlier version of this report and for having suggested modification which have greatly improved the draft manuscript, Susanne Veng Christensen is thanked for her help with the layout of this report.

### **Milestones of report:**

First draft January 2011, second draft mid of February 2011, report for layout beginning of March 2011 (after reviews of first draft; second draft and report for layout by Dr. Jochen Kolb and Lars Lund Sørensen).

Printing and distribution of the GEUS report 2011/31 mid of March 2011.

## References

- Allaart JH (1969) Geological map of Greenland, 1:100 000. Copenhagen: Geological Survey of Greenland.
- Appel WU, Secher K (1984) On a gold mineralization in the Precambrian Tartoq Group, SW Greenland. *Journal of the Geological Society*, 141: 273-278.
- Barrett TJ, MacLean WH (1994) Chemostratigraphy and hydrothermal alteration in exploration for VHMS deposits in greenstones and younger volcanic rocks. In: Lentz DR (ed) *Alteration and alteration processes associated with ore-forming systems. Short Course Notes, Volume 11*. Geological Association of Canada, pp 433-467.
- Best MG (1982) *Igneous and metamorphic petrology*. Freeman W.H. and Company, New York. 630 pages.
- Chadwick J (2010) Innovative Angel. *International Mining*, November 2010, Vol 6, Number 11: 10-14.
- Chadwick B, Garde AA (1996) Palaeoproterozoic oblique plate convergence in South Greenland; a reappraisal of the Ketilidian Orogen. In: Brewer TS (ed) *Precambrian crustal evolution in the North Atlantic region*. Geological Society Special Publications 112: 179-196.
- Debon F, Le Fort P (1983) A chemical-mineralogical classification of common plutonic rocks and associations. *Transactions of the Royal Society of Edinburgh: Earth Sciences* 73: 135-149.
- Dinel E, Fowler AD, Ayer J, Still A, Barr E (2008) Lithogeochemical and stratigraphic controls on gold mineralization within the metavolcanic rocks of the Hoyle Pond Mine, Timmins, Ontario. *Economic Geology* 103: 1341–1363.
- Dumka D, Thalenhorst H (2001) Underground Bulk Sampling Program Nalunaq Gold Project Greenland. Internal report, Strathcona Mineral Services Limited, GEUS reference number 21771, 61 pp., 8 appendices, 1 CD-ROM [appendix 3], 12 plates.
- Eilu P, Mikucki EJ (1998) Alteration and primary geochemical dispersion associated with the Bulletin lode-gold deposit, Wiluna, Western Australia. *Journal of Geochemical Exploration* 63: 73-103.
- Eilu P, Mikucki EJ., Dugdale AL (2001) Alteration zoning and primary geochemical dispersion at the Bronzewing lode-gold deposit, Western Australia. *Mineralium Deposita* 36: 13-31
- Eilu P, Groves DI (2001) Primary alteration and geochemical dispersion haloes of Archaean orogenic gold deposits in the Yilgarn Craton: the pre-weathering scenario. *Geochemistry: Exploration, Environment, Analysis* 1: 183-200.
- Eilu P, Garofalo P, Appel PWU, Heijlen W (2006) Alteration patterns in Au-mineralised zones of Storø, Nuuk region - West Greenland. *Danmarks og Grønlands Geologiske Undersøgelse Rapport 2006/30*, 73 pp.
- Evans DM, King AR (1993). Sediment and shear-hosted gold mineralization of the Tartoq group supracrustals, southwest Greenland. *Precambrian Research* 62: 61-82.
- Finlow-Bates T, Stumpfl EF (1981) The behaviour of so-called immobile elements in hydrothermally altered rocks associated with volcanogenic submarine-exhalative ore deposits. *Mineralium Deposita* 16: 319-328.

- Gowen J; Christiansen O; Grahl-Madsen L; Pederson J, Petersen JS; Robyn TL (1993) Discovery of the Nalunaq Gold Deposit, Kirkespirdalen, SW Greenland. *International Geology Review*, 1938-2839, Volume 35, Issue 11, 1993, Pages 1001 – 1008.
- Goldfarb R, Baker T., Dube B, Groves DI, Hart CJR, and Gosselin P (2005) Distribution, character and genesis of gold deposits in metamorphic terranes. In: *Economic geology 100th Anniversary volume*. Society of Economic Geologists, Littleton, Colorado, USA, pp. 407-450.
- Gowen J; Christiansen O; Grahl-Madsen L; Pederson J, Petersen JS; Robyn TL (1993) Discovery of the Nalunaq Gold Deposit, Kirkespirdalen, SW Greenland. *International Geology Review*, 1938-2839, Volume 35, Issue 11, 1993, Pages 1001 – 1008.
- Grammatikopoulos T, Kristic S (1999) Mineralogical Characterization of Gold-bearing rocks from the Nalunaq gold deposit, Greenland. Internal report, Nalunaq I/S, GEUS report file no 21699, 20 pp., 4 appendices
- Groves DI, Goldfarb RJ, Robert F, Hart CJR (2003) Gold Deposits in Metamorphic Belts: Overview of Current Understanding, Outstanding Problems, Future Research, and Exploration Significance. *Economic Geology* 98: 1-29.
- Guy K, (1993) Cyprus Greenland Corporation, Nunaoil A/S, Greenland Project. Nalunaq, Nanisiaq and Nanortalik joint ventures summary report on exploration - 1993. Internal report, Cyprus Greenland Corporation & Nunaoil A/S, GEUS reference number 21358, 15 pp., 3 app., 19 plates.
- Hallberg A, (2001) Geochemistry and tectonic setting of volcanic units in the northern Västerbotten county, northern Sweden. In: Weihed P (ed) *Research Paper C 833, Economic geology research, Volume 1, 1999-2000*. Sveriges Geologiska Undersökning (Geological Survey of Sweden), pp 69-92. In: Weihed P (ed) *Research Paper C 833, Economic geology research, Volume 1, 1999-2000*. Sveriges Geologiska Undersökning (Geological Survey of Sweden), pp 93-131.
- Kaltoft K, Schlatter DM, Kludt L (2000) Geology and genesis of Nalunaq Palaeoproterozoic shear zone-hosted gold deposit, South Greenland. *Applied Earth Science* 109 (Section B), B23–B33.
- Kaltoft K (2000) The geology and genesis of the paleoproterozoic shear zone hosted gold deposit Nalunaq, South Greenland. Fluid inclusions, field observations and mineral chemistry. Progress report, April 2000. Department of Earth Sciences University of Aarhus. 37 pages, 4 appendices.
- Kjølsen T (1999) Exploration in the Nalunaq Concession, South Greenland 1998, Adit report. Internal Report, Nalunaq I/S, GEUS reference number 21683, 21 pp., 7 appendices.
- Kludt L., Schlatter D (2000) Exploration in the Nalunaq Concession, South Greenland 1999. Internal Report, Nalunaq I/S, GEUS reference number 21738, Volume 1, 16 pp., 7 appendices, 5 plates, Volume 2, 8 appendices.
- Lind M, Kludt L, Ballou B (2001) The Nalunaq gold prospect, South Greenland: test mining for feasibility studies. *Geology of Greenland Survey Bulletin* **189** , 70-75.
- MacLean WH, Barrett TJ (1993) Lithogeochemical techniques using immobile elements. *Journal of Geochemical Exploration* 48: 109-133.
- Petersen JS (1993) Nalunaq Project 1993. Results of geological investigations on gold mineralization in the Nalunaq area, Nanortalik Peninsula, SW Greenland. Internal report, Nunaoil, GEUS reference number 21357, 49 pp., 1 app., 6 plates.
- Petersen JS, Madsen AL (1995) Shear-zone hosted gold in the Archaean Taartoq greenstone belt, South-West Greenland, in Ihlen, P.M. et al. eds. *Gold mineralization in the*

- Nordic countries and Greenland. Extended abstracts and field trip guide, **95/10**: Copenhagen, Open File Series Grønlands Geologiske Undersøgelse, pp. 65-68.
- Petersen JS, Kaltoft K, Schlatter DM (1997) The Nanortalik gold district in South Greenland. In: Papunen, H. (ed.) Mineral deposits: research and exploration. Where do they meet? Rotterdam: Balkema), pp. 285-288.
- Pearce JA (1996). A user's guide to basalt discrimination diagrams. In: Wyman DA (ed) Trace element geochemistry of volcanic rocks: applications for massive sulphide exploration. Geological Association of Canada. Short Course Notes, Vol. 12: 79–113.
- Porritt L, (2000) Alteration surrounding the main Vein of the Nalunaq gold deposit, South Greenland, unpublished M.Sc. thesis, University of Exeter , GEUS reference number 22102, 92 pp., 1 app.
- Porritt L, (2003) Development of a new, high-grade gold discovery in south Greenland: Nalunaq gold deposit, Mineral Deposits Studies Group annual meeting, Leicester, January 2003, page B157.
- Rose AW, Hawkes E, Webb JS, (1979) Geochemistry in mineral exploration, London, Academic Press, 657 pages.
- Schlatter DM (1997) Kujataa 1996 report: Gold exploration in: Nalunaq, Lake 410, Niaqornaarsuk. Licence No. 01/92 and 04/97 [27/92]. Internal report, Nunaoil A/S, GEUS reference number 21517, 2 volumes. 34 pp. + 14 appendices., 3 plates.
- Schlatter DM (1998) Gold exploration on Nalunaq Mt./Lake 410 W, South Greenland - Kujataa - 1997 Report. Internal report, Nunaoil A/S, GEUS reference number 21567, 59. pp., 4 appendices, 3 plates, 1 disk.
- Schlatter DM, Aasly K (2001) Diamond core drilling in the Nalunaq Concession, South Greenland, 2001, Drill report. Internal report, Nalunaq I/S, GEUS reference number 21795, 36 pp., 5 appendices, 3.
- Schlatter DM (2007) Volcanic Stratigraphy and Hydrothermal Alteration of the Petiknäs South Zn-Pb-Cu-Au-Ag Volcanic-hosted Massive Sulfide Deposit, Sweden, Ph.D. thesis, Department of Chemical Engineering and Geosciences, Division of Ore Geology and Applied Geophysics. Luleå University of Technology, ISSN: 1402-1544, 193 pages.
- Schlatter DM, Christensen R (2010) Characterisation of host rocks and hydrothermal alteration of the Qussuk gold occurrence, southern West Greenland. Geological Survey of Denmark and Greenland bulletin 20: 63-66.
- Schlatter DM, Kolb J (2011) The hydrothermal gold system of the Archaean Greenstones in the Nuuluk area, Sermiligaarsuk Fjord, South West Greenland. CERCAMS 14 & MDSG 34, 5<sup>th</sup> – 7<sup>th</sup> January 2011, Abstract Volume with Programme, The Natural History Museum, London: page 43.
- Schlatter DM, Kolb J, Hoffritz SE (2011): Characterization of host rocks and hydrothermal alteration of the Nuuluk gold occurrences in the Sermiligaarsuk Fjord area, South West Greenland. In: Geophysical Research Abstracts Vol. 13. EGU General Assembly 2011; EGU2011-7359 (accepted)
- Secher K (2009) Greenland Mineral Exploration Newsletter, Minex 35, December 2009, 8 pages.
- Secher K, Stendal H, Stensgaard BM (2008) The Nalunaq gold mine. Geology and Ore 11, 12pp.
- Steenfelt A (2000) Geochemical signatures of gold provinces in South Greenland. Applied Earth Science 109 (Section B), B14–B22.

- Stendal H, Schönwandt HK (2000) Mineral exploration in the 1990s. *Applied Earth Science* 109 (Section B), B1–B5.
- Stendal H, Frei R (2000) Gold occurrences and lead isotopes in Ketilidian Mobile Belt, South Greenland. *Applied Earth Science* 109 (Section B), B6–B13.
- Steenfelt A (2001) Geochemical atlas of Greenland-West and South Greenland, Danmarks og Grønlands Geologiske Undersøgelse Rapport 2001/46, 40 pp.
- Sun S, McDonough WF (1989) Chemical and isotopic systematics of oceanic basalts: implication for mantle composition and processes. In: Saunders AD, Norry MJ (eds.) *Magmatism in the Ocean basins*. *Geol. Soc. London, Spec. Publ.* 42: 313–345.
- Sundblad K (2003) Metallogeny of gold in the Precambrian of Northern Europe. *Economic Geology* 98: 1271-1290.
- Tukiainen T, Christensen L (2001): GEUSGREEN. GimmeX database relateret til GEUS' nummersystem for geologiske prøver fra Grønland. (GimmeX database related to the GEUS number system used for geological samples from Greenland. In Danish). Danmarks og Grønlands Geologiske Undersøgelse Rapport 2001/132.
- Weihed P, Bergman Weihed J, Sorjonen-Ward P (2003): Structural evolution of the Björkdal gold deposit, Skellefte district, northern Sweden: implications for Early Proterozoic Mesothermal gold in the late stage of the Svecokarelian Orogen. *Economic Geology* 98: 1291–1309.
- Winchester JA, Floyd PA (1977) Geochemical discrimination of different magma series and their differentiation products using immobile elements. *Chemical Geology* 20: 325-343.
- Windley BF (1991) Early Proterozoic collision tectonics, and rapakivi granites as intrusions in an extensional thrust-thickened crust: The Ketilidian orogen, South Greenland. *Tectonophysics*, Volume 195: 1-10.

## List of Appendices on DVD

- Appendix I:** List of all the samples contained in the “Nalunaq rock library” (186), including sample description, location and information about where to find the sample in the collection. The samples are sorted according to the sample ID. For samples printed in green bold lithogeochemical data are available.
- Appendix 1:** Au contents (7164 gold analyses) and detailed sample information from the surface drill core samples.
- Appendix 2:** Au contents (458 gold analyses) and detailed sample information from the samples collected from surface outcrops.
- Appendix 3:** Au contents (723 gold analyses) and detailed sample information from the drill cores from underground drilling.
- Appendix 4:** Au contents (2041 gold analyses) and detailed sample information from samples belonging to the MV structure collected from underground exposures (adits and raises).
- Appendix 5:** Au contents (5478 gold analyses) and detailed sample information from samples belonging to the MV structure collected from underground exposures (underground development).
- Appendix 6:** Au contents (104 gold analyses) and detailed sample information from samples collected from underground exposures not belonging to the MV structure.
- Appendix a:** Geochemical data from 4520 samples (trace elements and K<sub>2</sub>O) and detailed sample information from drill cores, surface rocks; scree sediments, rocks from underground exposures, and underground bulk sampling.
- Appendix b:** Geochemical data (whole-rock geochemistry including major and trace elements) and detailed sample information from 510 samples. Samples include drill cores, surface rocks, scree sediments, rocks from underground exposures.
- Appendix c:** Geochemical data from 75 samples analysed by the Leco method for sulphur. Samples are from drill cores, surface, surface bulk samples and from underground exposures.
- Appendix d:** Geochemical data and sample information from the CO<sub>2</sub> analyses from 36 drill core samples.
- Appendix e:** Geochemical data and sample information from 196 samples analysed with the neutron activation method. The samples are from drill cores, surface and scree sediments. The geochemical data include the elements U and Th and the rare earth elements.
- Appendix f:** Geochemical data and detailed sample information from 13 drill cores analysed at the Geological Survey of Canada (GSC) for major and trace elements.
- Appendix g:** Geochemical data and detailed sample information from 151 surface samples analysed for Pt and Pd. Only a few rocks have elevated Pd contents with Pd > 100 ppb.

**Appendix h:** Geochemical data (whole-rock geochemistry including major and trace elements) from samples of the Nalunaq rock library that were previously analysed.

**Appendix i:** Geochemical data (whole-rock geochemistry including major and trace elements analysed by GEUS) from 95 rocks sampled regionally in the Kirkespir valley.

**Appendix j:** Geochemical data (whole-rock geochemistry including major and trace elements) from 98 samples collected regionally in the Kirkespir valley. The data of the samples of “Appendix j” is reported in the report by Petersen (1993) under GEUS report file no 21357.

**Appendix k:** Geochemical data (whole-rock geochemistry including major and trace elements) from 79 samples collected regionally in the “Lake 410” area. The data of the samples of “Appendix k” is reported in GEUS report file no 21517.

**Appendix A:** Geochemical whole-rock data from 444 altered and 12 least altered amphibolite, dolerite and amphibolite containing quartz veinlets. The appendix includes also information about the chemical classification and the magmatic affinity of these samples.

**Appendix B:** Example of how mass change calculations were carried out for 116 basalt 1 samples. Shown are SiO<sub>2</sub> wt. %, TiO<sub>2</sub> wt. %, Al<sub>2</sub>O<sub>3</sub> wt. %, FeO wt. %, MnO wt. %, MgO wt. %, CaO wt. %, Na<sub>2</sub>O wt. %, K<sub>2</sub>O wt. %, P<sub>2</sub>O<sub>5</sub> wt. %, Cr<sub>2</sub>O<sub>3</sub> wt. %, Y ppm, Zr ppm, Nb ppm for the untreated data (normalized to LOI-free basis), the precursor value (single precursor), the reconstituted value (based on untreated data times Zr correction factor) and the mass changes (see also Appendix 1 in Barrett TJ, MacLean WH, 1994). The criteria used to identify least altered samples were Au < 20 ppb, As < 200 ppm, Ba < 70 ppm, LOI (loss on ignition) < 2%, and Bi, W, Sb and Mo below detection limit. In addition, the rock description and the sample location was examined to avoid samples where hydrothermal alteration was noted and from the main vein structure. The appendix also shows a graphic illustration of how the mass changes were calculated.

**Appendix C:** Results of mass change calculations for 410 altered amphibolite and dolerite samples. For some of the samples the mass changes were not calculated, either because the rocks are not altered (e.g. pegmatite), or because it was not possible to determine a probable precursor (e.g. for skarn samples and samples from the silicified siltstones).